SEMMELWEIS EGYETEM

DOKTORI ISKOLA

Ph.D. értekezések

3278.

PÉTERFFY BORBÁLA

Molekuláris és experimentális onkológia

című program

Programvezető: Dr. Bödör Csaba, egyetemi tanár

Témavezető: Dr. Alpár Donát, tudományos főmunkatárs

GENOMIC AND TRANSCRIPTOMIC PROFILING REVEALS NOVEL BIOMARKERS IN PEDIATRIC ACUTE LYMPHOBLASTIC LEUKEMIA

PhD thesis

Borbála Péterffy

Semmelweis University Doctoral School

Pathological and Oncological Division

Supervisor: Donát Alpár, Ph.D

Official reviewers: Tibor Szarvas, Ph.D

Károly Szuhai, MD, Ph.D

Head of the Complex Examination Committee: Attila Tordai, MD, DSc.

Members of the Complex Examination Committee: Péter Attila Király, MD, Ph.D

Zoltán Wiener, Ph.D

Budapest

2025

TABLE OF CONTENTS

LIST OF ABBREVIATIONS

ABL1/2	Abelson tyrosine-protein kinase 1
AFDN	Adherens junction formation factor
AFF1	ALF transcription elongation factor 1
ALL	Acute lymphoblastic leukemia
ANOVA	Analysis of variance
AUC	Area under curve
B-ALL	B-cell precursor acute lymphoblastic leukemia
BCR	Breakpoint cluster region
BM	Bone marrow
BRAF	Proto-oncogene B-Raf and v-Raf murine sarcoma viral oncogene homolog B
CDKN2A/B	Cyclin dependent kinase inhibitor 2A/B
cDNA	Complementary DNA
cfDNA	Cell-free deoxyribonucleic acid
CNA	Copy number alteration
CNS	Central nervous system
CNSamb	CNS-ambivalent
CNSL	Central nervous system leukemia
CNSmin	CNS-minimal
CNSneg	CNS-negative
CNSpos	CNS-positive
COSMIC	Catalogue of Somatic Mutations in Cancer
CREBBP	CREB (cAMP response element-binding protein)-binding protein
CRLF2	Cytokine receptor-like factor 2
ctDNA	Circulating tumor deoxyribonucleic acid
CXCL12	C-X-C motif chemokine ligand 12
CXCR4	C-X-C motif chemokine receptor 4
CSF	Cerebrospinal fluid
DALY	Disease-adjusted life-years
dbSNP	Database of Single Nucleotide Polymorphisms
ddPCR	Droplet digital PCR

DNA	Deoxyribonucleic acid
DUX4	Double homeobox 4
Dx	Diagnosis
EFS	Event-free survival
EOC	End of consolidation
EOI	End of induction
EPOR	Erythropoietin receptor
ERG	ETS transcription factor ERG
ETV6	ETS variant transcription factor 6
FBXW7	F-box and WD repeat domain containing 7
FCM	Flow cytometry
FFPE	Formalin-fixed paraffin-embedded
FISH	Fluorescence in situ hybridization
FLT3	Fms related receptor tyrosine kinase 3
gnomAD	Genome Aggregation Database
HLF	Hepatic leukemia factor
HR	High risk
iAMP21	Intrachromosomal amplification of chromosome 21
ICC	International Consensus Classification
IGH	Immunoglobulin heavy locus
IKZF1	IKAROS family zinc finger 1
IL3	Interleukin 3
IL7R	Interleukin 7 receptor
IR	Intermediate risk
ITGA6	Integrin subunit alpha 6
JAK1/2	Janus kinase 1/2
KMT2A	Lysine (K) Methyltransferase 2A
KRAS	Kirsten rat sarcoma viral oncogene homolog
LBL	Lymphoblastic lymphoma
LNK1	Lymphocyte adaptor protein
MEF2D	Myocyte-specific enhancer factor 2D
miR	MicroRNA

miRmin	miRminimal
miRsign	miRsignificant
MLLT1	Mixed lineage leukemia translocated to, 1
MLLT3	Mixed lineage leukemia translocated to, 3
MLPA	Multiplex ligation-dependent probe amplification
MRD	Measurable residual disease
MTAP	Methylthioadenosine phosphorylase
MYC	Myeolcytomatosis oncogene
NF1	Neurofibromin 1
NGS	Next generations sequencing
NOTCH1	Neurogenic locus notch homolog protein 1
NRAS	Neuroblastoma rat sarcoma viral oncogene homolog
NT5C2	5'-Nucleotidase, Cytosolic II
NUTM1	NUT midline carcinoma family member 1
OS	Overall survival
PAR1	Pseudoautosomal region 1
PAX5	Paired box 5
PBX1	Pre-B-Cell Leukemia Homeobox 1
PCR	Polymerase chain reaction
PHF6	Plant homeodomain-like finger protein 6
PTEN	Phosphatase and tensin homolog deleted on chromosome 10
PTPN11	Protein tyrosine phosphatase non-receptor type 11
QC	Quality control
qPCR	Quantitative PCR
RBC	Red blood cell
RNA	Ribonucleic acid
ROC	Reciever operating characteristic
RT-PCR	Real-time PCR
RUNX1	Runt-related transcription factor 1
SD	Standard deviation
SE	Standard error
SNP	Single nucleotide polymorphism

SNV	Single nucleotide variant
SR	Standard risk
SRCIN1	SRC Kinase Inhibitor 1
STAT5B	Signal transducer and activator of transcription 5B
STIL	STIL centriolar assembly protein
TAL1	T-cell acute lymphoblastic leukemia protein 1
T-ALL	T-cell precursor acute lymphoblastic leukemia
TARGET	Therapeutically Applicable Research to Generate Effective Treatments
TCF3	Transcription factor 3
TLP	Traumatic lumbar puncture
TP53	Tumor protein 53
USP2	Ubiquitin specific peptidase 2
VAF	Variant allele frequency
VEGFA	Vascular endothelial growth factor A
VEP	Variant Effect Predictor
VPREB1	V-set pre-B cel surrogate light chain 1
WBC	White blood cell
WHO	World Health Organization
WT1	Wilms' tumor gene 1
ZEB2	Zinc finger E-box binding homeobox 2
ZNF384	Zinc finger protein 384

1. INTRODUCTION

1.1 Epidemiology and pathophysiology of pediatric acute lymphoblastic leukemia

Leukemias are responsible for over one third of disability-adjusted life-years among children with cancer, thus representing the most significant burden in the field of pediatric oncology (1). Acute lymphoblastic leukemia (ALL) is the most prevalent form of malignancy in childhood. In Hungary, an estimated 60 to 70 children are diagnosed with ALL annually (2). Due to considerable advances in therapeutic strategies and patient stratification, the 5-year survival rates have remarkably improved during the past few decades, reaching 85-90 % in developed countries (3). Consequently, an increasing emphasis is being put on the scrutiny of potentially less intensive treatment options in order to alleviate long-term adverse effects. Of note, disease progression and relapse still pose a significant challenge to the clinical management of ALL. Deeper understanding of the underlying molecular mechanisms driving leukemia development, progression and relapse may greatly help achieve a fine balance with sufficient treatment preventing relapse and with reduced amount of cytotoxic agent alleviating potential long-term, harmful consequences.

Extensive research has been devoted in recent decades to comprehend the genetic mechanisms characterizing the various subtypes of ALL. The emergence of next-generation sequencing (NGS) has facilitated the discovery of previously unknown recurrent genetic alterations and transcriptional patterns, resulting in the establishment of novel disease subgroups (4–7). Accurate risk assessment indeed appears to depend on thorough molecular characterisation, as survival rates in certain genetically defined patient groups fall considerably below the average. Hence, the use of cutting-edge high-throughput molecular methods seems inevitable even in the diagnostic context (8). In addition, comprehensive genomic and transcriptomic characterization of leukemic blasts may aid the identification of prognostic indicators and/or potentially actionable alterations, paving the way for precision medicine.

The clinical presentation of pediatric ALL is usually preceded by a latent pre-leukemic state, commonly initiated by an early genomic aberration, often occurring prenatally, as evidenced in major genetic subgroups of the disease. Subsequent emergence of secondary alterations, required for the clinically manifest leukemia, typically confer a branching subclonal architecture(9,10). The genomic heterogeneity of ALL is represented by the current (5th) WHO classification, including 13 subgroups of B-cell precursor ALL (B-ALL), determined by either copy number changes on chromosomal (B-ALL with high hyperdiploidy / hypodiploidy) or subchromosomal level (B-ALL with iAMP21), gene fusions (B-ALL with *BCR::ABL1*, *ETV6::RUNX1*, *TCF3::PBX1*, *IGH::IL3*, *TCF3::HLF* fusion, *KMT2A* rearrangements), or gene expression profiles (B-ALL with *BCR::ABL1*-like / *ETV6::RUNX1*-like features)(11). Of note, the International Consensus Classification (ICC) recognizes additional distinct subgroups not included in the current WHO classification, such as patients characterized by *MYC, DUX4, MEF2D* or *ZNF384*-rearrangement, or harbouring *IKZF1* N159Y and *PAX5* P80R mutations (12). The current classification of ALL subtypes according to the 5th WHO and ICC is presented in Supplementary Table 1 (see: Appendix).

1.2 Molecular methods aiding the diagnostics of pediatric ALL

Due to the broad spectrum of genomic and transcriptomic changes in ALL, a wide range of molecular methods are employed across clinical laboratories, mainly for screening for subtype-defining alterations. In the diagnostics of ALL, identification of gene fusions is also crucial for risk assessment and patient stratification (13–15). While fluorescence *in situ* hybridization (FISH) and real-time PCR (RT-PCR) are commonly used for this purpose in routine diagnostics, those only allow for the analysis of a limited number of genomic loci. RNA sequencing offers a valuable alternative to these techniques by allowing for the simultaneous interrogation of a high number of genes recurrently affected by disease associated alterations, thus enabling the specific detection of rare fusions, in addition to all translocations commonly analyzed by more conventional methods (16–18).

Besides genetic subtype defining whole chromosome gains and losses conferring ploidy changes such as hyper- and hypodiploidy, the clinical importance of subchromosomal copy number alterations (CNAs) has been the subject of numerous

research studies, which identified a variety of prognostic biomarkers in pediatric ALL (19). Digital multiplex ligation-dependent probe amplification (digitalMLPA), a method primarily developed for CNA detection allows for a comprehensive, at the same time targeted, thus resource rationalized identification of whole chromosome aberrations and large CNAs, as well as for the exon-level investigation of specific genes playing driving roles in ALL development, progression and treatment resistance (20). digitalMLPA streamlines the identification of patients with *IKZF1*^{plus} genotype, which is characterized by the co-deletion of *CDKN2A/B*, *PAX5* or PAR1 in the absence of *ERG* deletion, and associated with very poor prognosis in an MRD-dependent manner (21). While standard MLPA requires two reactions – one with the P335 probemix, and another one with a different probemix covering *ERG* (P202 or P327) - the respective D007 digitalMLPA assay interrogates all genomic regions of interest simultaneously, hence enabling a rapid screening of *IKZF1*^{plus} status in a single reaction.

Currently, several combined prognostic scores exist based on the integration of cytogenetic alterations and CNAs into risk classification systems (5,20,22–24). Utilizing digitalMLPA and targeted RNA sequencing, all aberrations required for the patient-specific establishment of these integrative risk scores are detectable, without a need for orchestrating several labor-intensive conventional techniques such as karyotyping, FISH with numerous probes and conventional MLPA with multiple probemixes.

Deep mutational profiling by targeted DNA-seq is a well-suited technique for the identification of point mutations and small insertions/deletions with potential prognostic and/or therapeutic significance. Deep NGS analysis also enables the detection of mutations that are present with low variant allele frequencies (VAF) at the time of diagnosis, facilitating the early identification of subclones prone to drive relapse, and aiding the early adjustment of treatment strategies.

Since the identification of all aforementioned aberration classes is of high importance in the clinical management of pediatric ALL, the use and optimized integration of advanced methods in the diagnostic workflow is indispensable for a contemporary, state-of-the-art patient care.

1.3 Challenges in the clinical management of pediatric ALL

Relapse is the primary reason for treatment failure in pediatric ALL, and it is associated with the emergence or enrichment of certain genetic alterations harbored by the leukemic blasts (25,26). Deepening our insight on complex processes driving leukemia evolution, and on the mutational repertoire contributing to relapse, may translate directly into the advancement of clinical care, facilitating a fine-tuned, personalized therapy planning and patient management. Early identification of alterations conferring disease progression can help assess the likelihood of relapse and inform treatment focused clinical decisions. It may even enable a target specific eradication of subclones that are destined to relapse, prior to clonal re-diversification and occurrence of secondary resistance.

Another immensely challenging area of modern ALL diagnostics and therapy includes the sensitive detection, monitoring and clinical management of leukemic invasion affecting the central nervous system (CNS). Prior to the incorporation of CNS-directed therapy into ALL treatment, relapse rate involving the CNS had been as high as 80%. Early studies unraveled that CNS-directed therapy is indispensable even in cases without any clinical or cytological sign of CNS-involvement (27,28). Due to its detrimental side effects, craniospinal irradiation has largely been removed from contemporary treatment protocols, and replaced with intrathecal and high dose systemic chemotherapy (29,30). Finding a balance between sufficient treatment to prevent relapse and reduction of cytotoxic therapy to alleviate long-term harmful consequences is a pivotal challenge of modern ALL therapy. Despite considerable efforts made in the clinical management to eliminate leukemic blasts from the CNS, approximately 30-40% of relapses still include this compartment (31,32). The lack of sensitive diagnostic tools and biomarkers for interrogating the cerebrospinal fluid (CSF) is a major hurdle, preventing the precise identification of patients with clinically significant CNS involvement and a high risk of relapse in the CNS. In fact, the gap is evident, considering the 10^{-3}-10^{-5} (<0.001%) sensitivity level reachable with measurable residual disease (MRD) monitoring in the bone marrow, compared to the corresponding value of 10^{-1}-10^{-2} in the CSF (33–35).

The mechanism underlying the transendothelial migration of leukemic blasts into the central nervous system is still unclear. VEGFA, ITGA6, IL7R, and CXCL12/CXCR4 proteins are suggested to play a crucial role in the process of CNS invasion (36–39).

Anatomically, it has been established that the blood-CSF barrier, the Virchow-Robin spaces, and their outflow into the CSF are cardinal components in CNS invasion (32,38,40). Leukemic blast cells from the circulating CSF can adhere to the arachnoid mater, as evidenced by the significant leptomeningeal deposits found in patients with CNS leukemia (CNSL) in early autopsy investigations (40,41). It is important to note, that many individuals with negative CSF cytology have evident occult leptomeningeal illness or CNS relapse, indicating a very limited predictive power of CNS cytology for meningeal involvement (42,43). Nevertheless, the most commonly used contemporary methods such as cytospin-based cytology and flow cytometry (FCM) are still based on the detection of circulating blasts in the cerebrospinal fluid. For these techniques, it is essential to stabilize and process the leukemic blasts, due to the rapid ex vivo degradation of cells (44,45). The most widely recognized theory nowadays is that virtually all ALL patients present with some degree of CNS manifestation at the time of diagnosis (41). Accordingly, there appears to be a strong need for more sensitive molecular approaches, interrogating the cell-free fraction of the CSF and thus guiding CNS directed therapies more efficiently.

According to recent findings, circulating tumor DNA (ctDNA), isolated from the CSF could serve as an informative biomarker for CNSL. ctDNA comprises short extracellular double-stranded DNA fragments originating specifically from tumor cells and representing a fraction of cell-free DNA (cfDNA). Identification and longitudinal screening of leukemia associated genetic markers, for example specific immunoglobulin or T-cell receptor rearrangements may be suitable for CNSL diagnostics and monitoring using the cell-free phase of the CSF (46).

Another promising approach is the detection of microRNAs (miRs) in the CSF. These short non-coding RNA molecules have a broad regulatory impact on tumor growth, also facilitating the extramedullary dissemination of ALL (47). In a previous study, our colleagues suggested that members of the microRNA-181 (miR-181) family can be used as MRD markers for monitoring ALL in the peripheral blood (48). In addition, another previous study demonstrated the association between ALL burden and levels of miR-181 family, assessed by qPCR in the bone marrow and in CSF samples (49).

As evidenced by the aforementioned genetic heterogeneity of ALL, incorporating advanced molecular methods into the technological repertoire of clinicopathological

diagnostics is inevitable to efficiently address major challenges in the contemporary treatment of ALL. Since high-risk genetic alterations and/or CNS involvement are prominent obstacles yet to overcome in the clinical management of patients, my doctoral research seeks to address these challenging areas, by investigating alterations with potential prognostic and/or predictive relevance and discovering biomarkers for the early detection of leukemic CNS involvement. Identifying patients with a higher risk of CNS involvement or relapse based on genomic and transcriptomic features could aid clinical decision-making and enhance a more sophisticated, risk-adapted therapy selection.

2. OBJECTIVES

In my PhD work, we aimed:

- To interrogate the genomic and transcriptomic landscape of Hungarian children with ALL.
- To develop a targeted panel, specifically for the detection of mutations with clinical significance in ALL.
- To identify genetic alterations with therapeutic and/or prognostic relevance.
- To compare the landscape of genetic alterations in matching samples obtained at the time of diagnosis and relapse.
- To investigate hsa-miR-181a-5p as a potential biomarker for the diagnosis and monitoring of leukemic infiltration in the CNS.
- To investigate the associations between genetic alterations of the leukemic blasts, miR-181a expression and CNS involvement.
- To assess the diagnostic value and feasibility of miR-181a quantification by droplet digital PCR in CNSL diagnostics.

3. METHODS

3.1 Patients and samples

In the frame of the Hungarian Pediatric Leukemia Molecular Profiling Program, 192 patients diagnosed with B-cell precursor lymphoblastic leukemia (B-ALL, n=150) or lymphoblastic lymphoma (B-LBL, n=3), and T-cell precursor ALL (T-ALL, n=30) or lymphoblastic lymphoma (T-LBL, n=9) were analysed by combined genomic and transcriptomic profiling. Female to male ratio was 1.4:1, and the median age at the time of diagnosis was 5 years (range: 1-17 years, interquartile range: 9.46). Blast ratio of the diagnostic samples (bone marrow n=171, peripheral blood n=12, lymph node n=5, pleural fluid n=2, skin n=2) was assessed by flow cytometry and presented between 20 and 99% (mean±standard deviation: 78% ± 19.9%). Patients were diagnosed between 2018 and 2021 in the Department of Pathology and Experimental Cancer Research - Semmelweis University, in the Department of Pathology - University of Pécs, or in the Department of Laboratory Medicine - University of Debrecen according to standard morphological, immunophenotypical and genotypical criteria (50). Risk stratification and treatment selection were based on ALL IC-BFM 2002, ALL IC-BFM 2009, I-BFM NHL LL 2009, LBL 2018 and Interfant-06 protocols (51,52). Follow-up time ranged from 0 to 135 months, with an average of 29 months. Furthermore, samples of 19 patients (15 B-ALL and 4 T-ALL patients) drawn at the time of first, second or third relapse were collected in addition to the respective diagnostic samples. Measurable residual disease assessment on days 15 (n=177), 33 (n=180) and 78 (n=180) of therapy was performed on bone marrow samples using a 10-color BD FACSLyric™ or an 8-color BD FACSCanto II flow cytometer (BD Bioscience, Franklin Lakes, New Jersey, USA) and Kaluza 2.1.1 (Beckman Coulter, Brea, California, USA), with a minimum of 500,000 events measured at each time point (53,54).

Density-gradient centrifugation was performed for enrichment of the mononuclear cells, using Lymphoprep density gradient medium (Stemcell Technologies, Vancouver, Canada). DNA and RNA extraction was carried out with Allprep DNA/RNA/miRNA Universal Kit (Qiagene, Hilden, Germany), following the manufacturer's instructions.

For the investigation of CNSL, diagnostic bone marrow (BM) and CSF samples of 35 children with B-ALL (n=28) or T-ALL/LBL (n=7) were collected and analyzed.

Blast ratio of diagnostic samples ranged between 25 and 98% (average 85%). Serial follow-up CSF samples were collected on day 15, day 33 and around day 100 of treatment. Altogether, 92 CSF samples and 36 BM samples were analyzed. CSF samples were processed within 2 hours and frozen at -80 °C until further use, after separating the cell-free fraction by centrifugation (300*g*; 5 minutes). Conventional cell counting, microscopic cytology, and flow cytometry were performed for analyzing the cell fraction of the CSF samples following the ALL IC-BFM protocols.

The study was conducted in accordance with the Declaration of Helsinki, and was approved by the Ethical Committee (ETT-TUKEB approval numbers: 45563-2/2019/EKU, 60106-1/2015/EKU and 6886/2019/EKU), and informed consent from the parents or guardians of the patients were obtained.

3.2 DNA copy number analysis

DNA copy number aberrations were screened using the SALSA® MLPA® P335-C1, P383-A2, and P202-B2 probemixes (MRC Holland, Amsterdam, The Netherlands). The P335 probemix contains probes specific for genes recurrently altered in B-cell precursor ALL, such as *EBF1, IKZF1, PAX5, CDKN2A/B, ETV6, BTG1, RB1* and the PAR1 region. In case of *IKZF1* deletion, subsequent analysis with the P202 probemix was also performed, in order to determine the copy number status of *ERG*. *STIL::TAL1* fusion, *LEF1, CASP8AP2, MYB, EZH2, CDKN2A/B, MTAP, MLLT3, NUP214::ABL*1 fusion-amplification, *PTEN, LMO1, LMO2, NF1, SUZ12, PTPN2* and *PHF6* alterations were investigated in samples of T-ALL patients. Each MLPA reaction was carried out using 50-100 ng of genomic DNA according to the manufacturer's instructions. Following probe amplification, fluorescent signals were quantified with ABI 3500 Genetic Analyser (Life Technologies, Bleiswijk, the Netherlands), and evaluated using the Coffalyser.Net Software (MRC Holland). After normalization against non-malignant controls, copy number status of each region was determined, also considering the leukemic blast purity measured by flow cytometry, as well as the cytogenetic data.

digitalMLPA reactions were performed using an in-development version of the D007 ALL probemix (version D007-X7, MRC Holland). The probemix included (*i*) target probes for regions recurrently affected by copy number alterations in B-cell or T-cell ALL; (*ii*) digital karyotyping probes covering all chromosome arms to identify gross

chromosomal alterations and functioning as reference probes for data normalization, and (*iii*) internal control probes for quality control and sample assessment.

Reactions were carried out according to previously published protocols (20,55). After mixing each sample with a unique barcode solution, those were denatured, followed by the addition of digitalMLPA probemix and buffer. Each probe constituted two or three oligonucleotides with a locus specific 25-30 bp hybridizing sequence. The matching oligonucleotides were designed to hybridize adjacently, and in case of an intact genomic locus, the ligase-65 enzyme ligated those into a single, complete probe. Ligation was followed by amplification using a universal primer pair compatible with Illumina sequencing platforms. Polymerase chain reaction products serving as NGS libraries were then pooled, and sequenced on a MiSeq platform (Illumina, San Diego, CA, USA) with MiSeq v.3 reagent kit and 115 bp single-read configuration. Data analysis was performed in two consecutive steps, using the Coffalyser digitalMLPA software v.004 (MRC Holland). First, intra-sample normalization was carried out by normalizing the read count for each individual probe by the read count of reference probes hybridizing to regions that are typically unaffected by copy number alterations. Subsequently, inter-sample normalization was performed by comparing the relative read count calculated for each probe with the corresponding values of all reference samples. If a region was not altered by CNA, the final probe ratio (dosage quotient) was around 1.0, while an increase or decrease in the final probe ratio indicated gain or loss of the respective locus. The proportion of leukemic blasts assessed by flow cytometry was also taken into account at the interpretation. If the dosage quotient of multiple consecutive probes fell outside the average±3SD range, at the same time did not reach the predicted level of monoallelic alteration as calculated based on the leukemic cell fraction, the aberration was considered subclonal.

3.3 Mutational profiling by deep DNA sequencing

Targeted NGS was performed using a QIASeq Targeted DNA Custom Panel (Qiagen) covering 103 disease-relevant genes frequently (>2%) altered in ALL (Table 1). Libraries were prepared using 40ng genomic DNA (FFPE samples: 100ng) according to the manufacturer's recommendations, including fragmentation, unique molecular index assignment and target enrichment using region-specific primers. After equimolar pooling,

libraries were sequenced on MiSeq platform (Illumina) using v.2 chemistry with 150bp paired-end configuration. Data processing and analysis were performed with the QIAseq Targeted DNA Panel Analysis pipeline (Qiagen) using the smCounter2 workflow utilizing unique molecular identifier-based variant calling which facilitates the accurate detection of low-frequency variants (56). For reliable detection of high-confidence mutations, called variants were filtered and excluded if did not pass the predefined quality criteria of smCounter2, occurred with a variant allele frequency (VAF) of <2% or the coverage at the affected locus did not reach 100x. Furthermore, we excluded synonymous variants, intronic variants, variants present with a minor allele frequency of >1% in The Genome Aggregation Database (gnomAD 2.1) or in the 1000Genomes database (Phase 3 v5a), as well as novel variants classified as benign or likely benign based on the aggregated prediction by *in silico* pathogenicity predictors such as VarSome and Franklin(57) (https://franklin.genoox.com). Putative germline variants detected with a variant allele frequency of 45-55% and confirmed in available samples of remission were not reported. SnpSift version 4.3t was used for annotating variants with dbSNP (v151), ClinVar (2019-02-04) and COSMIC (v84) coding mutations, and variant consequence / impact was analyzed using Ensembl VEP (build 91).

Table 1. List of genes covered by the QIASeq Targeted DNA Custom Panel.

ABL1	*BCL9*	*DDX3X*	*GATA3*	*KIT*	*NOTCH2*	*PRPS1*	*STAT2*	*USP7*
ABL2	*BCL9L*	*DNM2*	*GNAO1*	*KMT2A*	*NOTCH3*	*PTEN*	*STAT3*	*USP9X*
ARID1A	*BCORL1*	*DNMT1*	*IDH1*	*KMT2C*	*NR3C1*	*PTPN11*	*STAT5A*	*VPREB1*
ASMTL	*BRAF*	*DNMT3A*	*IDH2*	*KMT2D*	*NRAS*	*RB1*	*STAT5B*	*WHSC1*
ASXL2	*BTK*	*DOT1L*	*IKZF1*	*KRAS*	*NSD2*	*RPL10*	*TBL1XR1*	*WT1*
ASXL3	*CBL*	*EBF1*	*IKZF2*	*LEF1*	*NT5C2*	*RPL22*	*TCF3*	*ZEB2*
ATRX	*CCND3*	*EP300*	*IKZF3*	*MPL*	*NTRK3*	*RUNX1*	*TP53*	*ZFP36L2*
BCL11B	*CDKN2A*	*ETV6*	*IL7R*	*MSH6*	*PAG1*	*SETD2*	*TUSC3*	
BCL2	*CDKN2B*	*EZH2*	*JAK1*	*MYC*	*PAX5*	*SH2B3*	*TYK2*	
BCL2A1	*CREBBP*	*FBXW7*	*JAK2*	*NCOR1*	*PDGFRA*	*SMARCA4*	*U2AF1*	
BCL2L2	*CRLF2*	*FLT3*	*JAK3*	*NF1*	*PHF6*	*SMARCC2*	*UBA2*	
BCL6B	*CTCF*	*GATA1*	*KDM6A*	*NOTCH1*	*PIK3R1*	*STAT1*	*USH2A*	

3.4 Gene fusion screening by targeted RNA sequencing

Gene fusions were analyzed using the TruSight RNA Pan-Cancer Panel (Illumina) covering 1,385 genes recurrently altered in various malignancies. Libraries were prepared following the manufacturer's instructions. After RNA fragmentation, reverse transcription and adapter ligation, ligated cDNA products were amplified. Targeted regions of interest were hybridized with sequence-specific baits and captured using Streptavidin magnetic beads, followed by amplification of the enriched libraries. Normalized libraries were pooled equimolarly and sequenced on a MiSeq platform using v.3 chemistry with 75bp paired-end configuration. Fusion transcripts were called with STAR-Fusion v1.9.0, FusionCatcher v1.20 and Pizzly v.0.37.3 software tools (58–60). Identified gene fusions were validated by FISH, quantitative RT-PCR or Sanger sequencing.

3.4 Droplet digital PCR

Reverse transcription and cDNA amplification were performed on total RNA samples, isolated from CSF, using TaqMan Advanced miRNA cDNA Synthesis Kit (Thermo Fisher Scientific, Waltham, MA, USA), enabling the non-biased amplification of the targets. The copy numbers of miR-181a, miR-532, and miR-16 were determined with a QX200 ddPCR system (Bio-Rad Laboratories, USA), using assays specific for the target miRNAs (TaqMan Advanced miRNA assay, 477857_mir, 478151_mir, 477860_mir; Thermo Fisher Scientific). ddPCR Supermix for probes (without dUTP) (Bio-Rad Laboratories) was used to carry out each PCR reaction. The results obtained were analysed and copy numbers determined using QuantaSoft software v1.7 (Bio-Rad Laboratories). Each sample was measured in duplicate, and the mean value of the two measurements was used in subsequent analyses.

3.5 Statistical analysis

The co-occurrence of genetic alterations and MRD positivity was evaluated using Fisher's exact test. Overall survival (OS) and event-free survival (EFS, defined as the time to relapse or death) were estimated using the Kaplan-Meier method and statistically compared with log-rank test. Analyses were performed and figures were prepared using SPSS Statistics 28.0.1.0 (IBM Corporation, Armonk, NY, USA) and GraphPad Prism

version 8.0.2 (GraphPad Software Inc., San Diego, CA, USA). Oncoplots were created using the PeCan ProteinPaint tool (61).

For statistical analysis of ddPCR results, the R language and environment was used (R Foundation for Statistical Computing, Vienna, Austria, version 4.2.1; accompanied by RStudio, Posit, PBC, USA, version 2023.06.1+524). As miR-532-5p showed reproducibly stable expression in CSF samples from patients with ALL in our previous experiments (49), we treated miR-532-5p as a background in miR expression data analysis. This way, as a normalization step, miR-532-5p copy numbers were subtracted from hsa-miR-181a-5p. The miR-16-5p expression was used for quality control of pre-analytical sample processing: if miR-16-5p copy number was under 100/well, the sample was considered non-informative and excluded from further analysis. Outliers above three standard deviations of the mean of the logarithm of miR-16-5p copy number were also subsequently discarded. Samples from patients who underwent traumatic lumbar puncture (TLP) were also removed from the analysis. CSF samples collected on the day of diagnosis were sorted by hierarchical cluster analysis based on Ward2 algorithm. The Euclidean distance was computed by taking the logarithm of hsa-miR-181a-5p copy numbers and correcting for miR-532-5p copy numbers. Three groups were further compared, based on the results of hierarchical cluster analysis. A multivariate linear regression model adjusted for gender and immunophenotype, and ANOVA were used to compare hsa-miR-181a-5p expression between the three groups. Diagnostic value of hsa-miR-181a-5p was determined using receiver operating characteristic (ROC) curve analysis (pROC package in R, version 1.18.0). For the binary transformation, a cut-off point was statistically defined for hsa-miR-181a-5p copy numbers based on the Youden index, and a blast rate of >0.1% was considered positive for FCM. Cytospin data were binary by nature.

4. RESULTS

4.1 Comprehensive genomic and transcriptomic profiling in the frame of the Hungarian Pediatric Leukemia Molecular Profiling Program

Comprehensive genomic and transcriptomic profiling was performed on the diagnostic samples of 180 patients diagnosed with B-ALL (n=150) or T-ALL (n=30) and 12 patients with B-LBL (n=3) or T-LBL (n=9). In total, targeted DNA- and RNA sequencing, as well as copy number analysis by MLPA was performed on the diagnostic samples of 165 patients (B-ALL: n=134; T-ALL: n=27; T-LBL: n=4), while in 27 cases (B-ALL: n=16; T-ALL: n=3; B-LBL: n=3; T-LBL: n=5) either NGS (DNA-seq or RNA-seq) or MLPA results were not available due to the paucity of samples or sample quality (Figure 1). Additionally, 114 samples (B-ALL: n=90; T-ALL: n=22; T-LBL: n=2) were also analyzed by digitalMLPA. Figure 2 depicts the distribution of WHO subtypes in the whole patient cohort (Figure 2.A) and across different age groups (Figure 2.B).

Figure 1.A

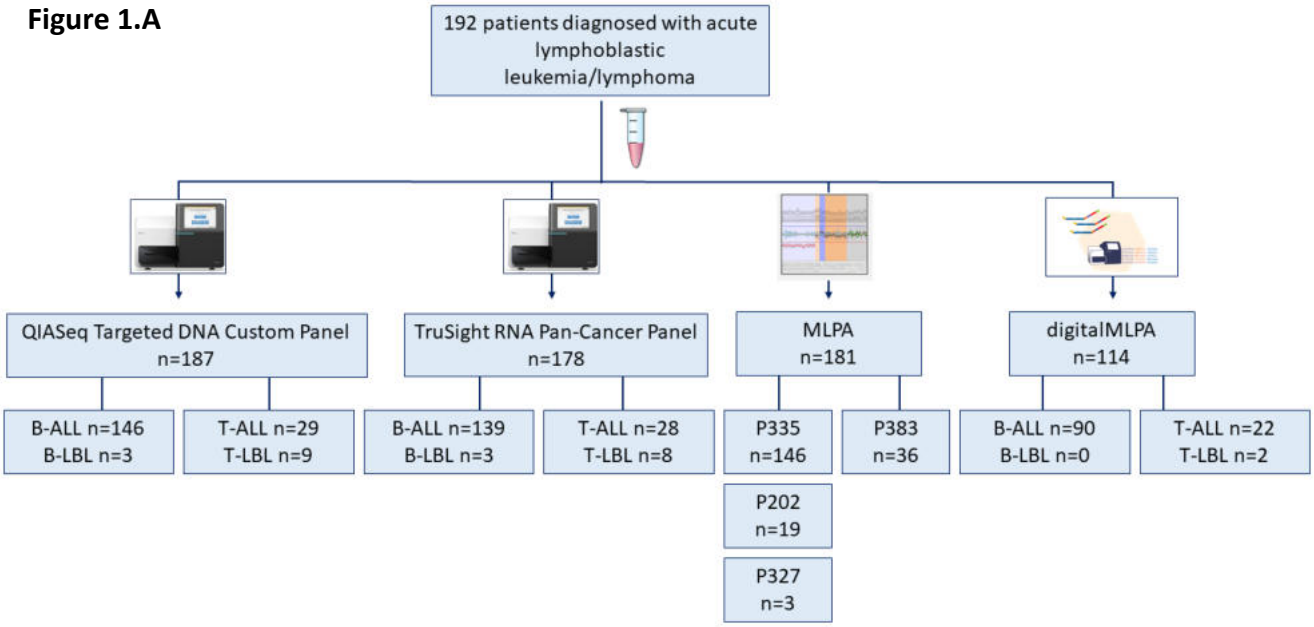

Figure 1.B

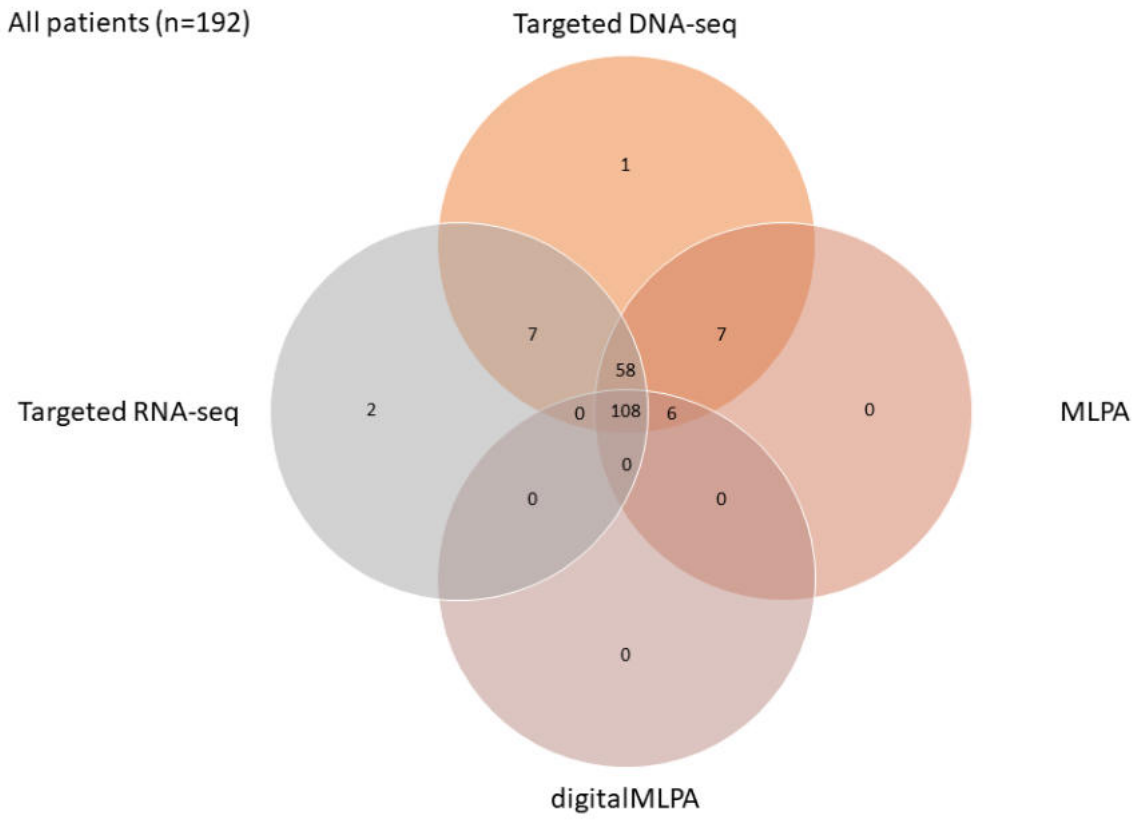

Figure 1. Molecular profiling strategy (62)**. A** Summary of the number of samples, and molecular methods used in this study. **B** Venn diagram depicting the number of diagnostic samples analyzed, and methods used for a combined genomic and transcriptomic characterization of 192 patients diagnosed with pediatric acute lymphoblastic leukemia/lymphoma.

Figure 2.A

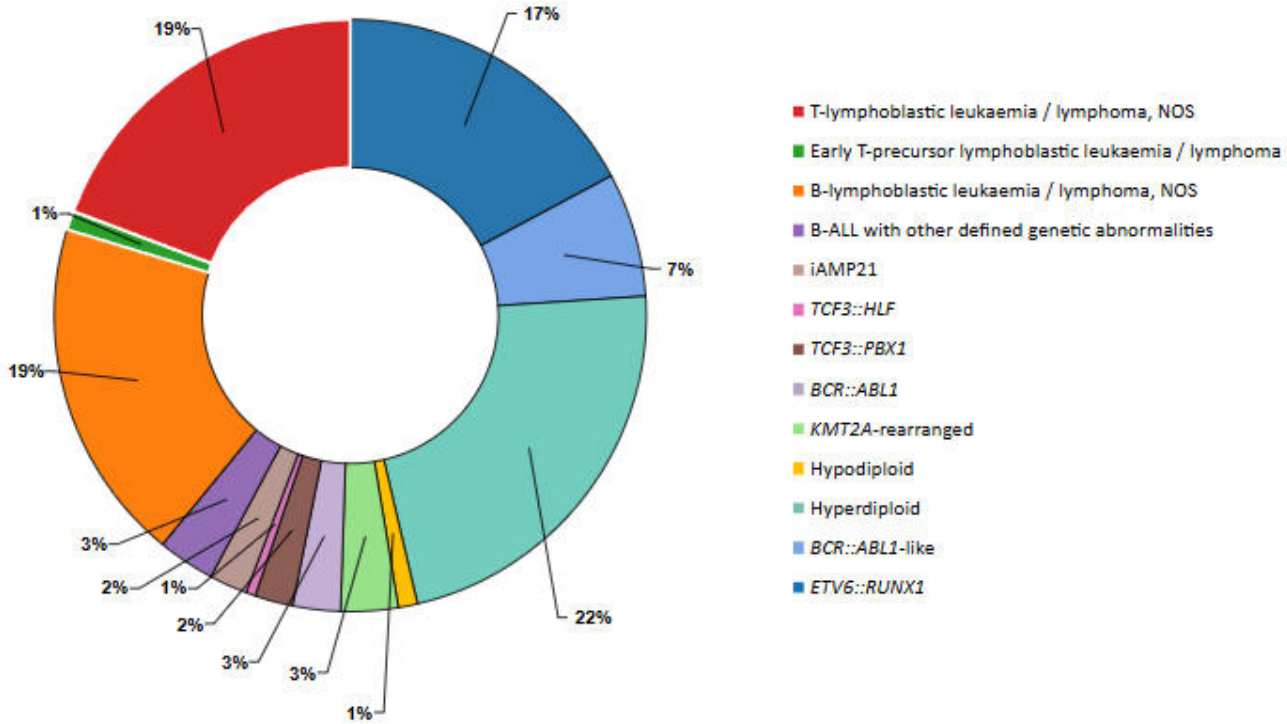

Figure 2.B

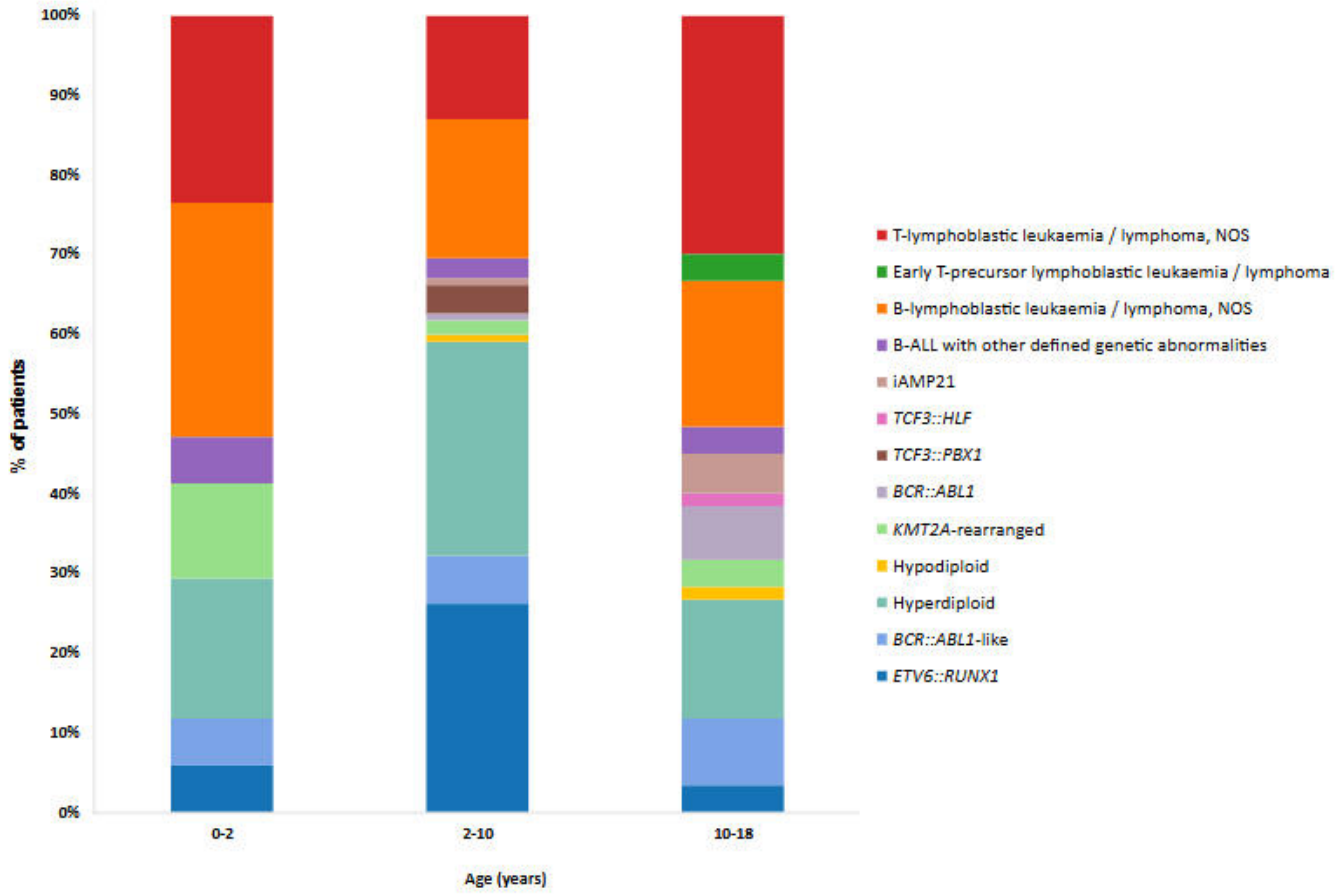

Figure 2. Distribution of molecular subtypes in our cohort (62)**. A** Distribution of WHO molecular subtypes among the 192 patients involved in the study. **B** Incidence of WHO categories in different age groups. Frequency of *KMT2A*-rearranged ALL was the most prominent in infants / young children (0-2 years), hyperdiploidy and *ETV6::RUNX1* fusion had the highest prevalence in the age group representing the peak incidence of pediatric ALL, while high-risk molecular alterations, such as *BCR::ABL1* fusion and iAMP21 presented predominantly in older children / teenagers.

4.2 Genetic aberrations unveiled by comprehensive profiling

Altogether, 401 single nucleotide variants and short insertions/deletions were detected in 187 samples interrogated (Figure 3). Seventy-five percent (74.9%, 140/187) of the patients harbored at least one mutation in 58 of the analyzed 103 genes, with an average of 1.78 mutations detected per sample (range: 0-10). In T-ALL/LBL patients, the average number of mutations was higher in comparison with that of B-ALL/LBL patients (1.5±1.4 vs 2.7±2.2; $p<0.001$, Figure 4.A). Mutations were most frequently identified in RAS-pathway genes (*KRAS* (18.5%; 27/146), *NRAS* (17.8%; 26/146), *FLT3* (10.3%; 15/146)), in B-ALL patients. In T-ALL patients, on the other hand, mutations in *NOTCH1* (58.6%; 17/29), *PHF6* (27.6%; 8/29), *PTEN* (17.2%; 5/29) and *WT1* (17.2%; 5/29) were the most prevalent. Missense mutations were the predominant mutation class in the interrogated genes (64.1%; 257/401), followed by frameshift alterations (15.2%; 61/401). Distribution of variant allele frequency of each alteration detected, broken down by genes, is presented in Figure 4.B.

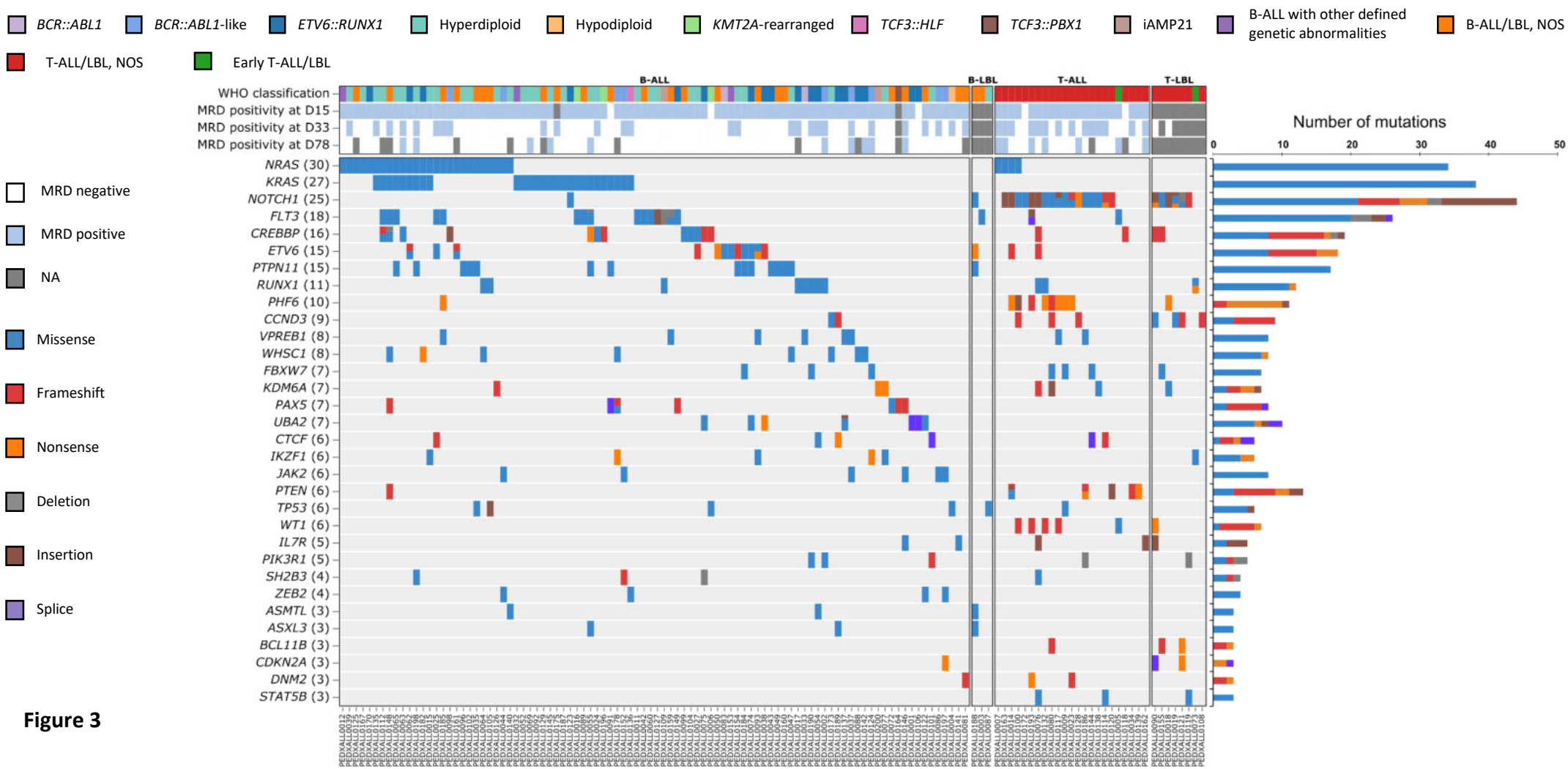

Figure 3

Figure 3. Oncoplot displaying the mutational profile of patients analyzed by targeted sequencing (62)**.** Mutations and short insertions/deletions identified by targeted DNA sequencing in diagnostic samples of 187 patients with pediatric ALL/LBL. Immunophenotype, WHO classification, measurable residual disease (MRD) status on days 15, 33 and 78 of therapy, mutation type and abundance of altered genes are also depicted. Genes affected in more than two patients are illustrated

Figure 4.A

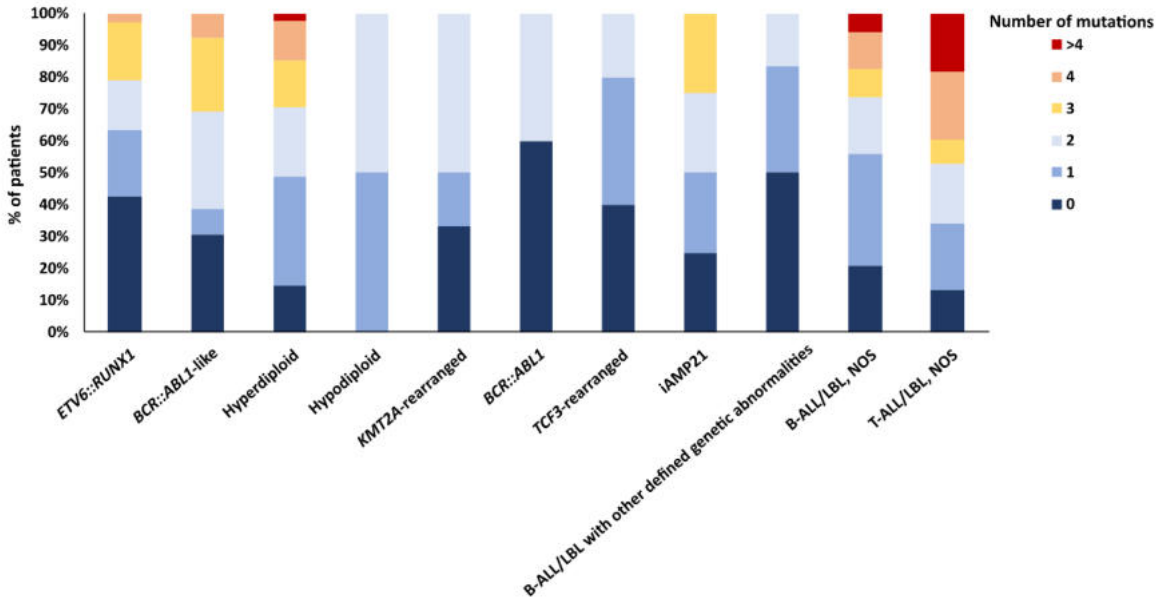

Figure 4.B

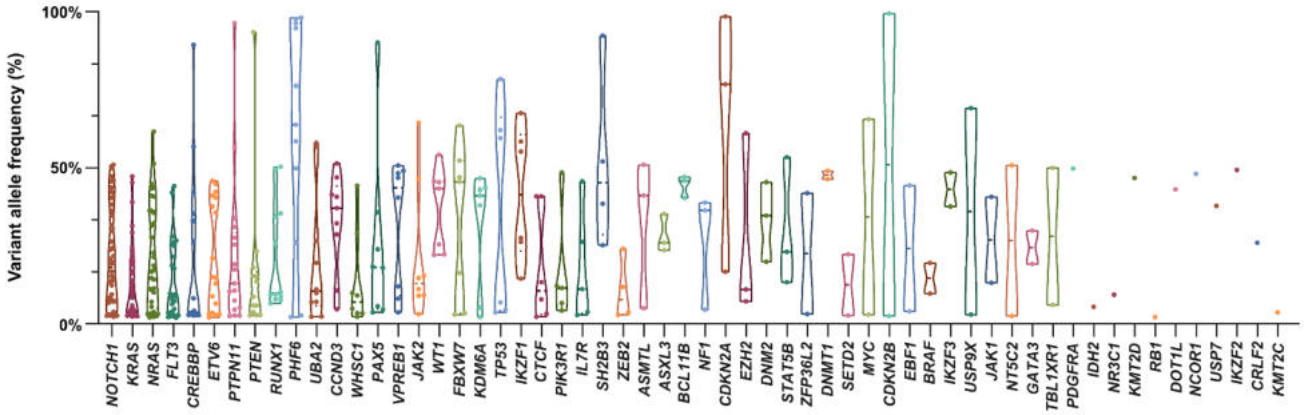

Figure 4. Distribution of mutation number across subtypes, and variant allele frequencies by genes (62)**. A** Number of mutations identified per patient at the time of diagnosis across different ALL subgroups. In T-ALL, higher mutation rate was observed compared to B-ALL subtypes. **B** Distribution of variant allele frequencies in the 58 mutated genes analyzed by targeted DNA-seq.

Figure 5.A

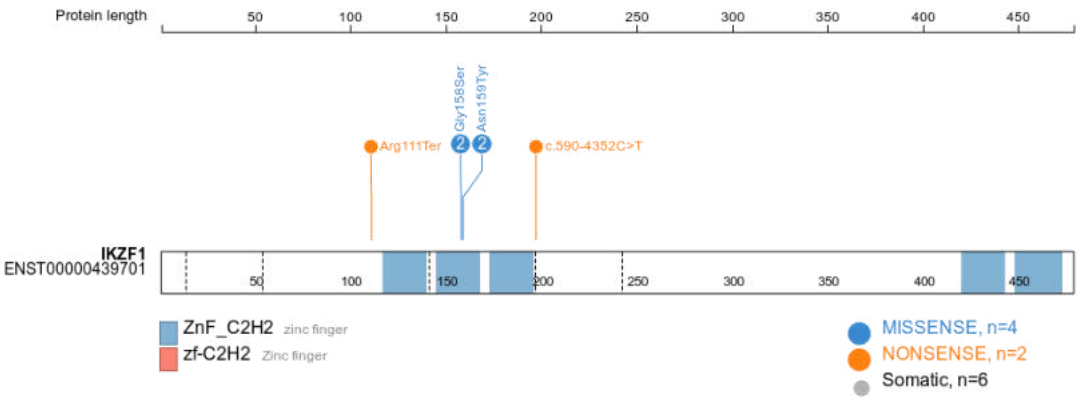

Figure 5.B

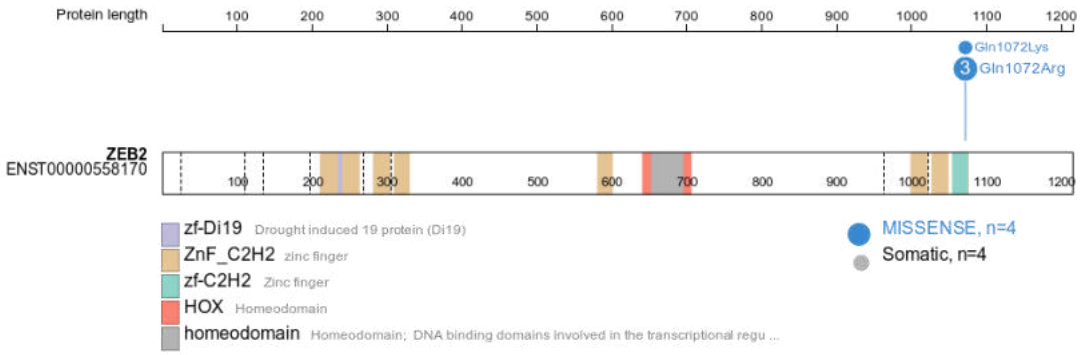

Figure 5.C

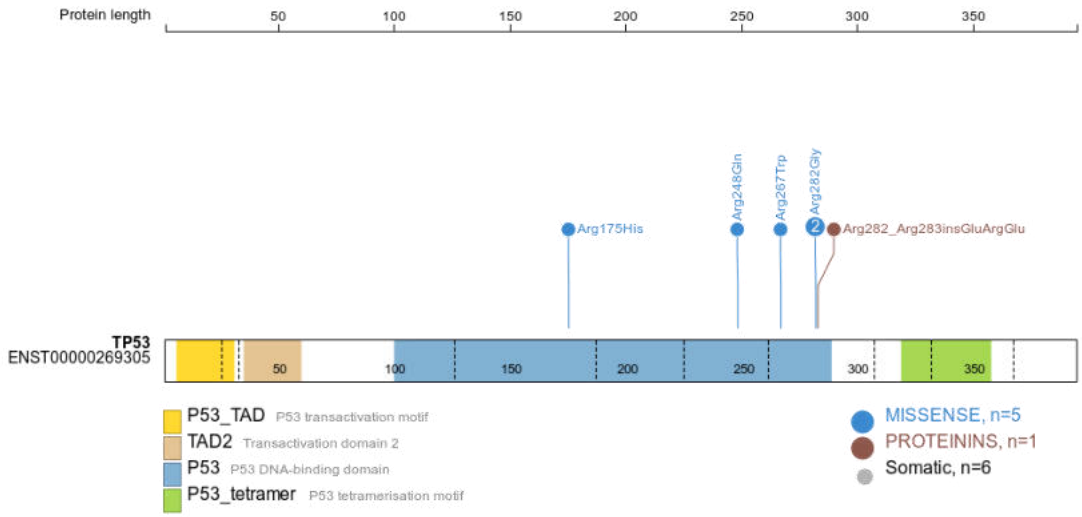

Figure 5. Short somatic variants in the *IKZF1* (A), *ZEB2* (B) and *TP53* (C) genes, identified by deep sequencing (62).

MLPA revealed copy number alterations in 55.5% (81/146) of B-ALL and 66.7% (20/30) of T-ALL patients. In B-ALL, *CDKN2B* (20.5%; 30/146), *CDKN2A* (19.9%; 29/146), *PAX5* (16.4%; 24/146) and *ETV6* (16.4%; 24/146) genes were most frequently affected by deletions (Figure 6.A). *IKZF1* deletion was present in 15.8% (23/146) of B-ALL patients, while seven of them displayed the *IKZF1*^{plus} (4.8%, 7/146) genotype. Most commonly identified alterations in T-ALL involved *CDKN2A* (56.7%; 17/30), *CDKN2B* (53.3%; 16/30) and *MTAP* (30.0%; 9/30) deletions, indicating the prevalent deletion of the 9p21 region in this subset of patients (Figure 6.B).

In 30 patients (24 B-ALL, 6 T-ALL), digitalMLPA unveiled CNAs in areas not covered by MLPA probemixes. This more comprehensive method identified CNAs in 95.6% (86/90) of B-ALL and 91.7% (22/24) of T-ALL patients. On average, 12.6 CNAs were identified per patient (mean subchromosomal alteration: 10.6, mean whole chromosome gain/loss: 2.0). Patients with hyperdiploid karyotype accounted for the majority (79.8%) of whole chromosome gains, with the most prevalent alterations being the gain of 14, 21, X, 6, 17, and 18 chromosomes. The modal chromosome number of twenty-two patients with a high hyperdiploid karyotype ranged from 51 to 58. One patient (PEDXALL113) exhibited near-triploid karyotype with 70 chromosomes. The most common subchromosomal aberrations in B-ALL patients were (37.8%; 34/90), *VPREB1* (25.6%; 23/90), *CDKN2A* (23.3%; 21/90), and *CDKN2B* (22.2%; 20/90), whereas *CDKN2A* (66.7%; 16/24), *CDKN2B* (62.5%; 15/24), *MTAP* (62.5%; 15/24) and *MLLT3* (29.2%; 7/24) were altered the most often in T-ALL patients. Biallelic losses primarily affected *CDKN2A* (31/121; 16 B-ALL, 15 T-ALL), *CDKN2B* (25/121; 12 B-ALL, 13 T-ALL) and *MTAP* (19/121; 7 B-ALL, 12 T-ALL) genes. Furthermore, subclonal alterations were uncovered in 42.1% (48/114) of the samples.

Figure 6. A Copy number aberrations detected by MLPA in diagnostic samples of 81/146 patients with B-ALL. **B** Copy number alterations detected in 20 samples of 30 T-ALL and 6 T-LBL patients, analyzed (62).

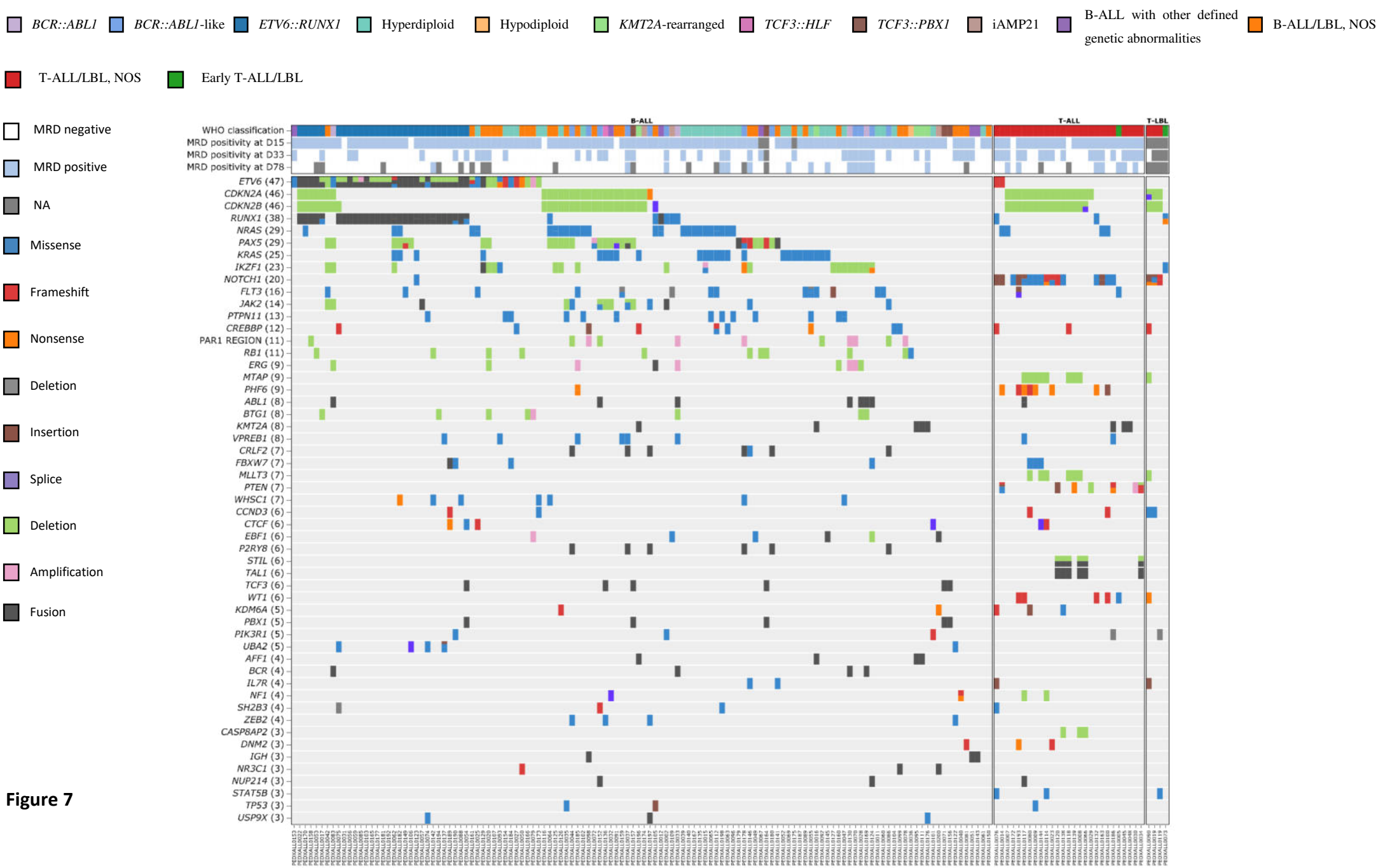
BCR::ABL1
BCR::ABL1-like
ETV6::RUNX1
Hyperdiploid
Hypodiploid
KMT2A-rearranged
TCF3::HLF
TCF3::PBX1
iAMP21
B-ALL with other defined genetic abnormalities
B-ALL/LBL, NOS
T-ALL/LBL, NOS
Early T-ALL/LBL
MRD negative
MRD positive
NA
Missense
Frameshift
Nonsense
Deletion
Insertion
Splice
Deletion
Amplification
Fusion
B-ALL
T-ALL
T-LBL
WHO classification
MRD positivity at D15
MRD positivity at D33
MRD positivity at D78
ETV6 (47)
CDKN2A (46)
CDKN2B (46)
RUNX1 (38)
NRAS (29)
PAX5 (29)
KRAS (25)
IKZF1 (23)
NOTCH1 (20)
FLT3 (16)
JAK2 (14)
PTPN11 (13)
CREBBP (12)
PAR1 REGION (11)
RB1 (11)
ERG (9)
MTAP (9)
PHF6 (9)
ABL1 (8)
BTG1 (8)
KMT2A (8)
VPREB1 (8)
CRLF2 (7)
FBXW7 (7)
MLLT3 (7)
PTEN (7)
WHSC1 (7)
CCND3 (6)
CTCF (6)
EBF1 (6)
P2RY8 (6)
STIL (6)
TAL1 (6)
TCF3 (6)
WT1 (6)
KDM6A (5)
PBX1 (5)
PIK3R1 (5)
UBA2 (5)
AFF1 (4)
BCR (4)
IL7R (4)
NF1 (4)
SH2B3 (4)
ZEB2 (4)
CASP8AP2 (3)
DNM2 (3)
IGH (3)
NR3C1 (3)
NUP214 (3)
STAT5B (3)
TP53 (3)
USP9X (3)

Figure 7

Figure 7. Short somatic variations, copy number aberrations, and gene fusions identified in diagnostic samples of 165 pediatric ALL/LBL patients by deep targeted DNA sequencing, RNA sequencing, and MLPA. Immunophenotype, WHO classification, and MRD status on days 15, 33, and 78 of therapy, as well as mutation types are also listed. Genes altered in at least 3 patients are depicted (62).

Targeted RNA sequencing revealed gene fusions in 34.9% (59/169) of B-ALL and 46.4% (13/28) of T-ALL patients. The most common changes found were *ETV6::RUNX1*, *STIL::TAL1*, *P2RY8::CRLF2,* and *TCF3::PBX1*. Less common chimeric genes with established clinical significance were also identified. Rearrangements involving *ABL1, ABL2, CRLF2, EPOR* and *JAK2* genes with a variety of different partner genes, indicated *BCR::ABL1*-like phenotype in 7.7% (13/169) of B-ALL patients. Additionally, rare fusions including *DUX4* (*DUX4::IGH,* n=2)*, MEF2D* (*MEF2D::BCL9*, n=1)*, NUTM1* (*ACIN1::NUTM1*, n=1) and *ZNF384* (*EP300::ZNF384*, n=1) genes were also discovered. Moreover, targeted RNAseq enabled the swift and specific identification of *KMT2A* fusion partners, such as *AFF1*, *AFDN, USP2* and *MLLT1,* which were previously either not detected by FISH or required labor-intensive karyotyping or multiple target-specific PCR tests for clinical diagnostics, prolonging the diagnostic process. Novel, formerly not reported fusions, affecting *JAK2* (*KDM4C::JAK2*), *KMT2A* (*KMT2A::KNSTRN*), *PAX5* (*PAX5::MLLT10*), *RUNX1* (*RUNX1::DNAJC15*, *RUNX1::SOX5::AS1*) and *NOTCH1* (*NOTCH1::IKZF2*) genes were also observed. Each gene affected by mutations, deletions, amplifications or gene fusions in at least three patients, is depicted in Figure 7.

4.3 Co-segregation of molecular alterations

Examining the relationship between distinct genetic alterations showed frequent co-occurrence or mutual exclusivity of several abnormalities. Altogether, 51 associations were revealed in the whole patient cohort. Frequent co-occurrence of *KRAS* mutations with *NRAS, BRAF, FLT3* and *CREBBP* mutations were observed in B-ALL (Figure 8.A), while in T-ALL the association of *STAT5B* mutations with *JAK1* mutations, or *NOTCH1* mutations with *PHF6* mutations were uncovered (Figure 8.B). These findings suggest that recurrent clonal selection mechanisms commonly converge on the same or interconnected pathways in individual patients. The frequency of RAS pathway mutations

(67.5%), such as *NRAS, KRAS, PTPN11,* and *FLT3* mutations were prominent in patients with hyperdiploidy. On the other hand, patients in this subgroup almost never harbored *CDKN2A/B, PAX5, ETV6, BTG1* and *RB1* deletions. *UBA2* mutations (85.7%) and *ETV6* deletion (66.7%) occurred primarily in the *ETV6::RUNX1* subgroup. All except for one patient with *BCR::ABL1* fusion carried *IKZF1* deletion, while in *BCR::ABL1*-like patients, *IKZF1, EBF1*, *PAX5* and PAR1 deletions, as well as *JAK2* and *ZEB2* mutations were enriched. In T-ALL, *CASP8AP2* deletion was only observed in the presence of *STIL::TAL1* fusion. In addition to the numerous concurrent deletion of genes located in chromosome region 9p21, several positive associations between *NOTCH1*, *PHF6*, *WT1*, *FBXW7, MLLT3* and *MTAP* alterations were present. Simultaneous or mutually exclusive presence of genetic events uncovered in B-ALL (Figure 8.A), or in T-ALL patients (Figure 8.B) is presented in Figure 8.

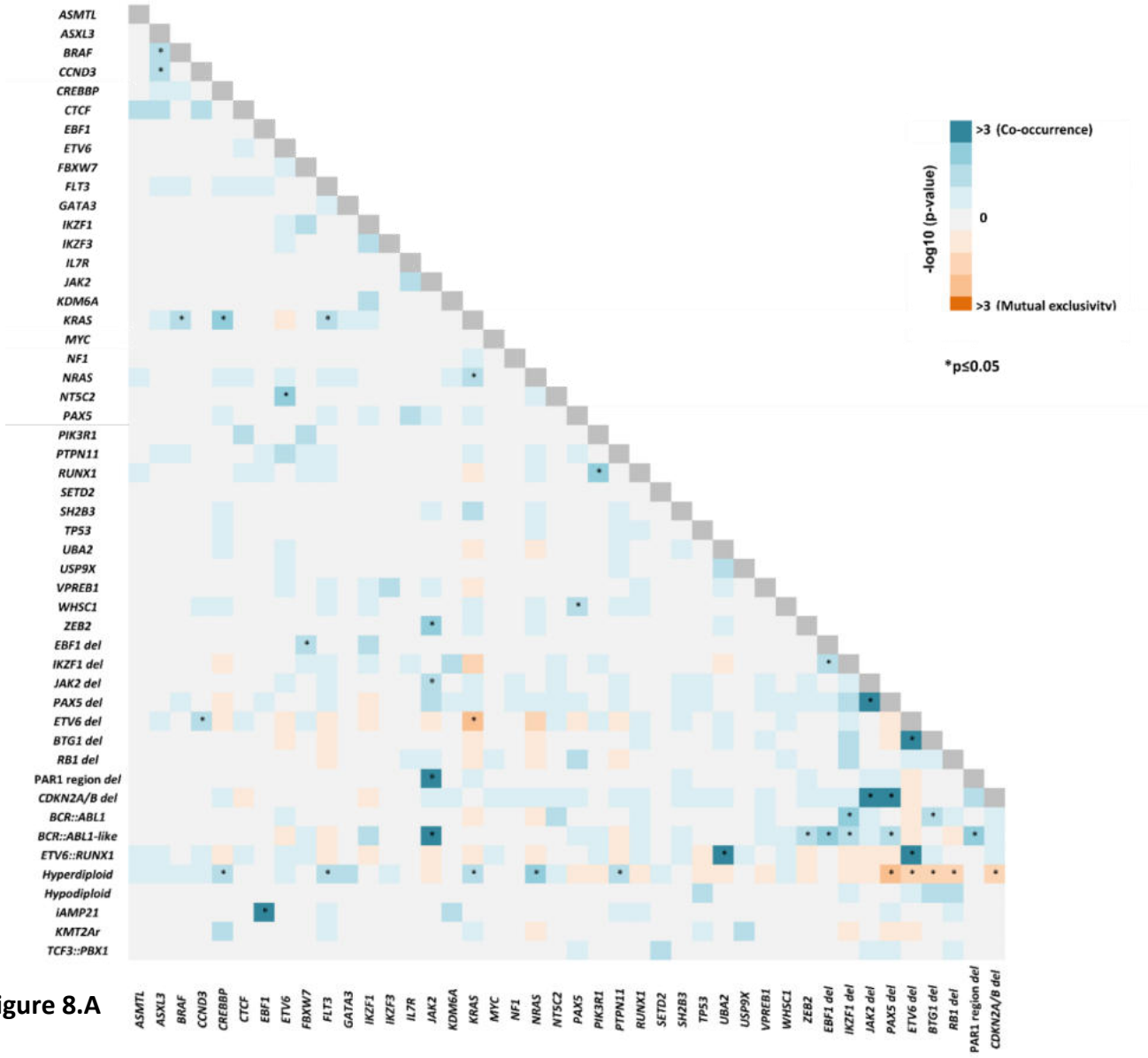

Figure 8.A

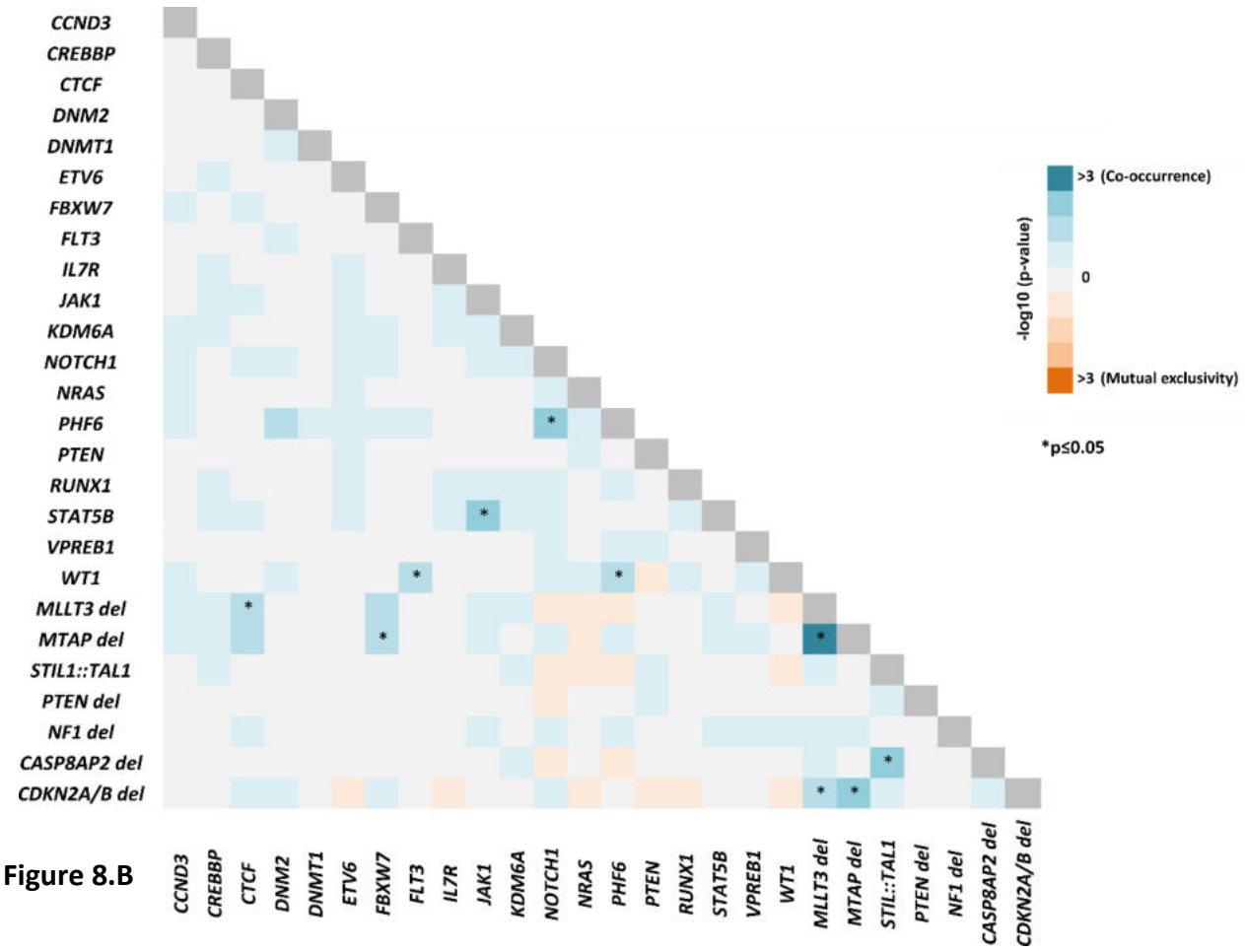

Figure 8. A Co-occurrence and mutual exclusivity of short somatic mutations and subchromosomal copy number aberrations in diagnostic samples of patients with B-ALL. **B** Co-occurrence and mutual exclusivity of short somatic mutations and subchromosomal copy number aberrations in B-ALL (62).

4.4 Genetic aberrations at relapse

Comprehensive molecular profiling was performed on paired samples of 19 patients (B-ALL: n=15, T-ALL: n=4), taken at the time of diagnosis and relapse. The duration between diagnosis and the first relapse ranged from 5 to 109 months, with an average of 31 months (Figure 9.A). Seventeen samples underwent targeted DNA and RNA sequencing combined with MLPA; while in the remaining cases, RNA-seq or MLPA analysis was impeded by sample quantity or quality. The average number of detected mutations was 2.4 (range: 0-5) in relapse samples, moderately surpassing the value observed in diagnostic samples (average: 2.0, range: 0-7). Twenty-seven percent (17/64)

of the somatic mutations detected at the time of diagnosis were absent from the relapse samples, 33% (21/64) persisted at the time of relapse, and 41% (26/64) emerged during the progression of the disease. *NT5C2* and *CDKN2A* mutations were solely identified, and the incidence of *TP53* and *CREBBP* mutations was increased in relapse samples. *TP53* and *CREBBP* exhibited the highest prevalence of alterations at relapse, both affecting 21% (4/19) of the patients (Figure 9.B). Somatic variants and copy number aberrations observed in the 19 relapsed patients at each time point analyzed, are presented in Figure 9.C. Higher variant allele frequencies at the time of relapse (VAF: 59% vs 74% and 4% vs 63%) indicated that both *TP53* mutant clones, which were present in two instances at the time of diagnosis, acquired selective survival advantage (Figure 9.D). Two patients developed *TP53* mutant clones during relapse, with one patient (PEDXALL0162) at the time of the second relapse, seven years after the initial diagnosis. In most of the cases (13/19), at least one mutation prevailed from diagnosis to relapse, the treatment eradicated additional variants in nine patients (9/19), and novel alterations arose at relapse in 8/19 patients (Figure 9.D). Four patients (PEDXALL0012, PEDXALL045, PEDXALL115, PEDXALL0136) presented with an entirely distinct mutational profile at the time of relapse. Further interrogation of the development of observed alterations over the course of the disease indicated perplexed clonal dynamics, with concurrently rising and declining subclones in two-thirds of the cases (Supplementary Figure S1, see: Appendix).

Figure 9.A

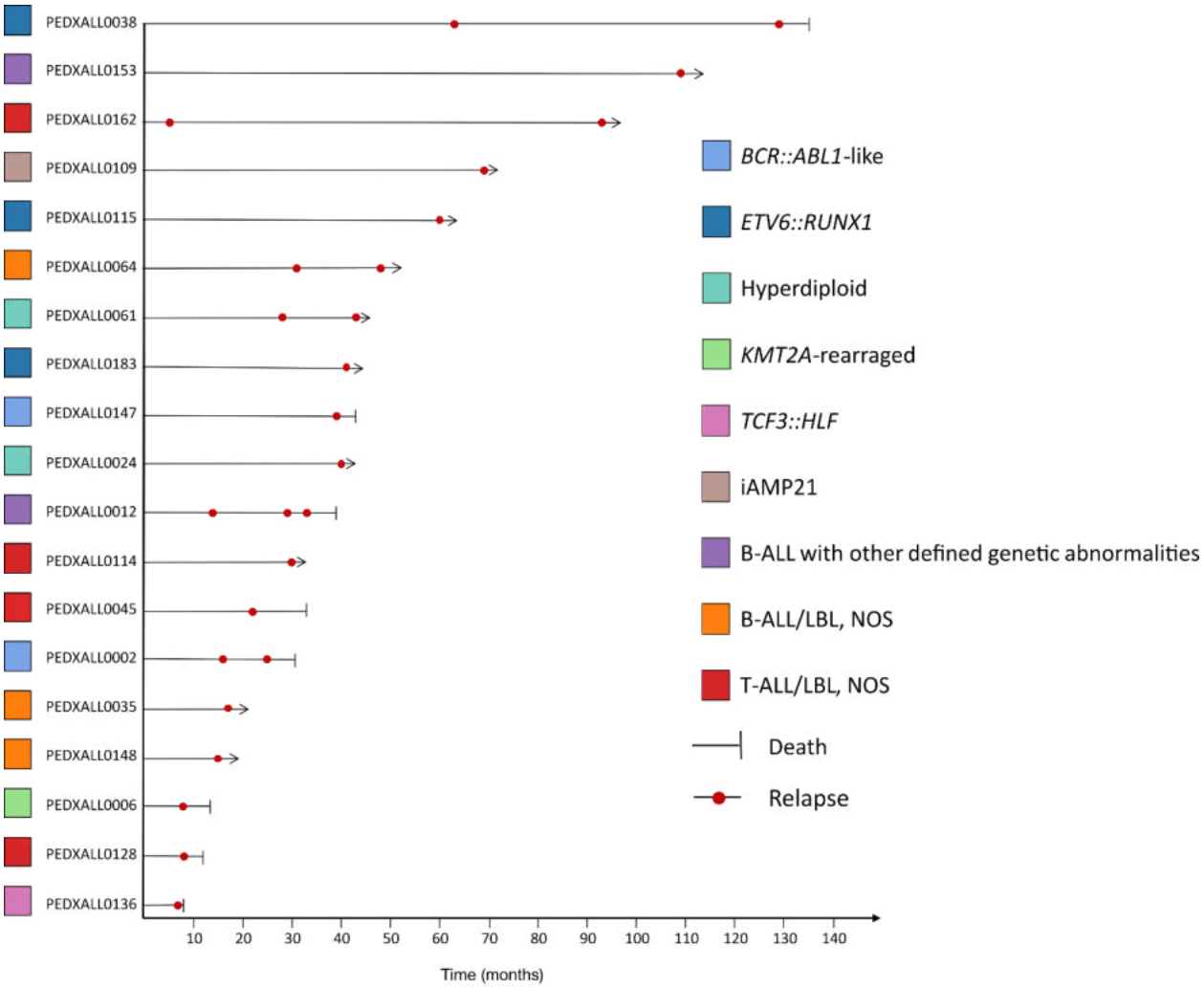
PEDXALL0038
PEDXALL0153
PEDXALL0162
PEDXALL0109
PEDXALL0115
PEDXALL0064
PEDXALL0061
PEDXALL0183
PEDXALL0147
PEDXALL0024
PEDXALL0012
PEDXALL0114
PEDXALL0045
PEDXALL0002
PEDXALL0035
PEDXALL0148
PEDXALL0006
PEDXALL0128
PEDXALL0136
10 20 30 40 50 60 70 80 90 100 110 120 130 140
Time (months)
BCR::ABL1-like
ETV6::RUNX1
Hyperdiploid
KMT2A-rearraged
TCF3::HLF
iAMP21
B-ALL with other defined genetic abnormalities
B-ALL/LBL, NOS
T-ALL/LBL, NOS
Death
Relapse

Figure 9.B

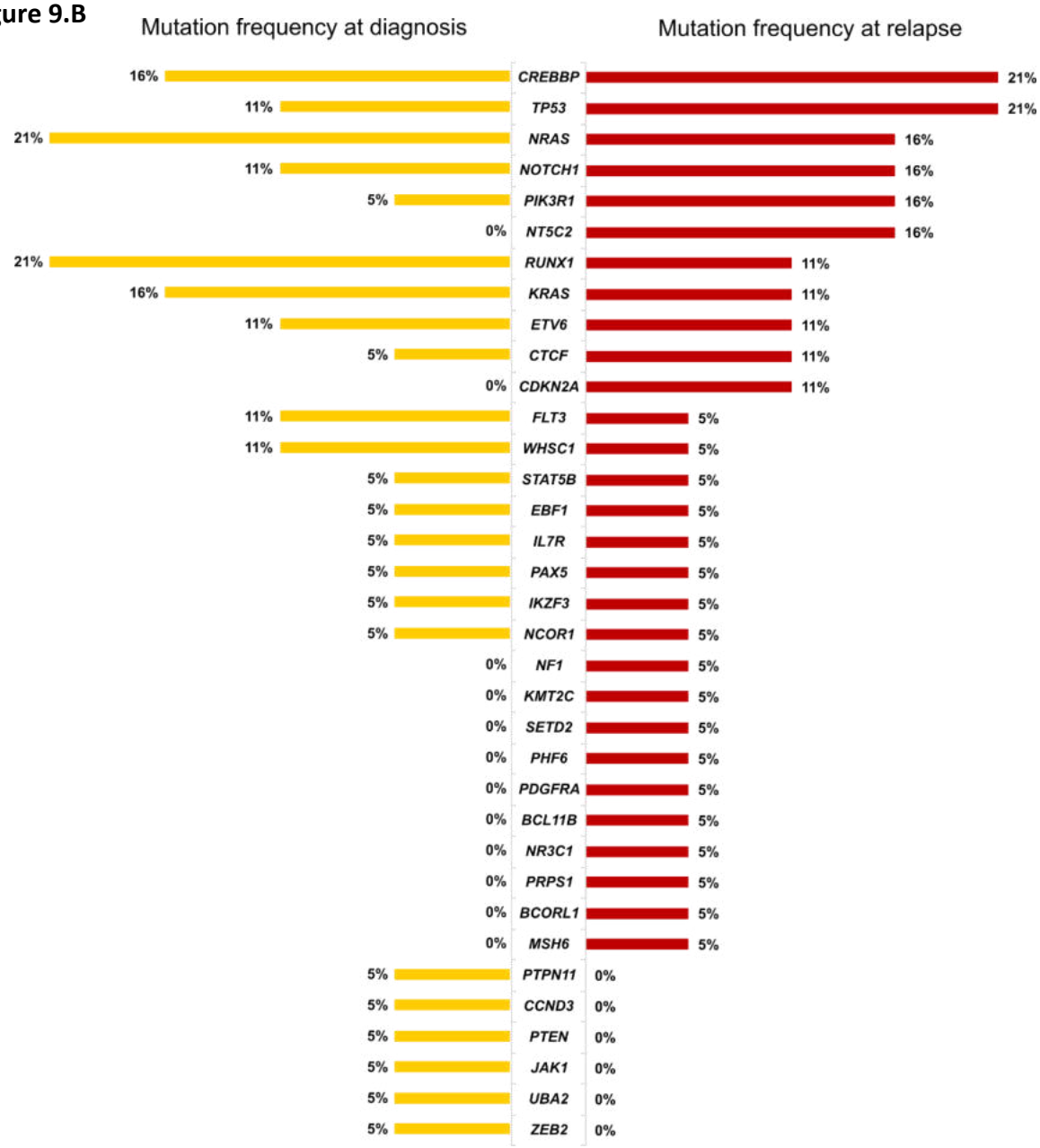
Mutation frequency at diagnosis
Mutation frequency at relapse
16% CREBBP 21%
11% TP53 21%
21% NRAS 16%
11% NOTCH1 16%
5% PIK3R1 16%
0% NT5C2 16%
21% RUNX1 11%
16% KRAS 11%
11% ETV6 11%
5% CTCF 11%
0% CDKN2A 11%
11% FLT3 5%
11% WHSC1 5%
5% STAT5B 5%
5% EBF1 5%
5% IL7R 5%
5% PAX5 5%
5% IKZF3 5%
5% NCOR1 5%
0% NF1 5%
0% KMT2C 5%
0% SETD2 5%
0% PHF6 5%
0% PDGFRA 5%
0% BCL11B 5%
0% NR3C1 5%
0% PRPS1 5%
0% BCORL1 5%
0% MSH6 5%
5% PTPN11 0%
5% CCND3 0%
5% PTEN 0%
5% JAK1 0%
5% UBA2 0%
5% ZEB2 0%

Figure 9.C

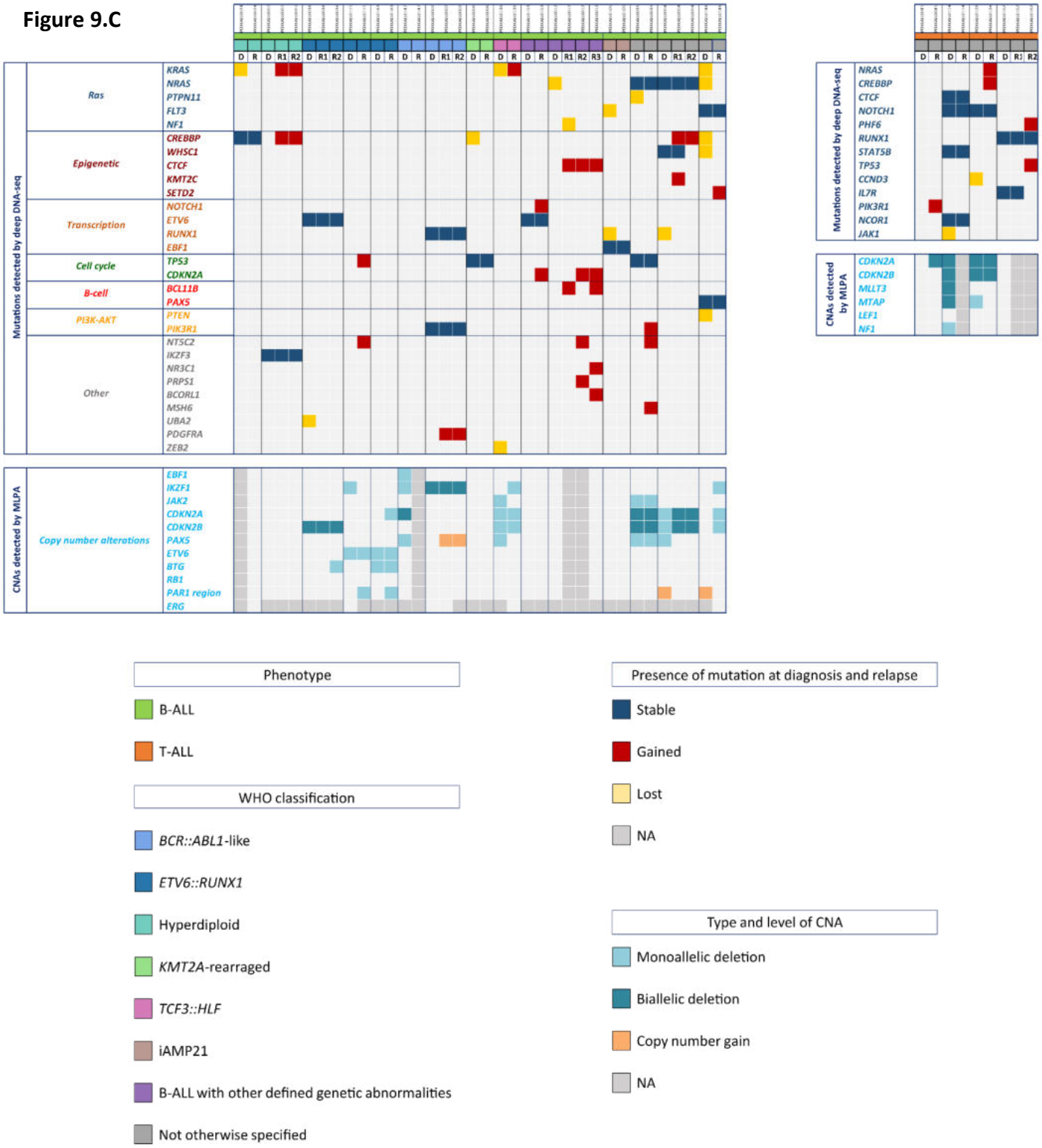

Phenotype

- B-ALL
- T-ALL

WHO classification

- *BCR::ABL1*-like
- *ETV6::RUNX1*
- Hyperdiploid
- *KMT2A*-rearraged
- *TCF3::HLF*
- iAMP21
- B-ALL with other defined genetic abnormalities
- Not otherwise specified

Presence of mutation at diagnosis and relapse

- Stable
- Gained
- Lost
- NA

Type and level of CNA

- Monoallelic deletion
- Biallelic deletion
- Copy number gain
- NA

Figure 9.D

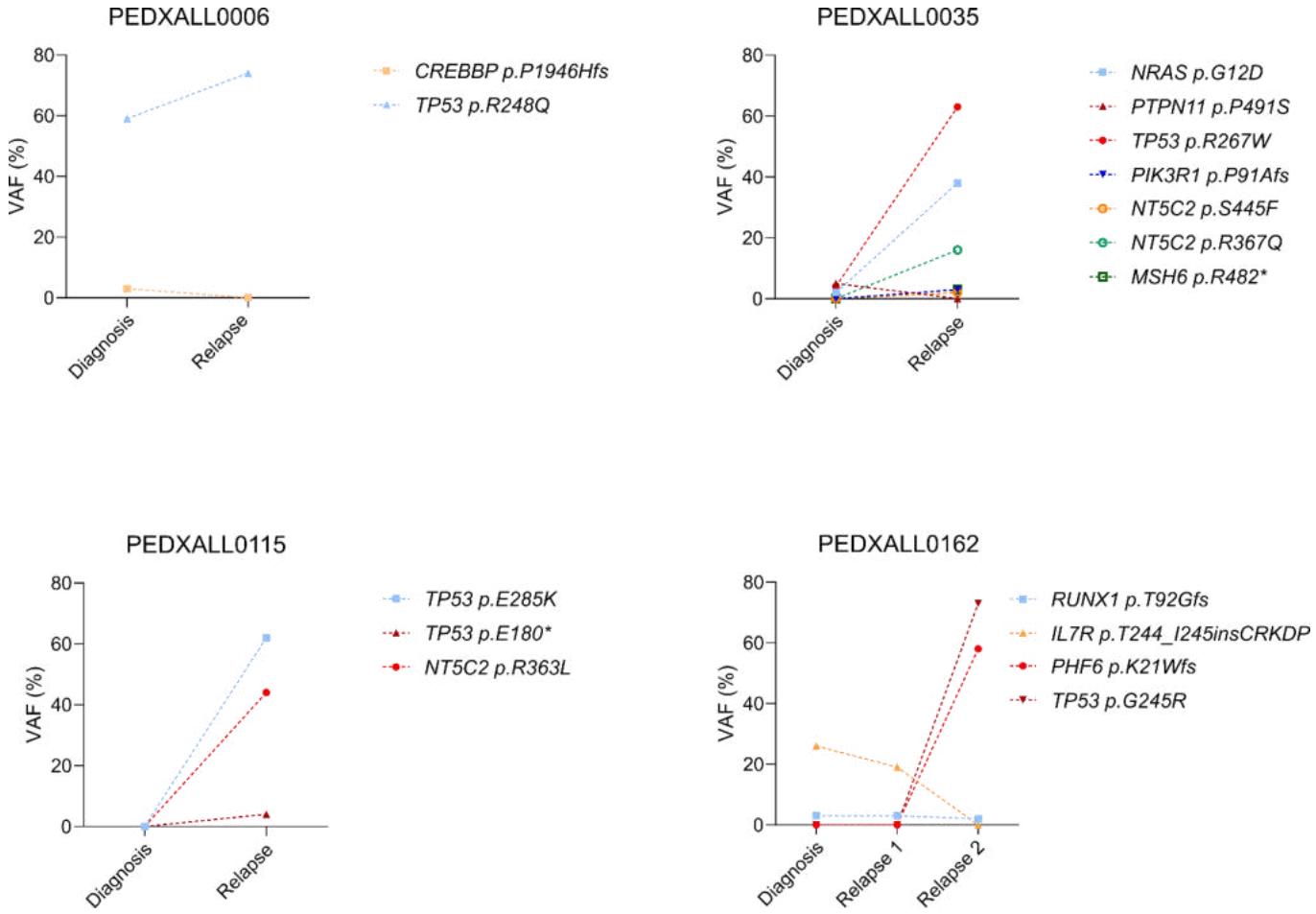

Figure 9. Comprehensive molecular profiling of diagnosis-relapse pairs (62)**. A** Timeline and WHO category of 19 relapsed patients. Red circles indicate the time of relapse. **B** Comparison of the mutation frequency in 35 altered genes between diagnostic and relapse samples. **C** Oncoplot displaying short somatic variants and copy number aberrations in 19 patients at the time of diagnosis and relapse. Distinctive colors are used for representing stable mutations (dark blue), which are present both at diagnosis and relapse, and unstable mutations, which are only present either at diagnosis (yellow) or at relapse (red). **D** Clonal dynamics and composition of mutations over the disease course in four selected patients harboring *TP53* mutation. (VAF: variant allele frequency).

4.5 Genetic alterations associated with therapeutic response and prognosis

Scrutinizing genetic aberrations in relation to MRD positivity evaluated by FCM, we found a strong positive association between *IKZF1* deletion and MRD positivity at days 33 and 78 of treatment (p=0.021 and p<0.001, respectively). Day 33 and day 78 MRD positivity was also more prevalent in *BCR::ABL1*-like subtype (p=0.014 and p=0.005, respectively). Conversely, all but one patients with *CCND3* mutation presented with MRD negative FCM results on days 33 and 78.

Patients with *KMT2A* rearrangement exhibited the most adverse prognosis across all B-ALL subtypes (3-year EFS, presence vs absence of *KMT2A* rearrangement; p=0.019). In addition, survival analysis of B-ALL patients indicated substantially shorter 3-year EFS in the presence of *TP53* mutation (mutant vs wild-type EFS; p=0.008; Figure 10.A) or *CREBBP* mutations (mutant vs wild-type EFS; p=0.010; Figure 10.B). On the other hand, there was no correlation between EFS or OS and the presence of other common alterations, including RAS pathway mutations, regardless of their clonal or subclonal nature. Interestingly, additional subgroup analyses revealed the negative prognostic impact of *TP53* mutations, even in patients with favorable clinical response to treatment. Patients with mutation and MRD negative FCM results on day 33 still showed unfavorable outcome (mutant vs wild-type EFS; p=0.0004; Figure 10.C).

Owing to the small number of *TP53* and *CREBBP* mutant cases in the original cohort, we used a combined dataset of 411 patients – including 265 patients from the TARGET ALL Phase 2 study – to conduct a second focused analysis of 3-year EFS on an expanded cohort. Survival analysis confirmed the poor prognosis of *TP53* and *CREBBP* mutant B-ALL patients in this larger cohort, in accordance with our previous findings (3-year EFS; *TP53* mutant vs wild-type: p=0.0009, Figure 10.D; *CREBBP* mutant vs wild-type p=0.013, Figure 10.E). Additionally, B-ALL patients displaying MRD negativity at the end of induction showed inferior survival in the presence of *TP53* mutation in the expanded dataset (3-year EFS, TP53 mutant vs wild-type; p=0.009; Figure 10.F).

Figure 10.A

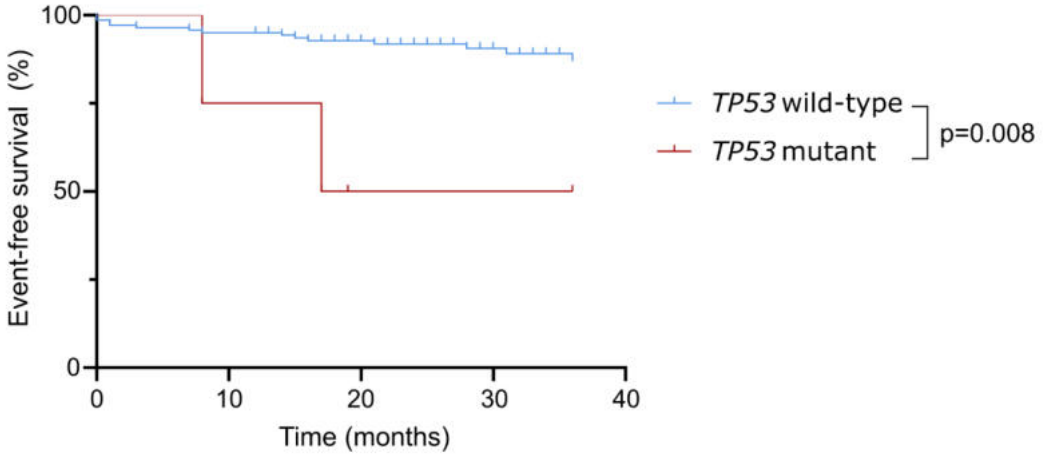

Figure 10.B

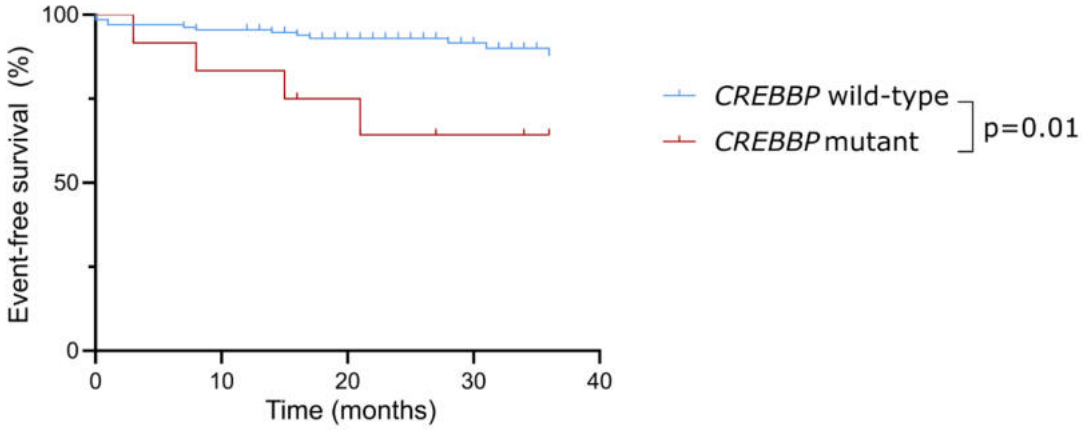

Figure 10.C

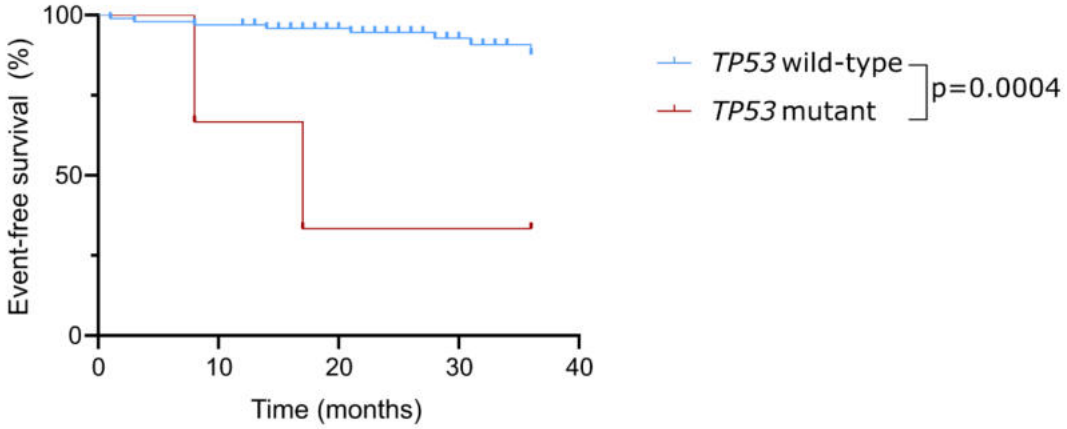

Figure 10.D

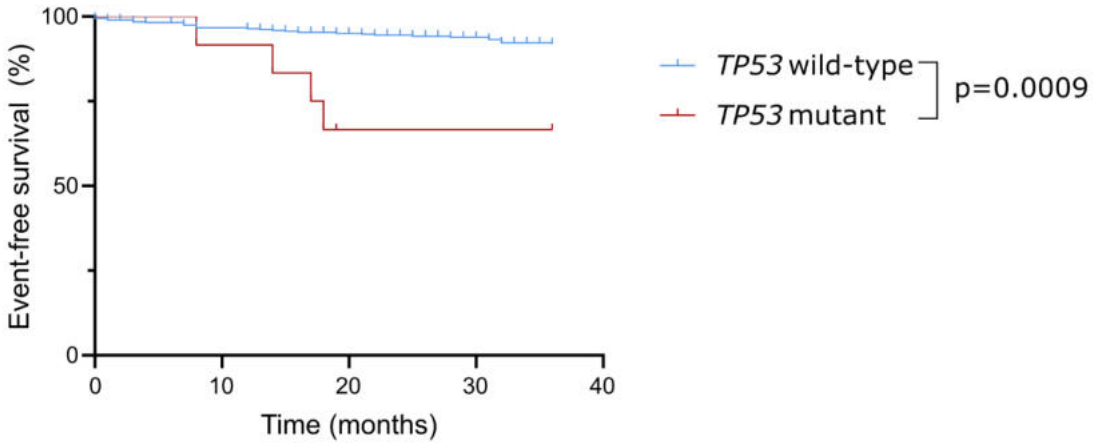

Figure 10.E

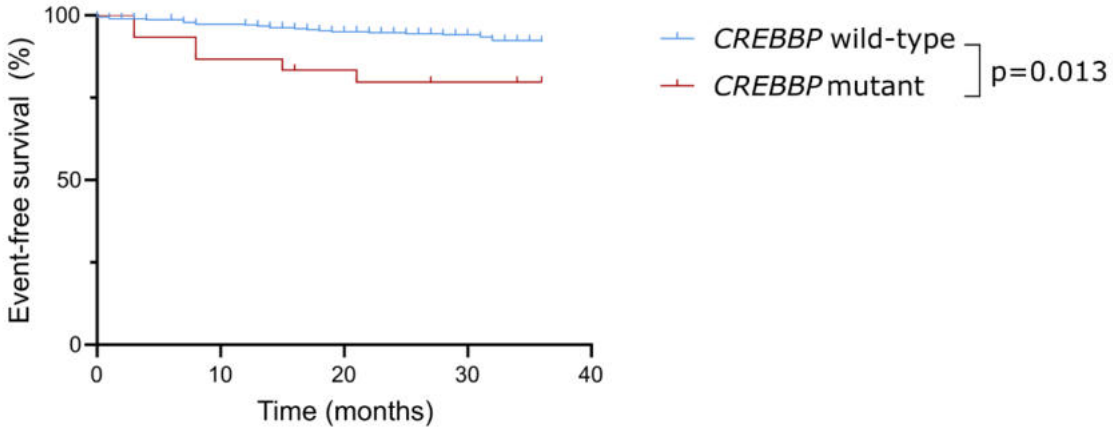

Figure 10.F

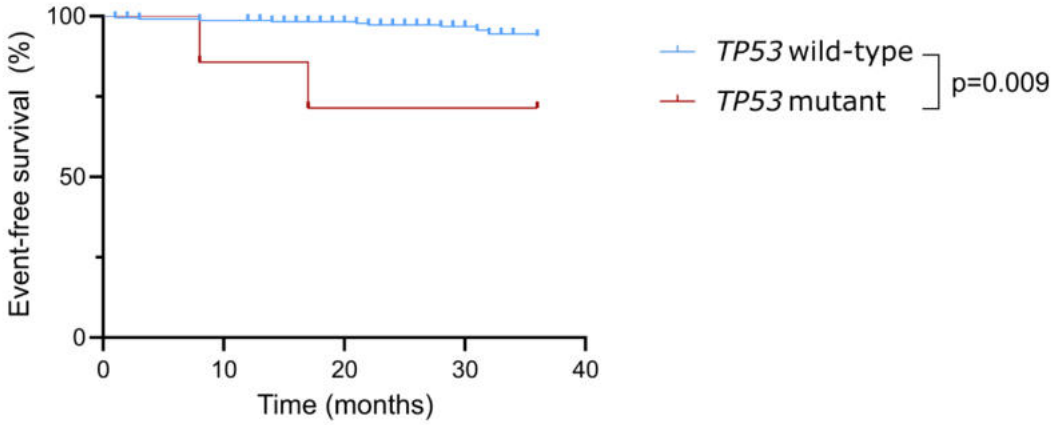

Figure 10. Event-free survival of our in-house cohort, and validation cohort, in the presence or absence of *TP53* or *CREBBP* mutation (62)**. A** Three-year event-free survival of B-ALL patients subclassified based on *TP53* mutation status. **B** Three-year event-free survival of B-ALL patients categorized based on *CREBBP* mutation status. **C** Three-year event-free survival of B-ALL patients MRD negative on day 33 and categorized based on *TP53* mutation status. **D** Three-year event-free survival of B-ALL patients with or without *TP53* mutation in the expanded cohort, including 265 patients from the TARGET ALL Phase 2 study. **E** Three-year event-free survival of B-ALL patients divided based *CREBBP* mutation status in the expanded cohort. **F** Three-year event-free survival of B-ALL patients showing MRD negativity at the end of induction and subclassified based on *TP53* mutation status in the expanded cohort. *TP53* mutations associated with dismal outcome, even in case of MRD negativity on day 33.

Further interrogation of the subset of patients with very early or early events (EFS<24 months) uncovered that 7 out of 13 B-ALL patients were stratified to the intermediate risk (IR) arm of the ALL IC-BFM 2009 protocol and treated accordingly. Four out of these seven IR patients carried either *TP53* (n=2) or *CREBBP* (n=3) mutation. Notably, in our in-house cohort, three of the five mutations presented subclonally with a VAF of 3-5%, which range is often precarious in terms of interpretation using conventional sequencing coverage instead of deep sequencing. Mutations with a VAF ≥10%, and fusions involving putatively targetable genes, including *NRAS, KRAS, PTPN11, NF1, FLT3, JAK2, IL7R, SH2B3, CRLF2, EPOR, ABL1, ABL2, KMT2A* and *NUP98* were identified in 55.9% (33/59) of ALL IC-BFM 2009 high-risk patients, and 31.6% (36/114) of standard/intermediate-risk patients (Figure 11, Supplementary figure 2; See: Appendix). Furthermore, deep sequencing allowed us to confidently detect 39 mutations in targetable genes with a VAF≤10%, affecting a total of 11 individuals.

Figure 11

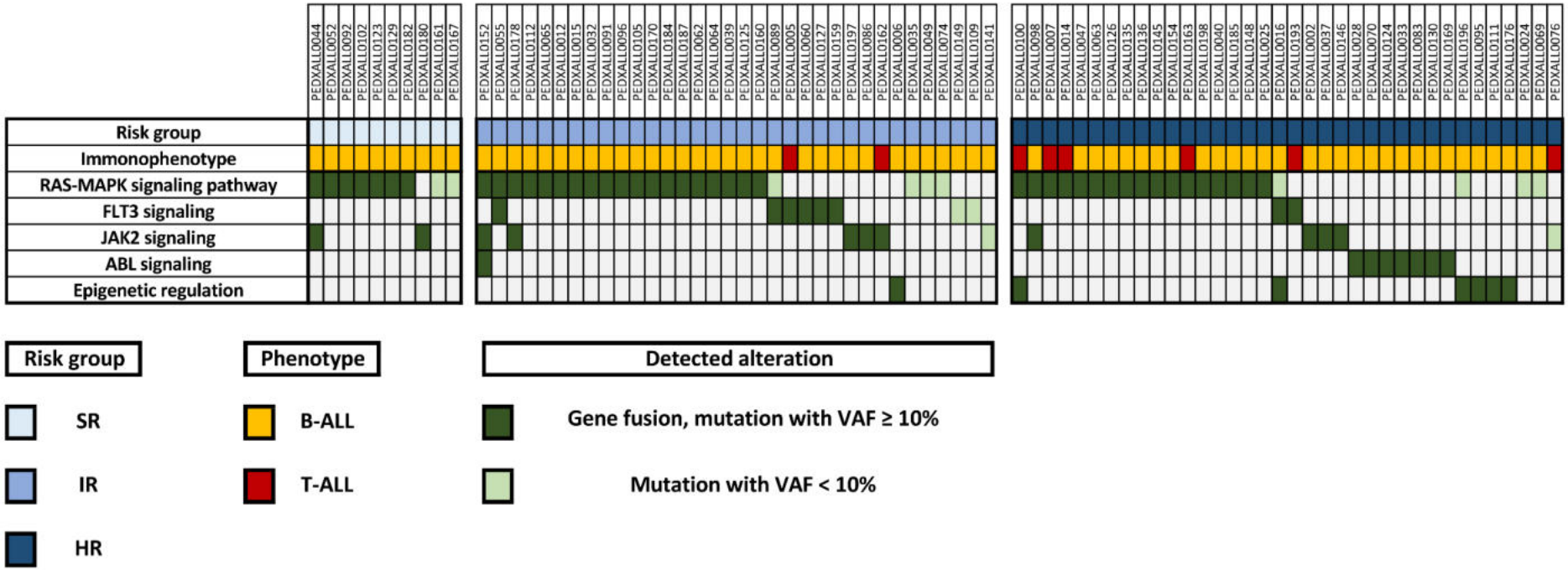
Risk group
Immonophenotype
RAS-MAPK signaling pathway
FLT3 signaling
JAK2 signaling
ABL signaling
Epigenetic regulation
Risk group
SR
IR
HR
Phenotype
B-ALL
T-ALL
Detected alteration
Gene fusion, mutation with VAF ≥ 10%
Mutation with VAF < 10%

Figure 11. Targetable signaling pathways affected by short somatic variants or gene fusions in B-ALL and T-ALL patients, treated according to ALL IC-BFM 2009 protocol. Risk group, immunophenotype, and pathways affected by mutations with VAF ≥10% or <10% are also illustrated with distinctive colors (62). SR: standard risk, IR: intermediate risk, HR: high risk, VAF: variant allele frequency

4.6 Reclassification of the level of CNS involvement based on the quantification of hsa-miR-181a-5p copy numbers

Most BFM treatment guidelines for childhood ALL suggest the classification of CNSL based on the white blood cell (WBC), blast cell and red blood cell counts in the initial CSF sample: CNS-1 refers to blast-free CSF with WBC≤5/µl, CNS-2 is used for cases with WBC≤5/µl and ≥2/µl unambiguous blast cells identified in CSF, while CNS-3 stands for WBC>5/µl with the majority of blasts. Instead of this conventional classification, we classified patients into newly established CNS-negative (CNSneg), CNS-ambivalent (CNSamb) and CNS-positive (CNSpos) groups. In this setting, CNSpos corresponded to CNS-3 status. The CNSneg group consisted of patients with CNS-1 status, restricted to patients clearly not containing blasts in the CSF based on classical cell-based methods. The CNSamb category included all patients classified as CNS-2 originally and those patients with CNS-1 status determined during the clinical care whose classification was uncertain due to inconclusive results of cytological methods, such as a negative cytospin along with unambiguous blast cells identified with insufficient sensitivity using FCM. All patients with traumatic lumbar puncture fulfilling the criterion that WBC/RBC ratio in the peripheral blood is at least two times higher than WBC/RBC ratio in the CSF were also included in the CNSamb group. Our classification aimed to address the clinical uncertainty originating from the inadequate sensitivity of existing cytological diagnostic methods.

This study examined the copy numbers of hsa-miR-181a-5p in 92 CSF samples collected at diagnosis or different follow-up time points. Based on previously outlined criteria, such as TLP or failure to meet quality requirements, 16 samples of 10 patients were excluded from further analysis. Normalized copy numbers of hsa-miR-181a-5p in samples obtained at the time of diagnosis from 28 patients were used for generating a hierarchical cluster dendrogram which yielded two primary branches (Figure 12.A). A

total of 13 patients were grouped in the left-hand branch, while 15 patients were grouped in the right-hand branch. Seven CNAamb samples and, notably, three CNSneg samples clustered together with all three CNSpos diagnostic samples. The samples in the left-hand branch were classified as 'miRsign', indicating 'significant' hsa-miR-181a-5p expression. The right-hand branch, consisting of 3 CNSamb and 12 CNSneg samples were labelled as 'miRmin', referring to minimal hsa-miR-181a-5p expression.

By integrating the miR-based CNSL classification with the routinely applied cellular methods, we reclassified the patients into three distinct groups indicative of initial CNS involvement: CNSneg or CNSamb samples on the right-hand branch (CNSmin & miRmin), CNSneg or CNSamb samples on the left branch (CNSmin & miRsign), and CNSpos samples (CNSpos & miRsign). The CNSneg and CNSamb samples were grouped together as the therapeutic consequence of CNS-2 category compared to CNS-1, with two additional intrathecal courses, is substantially less than the CNS-directed therapy escalation for the CNS-3 group. Composition of the novel, combined groups is summarized in Supplementary Table 2 (see: Appendix), the two-step reclassification process is depicted in Figure 12.B.

Figure 12.A

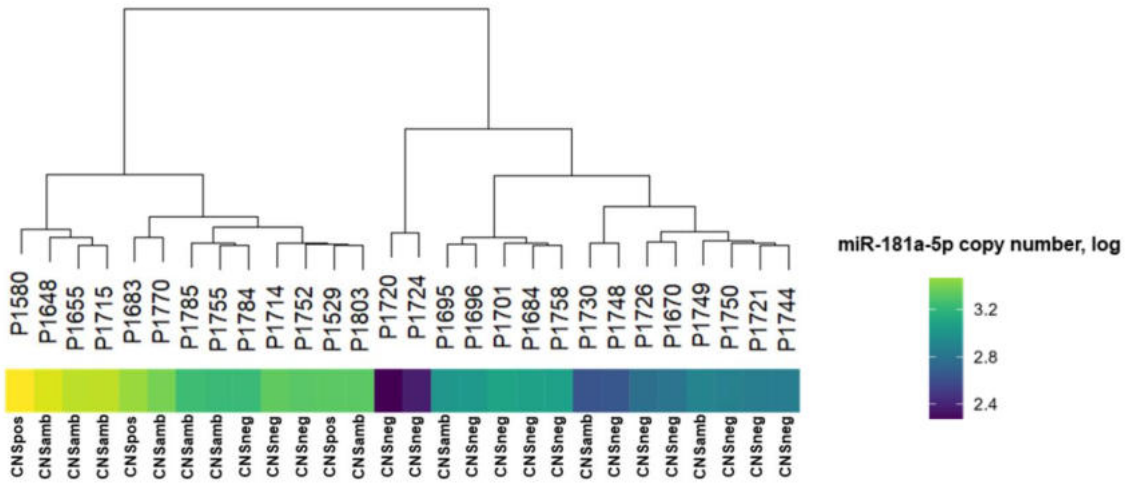

Figure 12.B

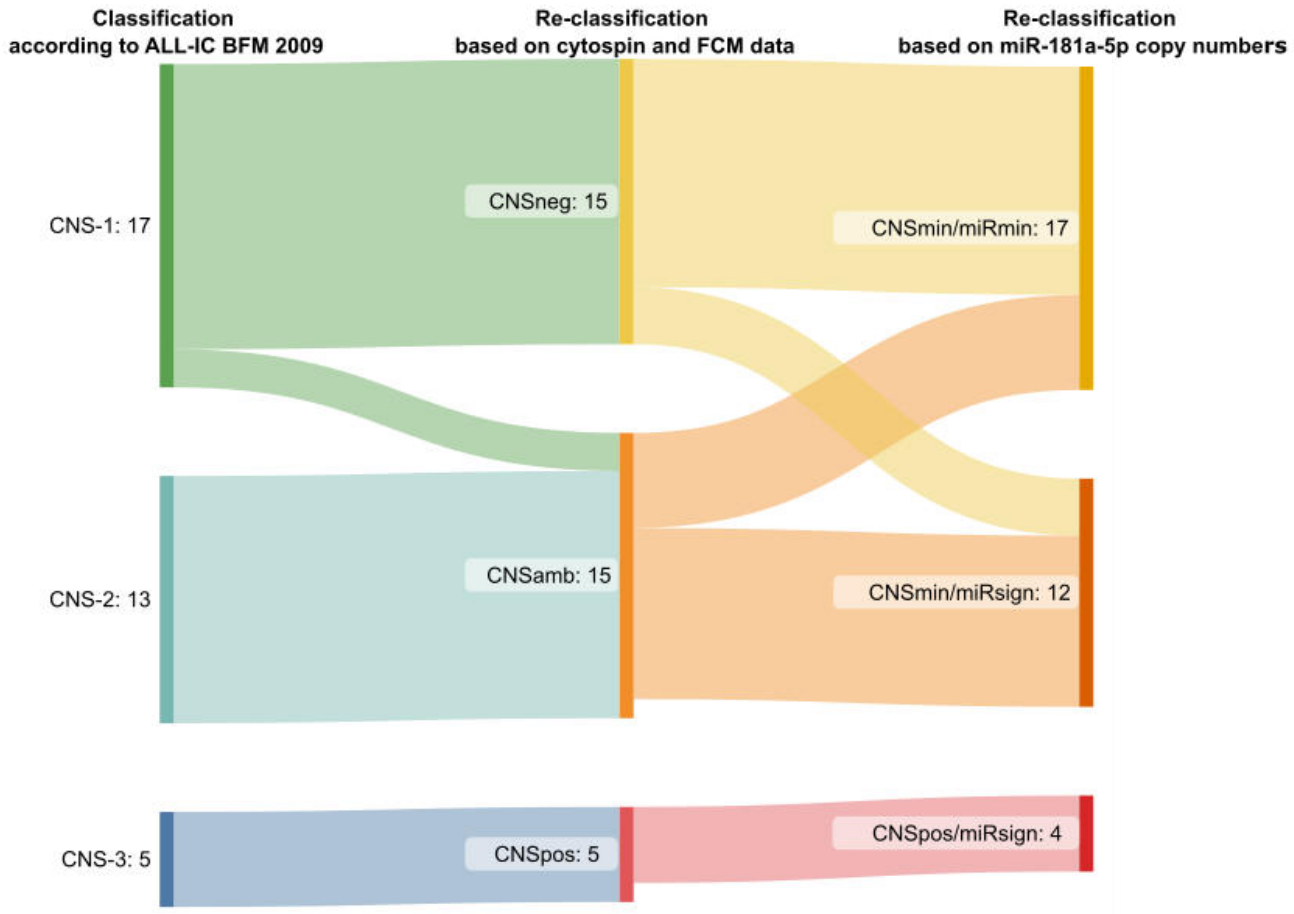

Figure 12. Classification applied in this study regarding CNS status (63)**. A** Dendogram, displaying the two main subgroups based on hsa-miR-181a-5p expression in the CSF, defined by hierarchical clustering. Each spike represents a patient. CNS status determined by cell-based methods is presented at the bottom. **B** Sankey diagram depicting the classification of patients according to current BFM guidelines applied in clinical setting (column on the left), newly established categories used in this study and reflecting the uncertainty of cell-based methods (column in the middle), and a proposed re-classification, implementing hsa-miR-181a-5p expression (column on the right)

4.7 Elevated hsa-miR-181a-5p copy numbers suggest latent CNSL and aid the classification of patients with ambiguous CNS status

Using linear regression, hsa-miR-181a-5p copy numbers of samples obtained at diagnosis were compared. Higher levels of hsa-miR-181a-5p were found in the CNSmin/miRsign

group and the CNSpos/miRsign group, as opposed to the CNSmin/miRmin group (mean copy number ± standard error (SE): 2503.50±275.89, 3300.70±809.69 and 744.02±86.81, respectively; p=1.13E-6 and p=2.16E-5 when comparing miRsign groups to CNSmin/miRmin group), as seen in Figure 13.A. Conversely, when the hsa-miR-181a-5p copy levels on days 15 and 33 were compared across the three groups, no discernible difference was found. The linear models revealed no statistically significant effect of the patients' gender or the leukemic blasts' immunophenotype. Analysing separately hsa-miR-181a-5p copy numbers at diagnosis in patients with ambiguous CNS status (CNSamb), we identified a higher mean copy number among CNSamb/miRsign compared to CNSamb/miRneg (mean copy number ± SE: 2729.06±362.87; 749.70±177.72; respectively; p=4.72E-3, Figure 13.B). Patients with FCM positivity (a minimum of 8 identified blast cells in the CSF) exhibited significantly elevated hsa-miR-181a-5p expression relative to those with negative CSF flow cytometry findings (p=0.016; Figure 13.C). However, there was no substantial difference in terms of hsa-miR-181a-5p copy number between cytospin-negative and positive cases (Figure 13.D). Various non-congruent trends were observed across the three novel CNS groups when analyzing the longitudinal dynamics of hsa-miR-181a-5p expression during the first 100 days of treatment, which impeded any conclusion about MRD and hsa-miR-181a-5p levels (Figure 14).

Figure 13.A

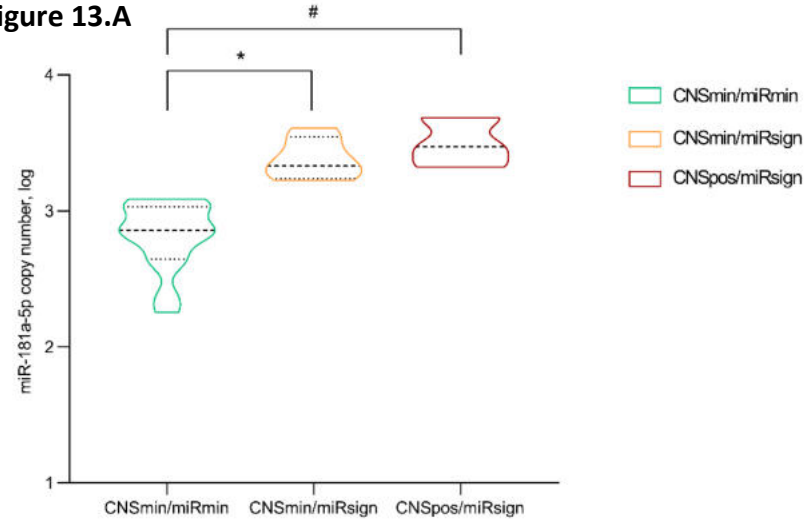

Figure 13.B

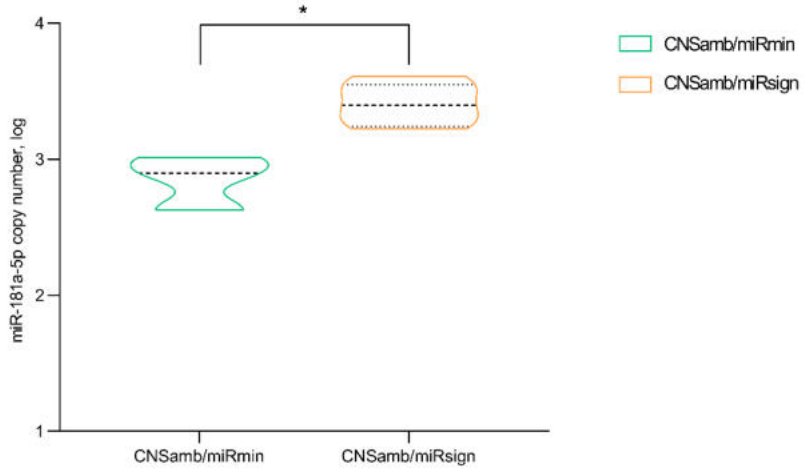

Figure 13.C

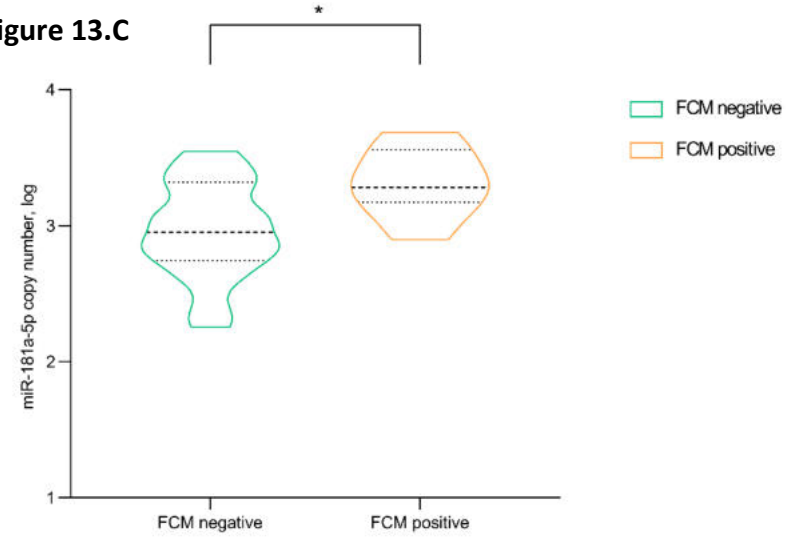

Figure 13.D

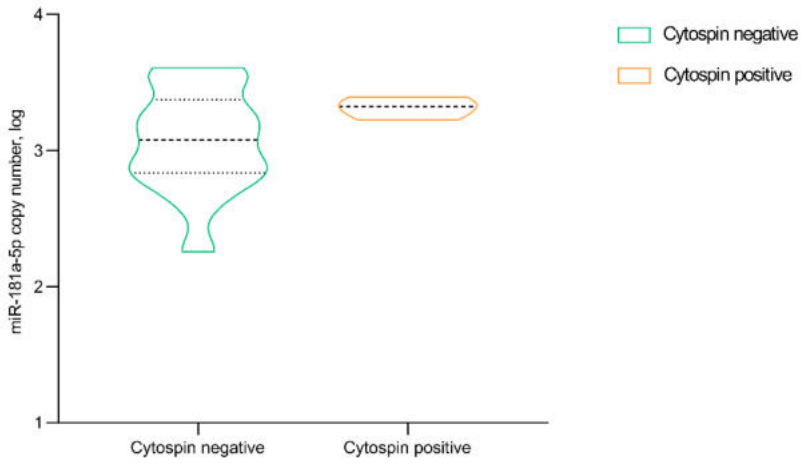

Figure 13. A Violin plot displaying the distribution of the logarithm of miR181-a-5p copy numbers of CSF samples collected at the time of diagnosis, measured by ddPCR. CNSmin/miRmin: green, CNSmin/miRsign: orange, CNSpos/miRsign: red; * p=1.13E-6; # p=2.16E-5 **B** Violin plot presenting the distribution of the logarithm of miR181-a-5p copy numbers in CSF samples collected at the time of the diagnosis, measured by ddPCR in CNSamb patients. CNSamb/miRmin: green, CNSamb/miRsign: orange; * p=0.0047. **C** Violin plot illustrating the distribution of the logarithm of miR181-a-5p copy numbers of CSF samples collected at the time of diagnosis in patients with either negative or positive CSF flow cytometry. FCM negative: green, FCM positive: orange; * p=0.016. **D** Violin plot showing the distribution of the logarithm of hsa-miR-181a-5p copy numbers in CSF samples collected at the time of diagnosis from patients with negative or positive cytospin findings. Cytospin negative: green, cytospin positive: orange. The contours in the figure show the distribution of data points. Dashed line represents the median, dotted lines represent upper and lower quartiles (63).

Figure 14

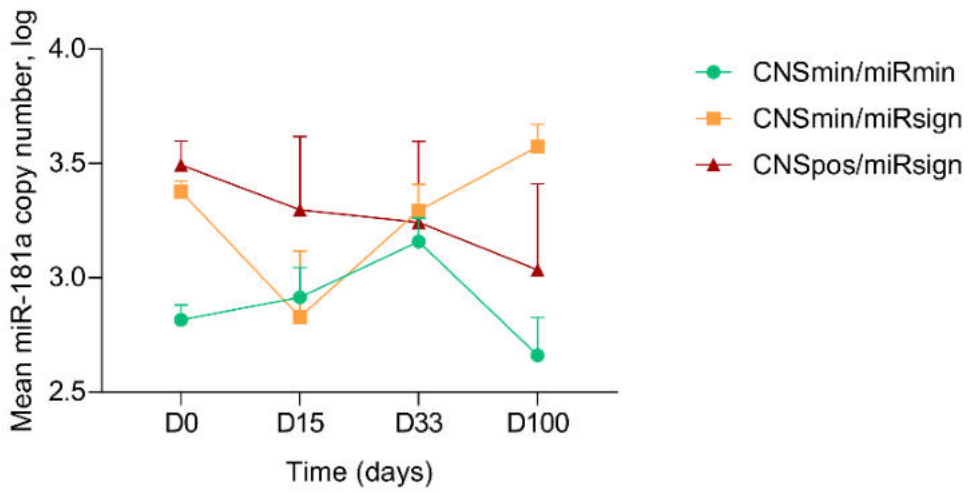

Figure 14. Mean expression of hsa-miR-181a-5p in miR-based groups per day, presented longitudinally. CNSmin/miRmin: green; CNSmin/miRsign: orange; CNSpos/miRsign: red. Sampling days were selected in accordance with the ALL IC-BFM 2009 guidelines. Whiskers indicate standard error of the mean (63).

4.8 Diagnostic value of ddPCR-based hsa-miR-181a-5p quantification

To evaluate the diagnostic value of hsa-miR-181a-5p copy number assessment by ddPCR, ROC analysis was conducted, comparing the feasibility of the novel biomarker with cell-based techniques, such as cytospin and flow cytometry. A cut-off value for hsa-miR-181a-5p copies was determined statistically, and as a result, copy numbers above 1,454 copies were considered positive in the consecutive binary transformation. Correspondingly, at least 8 blast cells detected by FCM was considered as CNSL positive for binary transformation of the FCM data. As the result of ROC analysis, the following area under the curve (AUC) values were assigned to the cytopsin, FCM and hsa-miR-181a-5p-based method, respectively: 0.6818, 0.8564, 0.8490 (Figure 15). Analysis of the curves indicates that our innovative hsa-miR-181a-5p copy number-based methodology outperformed cytospin and was non-inferior to FCM.

Figure 15

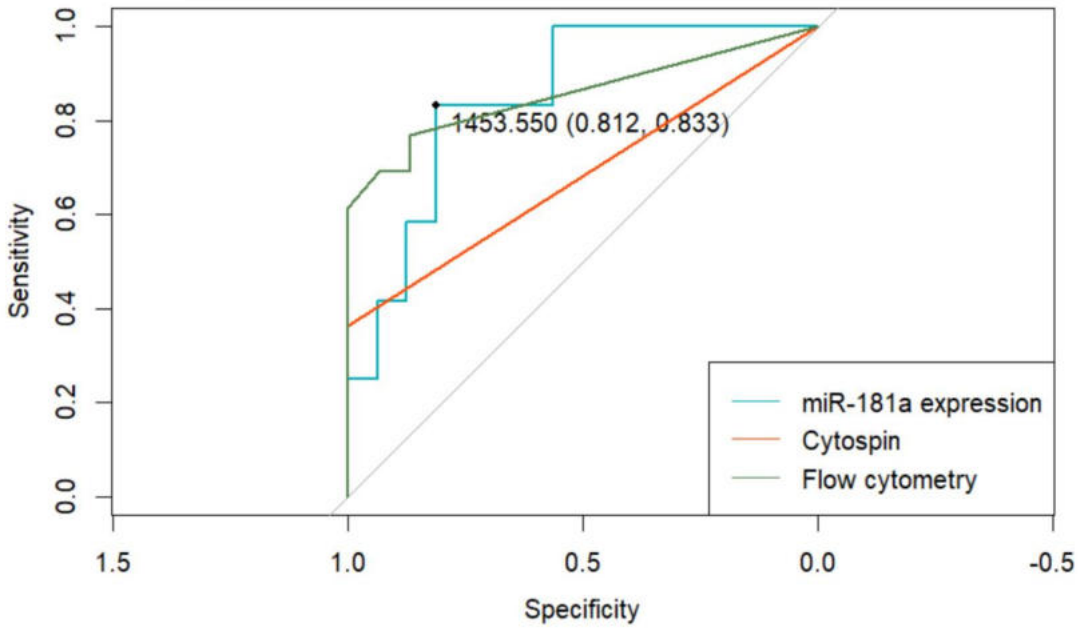

Figure 15. Receiver operating characteristic (ROC) curve illustrating the performance of the classification model predicated on hsa-miR-181a-5p quantification by ddPCR, in comparison with cytospin and flow cytometry. Blue line: hsa-miR-181a-5p quantification; red line: cytospin; green line: flow cytometry. Numbers indicate AUC values (63).

4.9 *SH2B3* alteration identified as CNSL-associated genetic feature

We also investigated the possible relations between hsa-miR-181a-5p copy numbers, molecular subtypes and small sequence variations (single nucleotide variants and small insertions/deletions) in disease-relevant genes detected in blast-rich BM samples. None of the patients with high hyperdiploid karyotype, hence associated with favorable outcome, were categorized as CNSpos/miRsign, while all patients harboring the high-risk iAMP21 alteration were classified in the miRsign groups (Figure 16.A). Twelve out of the 103 leukemia-relevant genes were mutated in at least 2 patients (Figure 16.B). There was no observable association between CNS or miR status and prognostically unfavorable clonal mutations in *TP53, NRAS, KRAS* or *CREBBP* genes. Strikingly, *SH2B3* mutations solely affected patients classified in miRsign groups (CNSmin/miRsign or CNSpos/miRsign), with no *SH2B3* mutation found in the miRmin group.

Figure 16.A

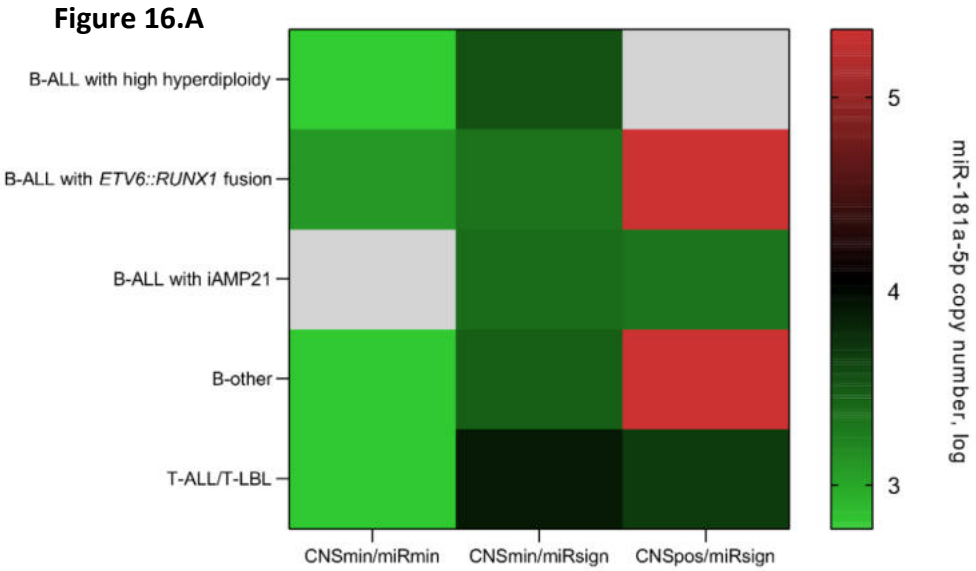

Figure 16.B

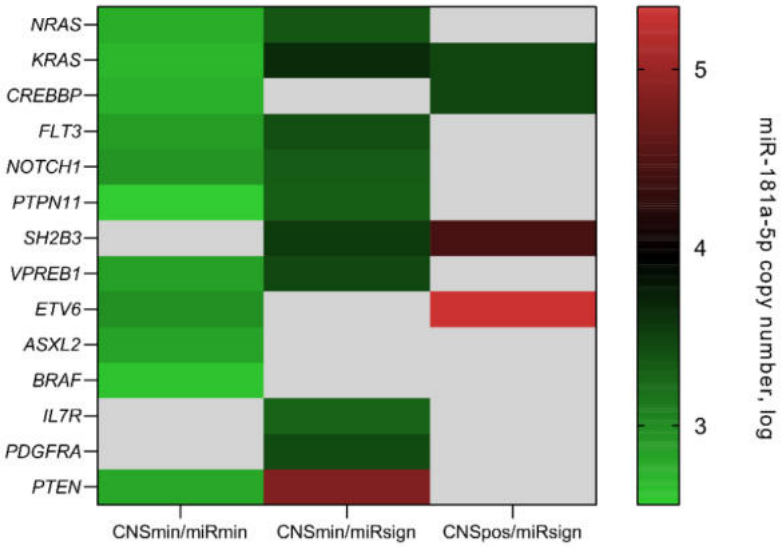

Figure 16. A Heatmap illustrating the logarithm of hsa-miR-181a-5p copy numbers and genetic subtypes of ALL. Only subtypes with at least two patients are shown. If no patient belonged to the subtype of interest, the field is presented in grey. **B** Heatmap, displaying the logarithm of hsa-miR-181a-5p copy numbers and genes altered in a minimum of two patients, illustrated by groups. Grey shaded fields indicate, that no mutation in the gene of interest was identified in the respective groups. The mean logarithm of hsa-miR-181a-5p copy number is presented for genes altered in several patients within a certain field (63).

5. DISCUSSION

The remarkable improvement in the survival rates of pediatric ALL is partially due to the continuously refined risk stratification of patients, and the implementation of personalized approaches, optimizing and carefully tailoring therapy selection(64,65). The swift advancement of next generation sequencing technologies revolutionized the molecular profiling of patients and enhanced our comprehension of the disease, laying the groundwork for personalized medicine(66,67).

We conducted a detailed genomic and transcriptomic analysis of pediatric ALL, as a part of a nationwide cooperation in the framework of the Hungarian Pediatric Leukemia Molecular Profiling Program. Aiming to identify subtype-defining aberrations, prognostic biomarkers, and putative therapeutic targets, we developed a targeted NGS panel, tailored for the deep genomic profiling of ALL, and present a suitable approach even for the routine diagnostic setting. Our findings indicate that the combination of targeted NGS and (digital)MLPA can be a powerful and beneficial tool to distinguish molecular subtypes, pinpoint putative therapeutic targets, and consequently contribute to further refinement of patient care.

A smaller subset of patients was also interrogated by digitalMLPA, enabling the determination of the modal chromosome number, the detection of CNAs in a genome wide manner, and the identification of *IKZF1*^{plus} subtype in a single reaction. *IKZF1* deletions were highly prevalent in *BCR::ABL*-like cases in our cohort, besides all but one *BCR::ABL1*-positive cases harboring *IKZF1* deletion. The high occurrence of Ikaros loss in these ALL subtypes is well-established(14,68–71). The prognostic significance of *IKZF1* status has also been in the spotlight of numerous studies, and *IKZF1* deletion is considered as an unfavorable prognostic indicator(72–75). Although patients with different *IKZF1* status had similar prognosis in our cohort with relatively a short follow-up period, a higher proportion of patients were found to be MRD positive on day 33 and 78 in the presence of *IKZF1* deletion, indicating unfavorable response to therapy.

We applied a commercially available targeted RNA sequencing kit to detect gene fusions, including subtype-defining, rare but of prognostic significance, potentially targetable or even novel, previously not described alterations. Besides observing alterations detectable by commonly used FISH and RT-PCR assays, we identified clinically relevant fusions that previously were not routinely tested for. Based on our

results, targeted RNA-seq may serve as an alternative for some of the standard tests. In line with our finding, the applicability and reliability of the TruSight RNA Pan-Cancer Panel in hematological malignancies has been demonstrated by others(17,76–78). Rare fusions in 'B-other' cases, involving *DUX4, MEF2D, NUTM1* and *ZNF384* genes have been unveiled, enabling the refinement of these patients' classification into recently described subgroups(15,79–82). As *KMT2A* rearrangements are usually screened by break-apart FISH probes - only used for indicating the presence of the rearrangement of *KTM2A* gene, but not the fusion partner - the detection of the partner genes with RNA sequencing allows for MRD monitoring in these cases, as *KMT2A* fusions are reliable MRD markers(83–85). The outstandingly dismal prognosis seen in *KMT2A*-rearranged cases in our cohort calls for novel therapeutic options, that menin inhibitors may putatively offer(85). Potentially actionable kinase fusions were also revealed, involving *ABL1*, *ABL2*, *JAK2* and *CRLF2*, paving the way for targeted therapy(13,14).

As anticipated, we observed substantially different mutation patterns across various ALL subtypes. Even though RAS pathway mutations were prevalent in all molecular subgroups of B-ALL, hyperdiploid patients showed the highest incidence of *NRAS*, *KRAS, PTPN11* and *FLT3* alterations. The relationship between hyperdiploidy and RAS pathway mutations has been described(86). Some studies associate RAS pathway mutations with therapy resistance and relapse(87,88). Jerchel et al. discovered that only clonal mutations are linked to dismal outcome, and Antić et al. also arrived to the conclusion that subclonal mutations do not serve as a prognostic indicator at the time of diagnosis(89,90). Mutations of the RAS pathway did not have an impact on outcome in our cohort, irrespective of the clonal or subclonal nature of the alteration. *UBA2* mutations were observed primarily in patients with *ETV6::RUNX1* fusion(91,92). Although previous studies have noted the occurrence of *UBA2* mutations in this subgroup(93), based on our findings, the frequency of these alterations appears to be significantly higher than formerly reported, almost exclusively detected in combination with *ETV6::RUNX1* fusion.

Mutational profiling with targeted sequencing specifically tailored to disease-relevant genes in ALL provides significant advantages by facilitating the identification of even infrequent variants with putative prognostic importance, such as *PAX5* p.P80R, *IKZF1* p.N159Y, or *ZEB2* p.H1038 and p.Q1072(6,94–96). *ZEB2* p.Q1072 hotspot

mutation was detected in four, and *IKZF1* p.N159Y in two patients, while *PAX5* p.P80R, and *ZEB2* p.H1038 variants were absent in our cohort. The limited number of mutant cases and the brief follow-up period precluded definitive conclusions about outcomes related to these hotspot mutations. On the other hand, existing literature data indicates that patients with *ZEB2* mutations are prone to relapse and are associated with shorter event-free survival, emphasizing the significance of early detection of these alterations(96). Accordingly, one patient with *ZEB2* mutation from our cohort went through a relapse as early as seven months after treatment initiation, and eventually succumbed to their disease at month 8 after diagnosis.

Notably, more than fifty percent of high-risk and over thirty percent of standard/intermediate risk patients exhibited putatively druggable mutations with a VAF above 10%, or actionable fusions, hence setting stage for targeted therapy for a substantial proportion of patients across all risk groups(14,97). Moreover, an additional 11 patients harbored potentially targetable mutations with a low VAF, as revealed by deep sequencing, further expanding the number of patients who may be stratified for targeted therapy in the future.

Survival analysis of the B-ALL subcohort indicated that event-free survival of *TP53* mutant patients was considerably shorter compared to wild-type cases. *TP53* mutations are present in approximately 10-15% of ALL patients, and have been linked to resistance to treatment, increased rate of relapse, and adverse prognosis (98–100). Furthermore, it is commonly acknowledged that *TP53* mutations affect approximately 90% of patients with low hypodiploidy(101,102). Despite the very small number of patients with low hypodiploidy in our dataset (n=2), *TP53* mutation was detected in both of them, accordingly. In addition, inferior outcome was observed in the presence of *TP53* mutation, even among patients with MRD negative FCM on day 33 of therapy. Taking into consideration that the evaluation of end-of-induction MRD is widely acknowledged as a strong prognostic predictor(103–105), yet, this specific genetic alteration further stratified patients within this subcohort with expected favorable outcome, makes our finding especially noteworthy. This discovery warrants additional exploration in larger patient cohorts, thus as a first step, we conducted a successful validation by augmenting our results with data from the TARGET ALL Phase 2 study.

Roughly 50% of those patients who experienced relapse or passed away within the first two years of therapy were stratified in the intermediate-risk arm. Four of these IR patients harbored *TP53* and/or *CREBBP* mutations, prompting the query, whether therapy intensification would have been advantageous for them. Three of these mutations presented with a low VAF (3-5%), highlighting the benefits of deep sequencing, and its widespread, unrestricted use, irrespective of risk groups. Notably, in chronic lymphocytic leukemia, it has already been demonstrated that low-burden *TP53* mutations are associated with dismal prognosis; hence, identifying low-burden variants at diagnosis may also carry clinical significance in acute leukemias(106–110).

We also compared the genetic alterations detected in matching paired samples of patients experiencing relapse. Of note, in relapsed cases, the most commonly mutated genes were the ones mentioned earlier, such as *TP53* and *CREBBP*. Studies have linked *CREBBP* mutations to glucocorticoid resistance and relapse(111–113). *TP53* are known to be enriched in relapse samples, and to frequently appear as progression related novel alteration, similar to what was seen at two patients in our cohort(114–116). Detectable *TP53* mutant clone did not appear until the second relapse, several years post-treatment of the first relapse, indicating a possible impact of prior administration of cytotoxic drugs on the course of the disease(117). The expansion of an initially smaller subclone at the time of relapse in two other *TP53* mutation positive patients suggests that the corresponding leukemic clone was not fully eradicated by the primary treatment, providing additional evidence of the association between *TP53* mutations and chemotherapy resistance(99,116). *NT5C2* mutations occurred exclusively at the time of relapse, consistent with prior research identifying these mutations as prevalent alterations specific to relapse and accountable for 6-merkaptopurin resistance(118–121). Based on the results of temporal mutational profiling, most cases showed branching clonal evolution, characterized by the concurrent emerging and vanishing subclones, shedding light to intricate evolutionary hierarchies with rivaling tumor cells, substantially complicating therapeutic considerations.

Even though extraordinary advances have been achieved in the survival of pediatric ALL, leukemic involvement of the CNS and meningeal relapse continues to be a prevalent cause of therapy failure, presenting as a leading therapeutic obstacle(41,122).

One of the key components of treatment-improvement is the accurate identification of children susceptible to CNS relapse, and sensitive monitoring of treatment-response. Nevertheless, currently used methods rely primarily on cell-based techniques, lacking the sensitivity and reproducibility needed for the refinement of risk-adapted CNS-directed treatment. Taking into account the generally accepted theory, that virtually all acute leukemia patients have sub-microscopic CNS involvement, already at the time of diagnosis, which conventional methods fail to identify, the introduction of more sensitive molecular techniques, analysing the cell-free component of the CSF seems indispensable(32,46,49,123).

In my PhD work, we evaluated hsa-miR-181a-5p as a potential novel biomarker for the assessment of CNS status, and for monitoring therapeutic response in ALL. We confirmed the prior discovery of the working group, that hsa-miR-181a-5p expression is elevated in patients with leukemic involvement of the CNS(49). Additionally, we proposed a novel classification, with complementary application of conventionally used methods (cytospin and FCM), and hsa-miR-181a-5p copy number quantification by ddPCR. For normalization and quality assurance of the measurements, miR-532 and miR-16 microRNAs were used as references, as the expression of these miRs is stable according to literature data(49,124–126). Incorporating hsa-miR-181a-5p expression into the patient assessment procedure allowed for the identification of a number of patients with initially unclear CNS status, with elevated level of hsa-miR-181a-5p. Interestingly, the highest average hsa-miR-181a-5p copy number on day 100 of the therapy was measured in the CNSmin/miRsign group. In the light of this result, the question arises as to whether or not the aforementioned patients would have profited from intensified CNS-directed therapy. This question, however, can only be resolved by meticulously designed prospective trials, including long-term follow-up surveillance of CNS relapses.

The role of hsa-miR-181a-5p has been investigated in solid tumors and hematological malignances(127–129), and shown to regulate the activation and development of lymphocytes(130–132). While the precise role of hsa-miR-181a-5p plays in hematological malignancies is currently unclear(133–135), recent studies indicate its involvement in the adaptation of leukemic cells to hypoxic environments, thereby promoting the chance of their survival in the CNS(136).

The connection that exists between hsa-miR-181a-5p and vascular endothelial growth factor A (VEGFA) is of particular interest. Overexpression of hsa-miR-181a-5p enhances angiogenesis in the tumor microenvironment by positively regulating VEGFA through the SRC Kinase Inhibitor 1 (SRCIN1) protein, as described in detail in colorectal carcinoma by Sun et al(137). Our workgroup has previously confirmed this relationship in ALL, by finding elevated VEGFA expression in CNS-positive ALL patients, along with high hsa-miR-181a-5p expression in the bone marrow as well as in the CSF(138). Elevated VEGFA expression also facilitates the transendothelial migration of lymphoblasts, as demonstrated in animal models, implying a mediator function in CNS invasion(139). In addition, bevacizumab, a VEGF inhibitor, was shown to diminish CNSL burden in rodents(37,136,139). All things considered, these findings raise the possibility of therapeutic intervention in the process of blast migration and survival in the CNS by targeting members of the hsa-miR-181a-5p-VEGFA axis(140).

Furthermore, we observed that all patients with *SH2B3* mutations were classified as miRsign, with identifiable CNS involvement. The *SH2B3* gene is responsible for the encoding of a lymphocyte adaptor protein (LNK), that has multiple functions, including participation in cell adhesion and migration processes, and modulation of integrin-cytokine interaction(141,142). Given the potential role of this protein in the transmigration of leukemic cells into the CNS, further studies are required to elucidate its specific role in CNS invasion. Publicly available miR target predictions, including TargetScan, miRDB and miRDIP indicate a highly likely interaction between *SH2B3* and hsa-miR-181a-5p. In fact, miRDIP assigns a high combined confidence score to the interaction, placing it in the top 5%(143).

From a clinical point of view, the primary concern is the diagnostic feasibility and performance of hsa-miR-181a-5p quantification from the CSF, with special regard to the classification of ambiguous cases. A limitation of the routinely employed cell-based methods is the insufficient sensitivity for revealing latent CNSL, thus the lack of a high-sensitivity gold standard approach for the affirmation of cases with high hsa-miR-181a-5p expression(144). In this study, with limited number of eligible samples, no CNS relapse was observed during the follow-up period. Nevertheless, the long-term relapse rate would be of particular interest in miRsign cases, with a special regard to CNSmin/miRsign cases, receiving CNS-directed therapy without intensification.

Integrating molecular methods into CNSL diagnostics, with a focus on hsa-miR-181a-5p quantification from the CSF, may enhance the identification of patients who could potentially profit from closer monitoring and fine-tuning of CNS-directed therapy.

To the best of our knowledge, we were the first to conduct ddPCR-based quantification of hsa-miR-181a-5p from CSF of pediatric ALL patients, determined the diagnostic value of our measurements, and discovered that its diagnostic power is comparable to that of flow cytometry, while cytospin underperforms both methods. Our results align with a prior observation by Schwinghammer et al, who highlighted the absolute quantitative nature of ddPCR and FCM, and revealed a higher level of concordance between MRD values assessed by FCM and ddPCR, than between FCM and qPCR results(145). Thus, ddPCR may complement FCM in CNSL diagnostics as a novel sensitive alternative.

After validation in an independent patient population, miR-181a expression may serve as a suitable diagnostic marker for leukemic infiltration of the CNS. We propose a method that could complement conventionally used cell-based techniques in the diagnostic workflow, since the diagnostic value of the approach is nearly identical to that of flow cytometry. Understanding the impact of *SH2B3* gene on CNS invasion may merit further investigation.

Two immensely challenging areas of the clinical management of ALL are relapse and the leukemic involvement of the CNS. Relapse represents a significant obstacle in modern ALL therapy, as it remains the primary reason for treatment failure and adverse clinical outcome. Furthermore, leukemic infiltration of the CNS presents substantial impediment, often complicating treatment and increasing the risk of relapse. We aimed to examine the molecular background of these two critical conditions - relapse and CNSL - besides establishing the genomic and transcriptomic profiles in a nationwide cohort of pediatric ALL patients using a range of advanced molecular methods. We have uncovered biomarkers with prognostic significance, explored the landscape of potentially targetable alterations, revealed novel gene fusions, and investigated the diagnostic value of a novel biomarker that can potentially facilitate the refinement of patient stratification based on CNSL status. We genuinely hope that our findings will contribute to the advancement of acute leukemia diagnostics and help overcome some of the remaining obstacles in the clinical management of ALL.

6. CONCLUSIONS

Novel findings of my thesis are the following:

- We present a systematic comprehensive molecular profiling approach as part of the diagnostic workflow for the molecular characterization of a nationwide consecutive cohort of children with ALL.
- We demonstrated that targeted RNA sequencing complemented by (digital)MLPA is a powerful diagnostic method for identifying recently introduced genetic subtypes of ALL and offers a viable alternative to existing diagnostic techniques.
- We conducted mutational screening, using targeted deep DNA sequencing with a self-developed panel, designed specifically to detect small genomic variants in ALL, even if they are present with a low variant allele frequency, witch may carry potential clinical relevance, as exemplified in other hematological malignancies.
- We observed inferior outcome among B-ALL patients harboring *TP53* or *CREBBP* mutation.
- We found shorter event-free survival in *TP53* mutant B-ALL patients, even among patients with favorable therapeutic response, testing negative for MRD by flow cytometry on day 33 of therapy.
- We compared the genomic profile of matched diagnostic and relapse samples of 19 ALL patients and shed light to the manifold evolutionary process and entangled clonal selection mechanisms.
- We propose hsa-miR-181a-5p as a novel biomarker in the cerebrospinal fluid for the diagnosis of CNSL and demonstrate a feasible quantification method by ddPCR.
- We tested the diagnostic power of hsa-miR-181a-5p quantification by ddPCR, and found that it is non-inferior to flow cytometry, and overperforms cytospin in identifying CNSL.
- We discovered an association between *SH2B3* mutations and hsa-miR-181a-5p expression, which might indicate a potential role of *SH2B3* mutations in the leukemic invasion of the CNS.

7. SUMMARY

Disease progression, relapse, and the detection of leukemic involvement of the central nervous system still raise prominent obstacles in the clinical management of ALL. The revolution of molecular genetics reshaped the field of diagnostics and risk assessment, and paved the way for targeted therapies, hence it was placed in the center of my PhD research.

Diagnostic bone marrow samples from 192 patients diagnosed with B-ALL/LBL (n=153) or T-ALL/LBL (n=39), and 92 CSF samples of 35 children with B-ALL/LBL (n=28) or T-ALL/LBL (n=7) were investigated. Additionally, samples drawn at the time of relapse were analysed from 19 patients. Comprehensive genomic and transcriptomic profiling was performed using TruSight RNA Pan-Cancer Panel targeting 1,385 genes, QIASeq Targeted DNA Custom Panel covering 103 disease-relevant genes, and MLPA or digitalMLPA, using the D007 ALL probemix. Copy numbers of miR-181a, miR-532 and miR-16 were quantified in the CSF using digital droplet PCR.

Novel fusions, involving *JAK2, PAX5, KMT2A* and *RUNX1* genes were observed, with *KMT2A*-rearranged patients showing the worst prognosis (3-year EFS: 24 months, p=0.013). Targeted deep sequencing revealed somatic mutations in 74.9% of the patients. B-ALL patients harboring *TP53* (p=0.008) or *CREBBP* (p=0.010) mutation displayed inferior EFS, and B-ALL patients with negative MRD at day 33 of therapy exhibited shorter EFS in the presence of *TP53* (p<0.001) mutation.

By combining the cytospin- and flow cytometry (FCM)-derived data with the miR-181a expression, we were able to reclassify patients into three novel groups representing CNSL status, and assign previously ambiguous cases. CNSpos/miRsign patients had overt CNS infiltration, CNSmin/miRsign patients had potentially clinically significant, but latent CNSL, while CNSmin/miRmin group had no sign of CNS involvement. ROC analysis revealed a diagnostic value of miR-181a quantification surpassing cytospin and comparable to FCM. *SH2B3* mutations were solely present in patients classified as miRsign.

Our work uncovers novel gene fusions and the prognostic importance of *TP53* and *CREBBP* mutations and demonstrates a novel biomarker in the field of CNSL diagnostics, offering valuable, therapeutically relevant insight into the genomic and transcriptomic landscape of children diagnosed with ALL.

8. REFERENCES

1. Force LM, Abdollahpour I, Advani SM, Agius D, Ahmadian E, Alahdab F, Alam T, Alebel A, Alipour V, Allen CA, Almasi-Hashiani A, Alvarez EM, Amini S, Amoako YA, Anber NH, Arabloo J, Artaman A, Atique S, Awasthi A, et al. The global burden of childhood and adolescent cancer in 2017: an analysis of the Global Burden of Disease Study 2017. Lancet Oncol [Internet]. 2019 Sep 1;20(9):1211–25. Available from: https://doi.org/10.1016/S1470-2045(19)30339-0
2. Garami M, Schuler D, Jakab Z. [Importance of the National Childhood Cancer Registry in the field of paediatric oncology care in Hungary]. Orv Hetil. 2014 May;155(19):732–9.
3. Teachey DT, Pui CH. Comparative features and outcomes between paediatric T-cell and B-cell acute lymphoblastic leukaemia. Lancet Oncol. 2019 Mar;20(3):e142–54.
4. Brady SW, Roberts KG, Gu Z, Shi L, Pounds S, Pei D, Cheng C, Dai Y, Devidas M, Qu C, Hill AN, Payne-Turner D, Ma X, Iacobucci I, Baviskar P, Wei L, Arunachalam S, Hagiwara K, Liu Y, et al. The genomic landscape of pediatric acute lymphoblastic leukemia. Nat Genet [Internet]. 2022;54(9):1376–89. Available from: https://doi.org/10.1038/s41588-022-01159-z
5. Paietta E, Roberts KG, Wang V, Gu Z, Buck GAN, Pei D, Cheng C, Levine RL, Abdel-Wahab O, Cheng Z, Wu G, Qu C, Shi L, Pounds S, Willman CL, Harvey R, Racevskis J, Barinka J, Zhang Y, et al. Molecular classification improves risk assessment in adult BCR-ABL1-negative B-ALL. Blood [Internet]. 2021 Sep 16 [cited 2022 Jun 28];138(11):948–58. Available from: https://pubmed.ncbi.nlm.nih.gov/33895809/
6. Gu Z, Churchman ML, Roberts KG, Moore I, Zhou X, Nakitandwe J, Hagiwara K, Pelletier S, Gingras S, Berns H, Payne-Turner D, Hill A, Iacobucci I, Shi L, Pounds S, Cheng C, Pei D, Qu C, Newman S, et al. PAX5-driven subtypes of B-progenitor acute lymphoblastic leukemia. Nat Genet [Internet]. 2019 Feb 1 [cited 2022 Jun 28];51(2):296–307. Available from: https://pubmed.ncbi.nlm.nih.gov/30643249/
7. Jeha S, Choi J, Roberts KG, Pei D, Coustan-Smith E, Inaba H, Rubnitz JE, Ribeiro

RC, Gruber TA, Raimondi SC, Karol SE, Qu C, Brady SW, Gu Z, Yang JJ, Cheng C, Downing JR, Evans WE, Relling M V, et al. Clinical Significance of Novel Subtypes of Acute Lymphoblastic Leukemia in the Context of Minimal Residual Disease–Directed Therapy. Blood Cancer Discov [Internet]. 2021 Jul 1 [cited 2022 Jun 28];2(4):326–37. Available from: https://aacrjournals.org/bloodcancerdiscov/article/2/4/326/665859/Clinical-Significance-of-Novel-Subtypes-of-Acute

8. Hunger SP, Mullighan CG. Redefining ALL classification: toward detecting high-risk ALL and implementing precision medicine. Blood. 2015 Jun;125(26):3977–87.

9. Anderson K, Lutz C, van Delft FW, Bateman CM, Guo Y, Colman SM, Kempski H, Moorman A V, Titley I, Swansbury J, Kearney L, Enver T, Greaves M. Genetic variegation of clonal architecture and propagating cells in leukaemia. Nature [Internet]. 2011;469(7330):356–61. Available from: https://doi.org/10.1038/nature09650

10. Notta F, Mullighan CG, Wang JCY, Poeppl A, Doulatov S, Phillips LA, Ma J, Minden MD, Downing JR, Dick JE. Evolution of human BCR–ABL1 lymphoblastic leukaemia-initiating cells. Nature [Internet]. 2011;469(7330):362–7. Available from: https://doi.org/10.1038/nature09733

11. Alaggio R, Amador C, Anagnostopoulos I, Attygalle AD, Araujo IB de O, Berti E, Bhagat G, Borges AM, Boyer D, Calaminici M, Chadburn A, Chan JKC, Cheuk W, Chng WJ, Choi JK, Chuang SS, Coupland SE, Czader M, Dave SS, et al. The 5th edition of the World Health Organization Classification of Haematolymphoid Tumours: Lymphoid Neoplasms. Leukemia [Internet]. 2022;36(7):1720–48. Available from: https://doi.org/10.1038/s41375-022-01620-2

12. Arber DA, Orazi A, Hasserjian RP, Borowitz MJ, Calvo KR, Kvasnicka HM, Wang SA, Bagg A, Barbui T, Branford S, Bueso-Ramos CE, Cortes JE, Dal Cin P, DiNardo CD, Dombret H, Duncavage EJ, Ebert BL, Estey EH, Facchetti F, et al. International Consensus Classification of Myeloid Neoplasms and Acute Leukemias: integrating morphologic, clinical, and genomic data. Blood [Internet]. 2022 Sep 15;140(11):1200–28. Available from: https://doi.org/10.1182/blood.2022015850

13. Tasian SK, Loh ML, Hunger SP. Philadelphia chromosome-like acute lymphoblastic leukemia. Blood. 2017 Nov;130(19):2064–72.
14. Roberts KG, Li Y, Payne-Turner D, Harvey RC, Yang YL, Pei D, McCastlain K, Ding L, Lu C, Song G, Ma J, Becksfort J, Rusch M, Chen SC, Easton J, Cheng J, Boggs K, Santiago-Morales N, Iacobucci I, et al. Targetable Kinase-Activating Lesions in Ph-like Acute Lymphoblastic Leukemia. N Engl J Med [Internet]. 2014 Sep 11;371(11):1005–15. Available from: https://doi.org/10.1056/NEJMoa1403088
15. Lilljebjörn H, Henningsson R, Hyrenius-Wittsten A, Olsson L, Orsmark-Pietras C, von Palffy S, Askmyr M, Rissler M, Schrappe M, Cario G, Castor A, Pronk CJH, Behrendtz M, Mitelman F, Johansson B, Paulsson K, Andersson AK, Fontes M, Fioretos T. Identification of ETV6-RUNX1-like and DUX4-rearranged subtypes in paediatric B-cell precursor acute lymphoblastic leukaemia. Nat Commun [Internet]. 2016;7(1):11790. Available from: https://doi.org/10.1038/ncomms11790
16. Grioni A, Fazio G, Rigamonti S, Bystry V, Daniele G, Dostalova Z, Quadri M, Saitta C, Silvestri D, Songia S, Storlazzi CT, Biondi A, Darzentas N, Cazzaniga G. A Simple RNA Target Capture NGS Strategy for Fusion Genes Assessment in the Diagnostics of Pediatric B-cell Acute Lymphoblastic Leukemia. HemaSphere [Internet]. 2019 Jun 1 [cited 2022 Jun 28];3(3). Available from: https://pubmed.ncbi.nlm.nih.gov/31723839/
17. Migita NA, Jotta PY, Nascimento NP do, Vasconcelos VS, Centoducatte GL, Massirer KB, Azevedo AC de, Brandalise SR, Yunes JA. Classification and genetics of pediatric B-other acute lymphoblastic leukemia by targeted RNA sequencing. Blood Adv. 2023 Jul;7(13):2957–71.
18. Brown LM, Lonsdale A, Zhu A, Davidson NM, Schmidt B, Hawkins A, Wallach E, Martin M, Mechinaud FM, Khaw SL, Bartolo RC, Ludlow LEA, Challis J, Brooks I, Petrovic V, Venn NC, Sutton R, Majewski IJ, Oshlack A, et al. The application of RNA sequencing for the diagnosis and genomic classification of pediatric acute lymphoblastic leukemia. Blood Adv [Internet]. 2020;4(5):930–42. Available from: https://www.sciencedirect.com/science/article/pii/S2473952920314580

19. Moorman A V, Barretta E, Butler ER, Ward EJ, Twentyman K, Kirkwood AA, Enshaei A, Schwab C, Creasey T, Leongamornlert D, Papaemmanuil E, Patrick P, Clifton-Hadley L, Patel B, Menne T, McMillan AK, Harrison CJ, Rowntree CJ, Marks DI, et al. Prognostic impact of chromosomal abnormalities and copy number alterations in adult B-cell precursor acute lymphoblastic leukaemia: a UKALL14 study. Leukemia [Internet]. 2022;36(3):625–36. Available from: https://doi.org/10.1038/s41375-021-01448-2

20. Kiss R, Gángó A, Benard-Slagter A, Egyed B, Haltrich I, Hegyi L, de Groot K, Király PA, Krizsán S, Kajtár B, Pikó H, Pajor L, Vojcek Á, Matolcsy A, Kovács G, Szuhai K, Savola S, Bödör C, Alpár D. Comprehensive profiling of disease-relevant copy number aberrations for advanced clinical diagnostics of pediatric acute lymphoblastic leukemia. Mod Pathol [Internet]. 2020;33(5):812–24. Available from: https://www.sciencedirect.com/science/article/pii/S0893395222008602

21. Stanulla M, Dagdan E, Zaliova M, Möricke A, Palmi C, Cazzaniga G, Eckert C, Te Kronnie G, Bourquin JP, Bornhauser B, Koehler R, Bartram CR, Ludwig WD, Bleckmann K, Groeneveld-Krentz S, Schewe D, Junk S V, Hinze L, Klein N, et al. IKZF1(plus) Defines a New Minimal Residual Disease-Dependent Very-Poor Prognostic Profile in Pediatric B-Cell Precursor Acute Lymphoblastic Leukemia. J Clin Oncol Off J Am Soc Clin Oncol. 2018 Apr;36(12):1240–9.

22. Bedics G, Egyed B, Kotmayer L, Benard-Slagter A, de Groot K, Bekő A, Hegyi LL, Bátai B, Krizsán S, Kriván G, Erdélyi DJ, Müller J, Haltrich I, Kajtár B, Pajor L, Vojcek Á, Ottóffy G, Ujfalusi A, Szegedi I, et al. PersonALL: a genetic scoring guide for personalized risk assessment in pediatric B-cell precursor acute lymphoblastic leukemia. Br J Cancer [Internet]. 2023;129(3):455–65. Available from: https://doi.org/10.1038/s41416-023-02309-8

23. Moorman A V, Enshaei A, Schwab C, Wade R, Chilton L, Elliott A, Richardson S, Hancock J, Kinsey SE, Mitchell CD, Goulden N, Vora A, Harrison CJ. A novel integrated cytogenetic and genomic classification refines risk stratification in pediatric acute lymphoblastic leukemia. Blood. 2014 Aug;124(9):1434–44.

24. Hamadeh L, Enshaei A, Schwab C, Alonso CN, Attarbaschi A, Barbany G, den Boer ML, Boer JM, Braun M, Dalla Pozza L, Elitzur S, Emerenciano M, Fechina

L, Felice MS, Fronkova E, Haltrich I, Heyman MM, Horibe K, Imamura T, et al. Validation of the United Kingdom copy-number alteration classifier in 3239 children with B-cell precursor ALL. Blood Adv. 2019 Jan;3(2):148–57.

25. Ma X, Edmonson M, Yergeau D, Muzny DM, Hampton OA, Rusch M, Song G, Easton J, Harvey RC, Wheeler DA, Ma J, Doddapaneni H, Vadodaria B, Wu G, Nagahawatte P, Carroll WL, Chen IM, Gastier-Foster JM, Relling M V, et al. Rise and fall of subclones from diagnosis to relapse in pediatric B-acute lymphoblastic leukaemia. Nat Commun [Internet]. 2015;6(1):6604. Available from: https://doi.org/10.1038/ncomms7604

26. Waanders E, Gu Z, Dobson SM, Antić Ž, Crawford JC, Ma X, Edmonson MN, Payne-Turner D, van de Vorst M, Jongmans MCJ, McGuire I, Zhou X, Wang J, Shi L, Pounds S, Pei D, Cheng C, Song G, Fan Y, et al. Mutational landscape and patterns of clonal evolution in relapsed pediatric acute lymphoblastic leukemia. Blood cancer Discov [Internet]. 2020 Jul 1 [cited 2022 Jul 26];1(1):96–111. Available from: https://pubmed.ncbi.nlm.nih.gov/32793890/

27. Aur RJA, Simone J, Hustu HO, Walters T, Borella L, Pratt C, Pinkel D. Central Nervous System Therapy and Combination Chemotherapy of Childhood Lymphocytic Leukemia. Blood [Internet]. 1971;37(3):272–81. Available from: https://www.sciencedirect.com/science/article/pii/S0006497120694587

28. Pui CH, Howard SC. Current management and challenges of malignant disease in the CNS in paediatric leukaemia. Lancet Oncol [Internet]. 2008;9(3):257–68. Available from: https://www.sciencedirect.com/science/article/pii/S1470204508700706

29. Pui CH, Cheng C, Leung W, Rai SN, Rivera GK, Sandlund JT, Ribeiro RC, Relling M V, Kun LE, Evans WE, Hudson MM. Extended Follow-up of Long-Term Survivors of Childhood Acute Lymphoblastic Leukemia. N Engl J Med [Internet]. 2003 Aug 14;349(7):640–9. Available from: https://doi.org/10.1056/NEJMoa035091

30. Hijiya N, Hudson MM, Lensing S, Zacher M, Onciu M, Behm FG, Razzouk BI, Ribeiro RC, Rubnitz JE, Sandlund JT, Rivera GK, Evans WE, Relling M V, Pui CH. Cumulative Incidence of Secondary Neoplasms as a First Event After Childhood Acute Lymphoblastic Leukemia. JAMA [Internet]. 2007 Mar

21;297(11):1207–15. Available from: https://doi.org/10.1001/jama.297.11.1207

31. Krishnan S, Wade R, Moorman A V, Mitchell C, Kinsey SE, Eden TOB, Parker C, Vora A, Richards S, Saha V. Temporal changes in the incidence and pattern of central nervous system relapses in children with acute lymphoblastic leukaemia treated on four consecutive Medical Research Council trials, 1985-2001. Leukemia. 2010 Feb;24(2):450–9.
32. Frishman-Levy L, Izraeli S. Advances in understanding the pathogenesis of CNS acute lymphoblastic leukaemia and potential for therapy. Br J Haematol [Internet]. 2017 Jan 1;176(2):157–67. Available from: https://doi.org/10.1111/bjh.14411
33. Thastrup M, Marquart HV, Schmiegelow K. Flow Cytometric Detection of Malignant Blasts in Cerebrospinal Fluid: A Biomarker of Central Nervous System Involvement in Childhood Acute Lymphoblastic Leukemia. Biomolecules. 2022 Jun;12(6).
34. Gaipa G, Basso G, Biondi A, Campana D. Detection of minimal residual disease in pediatric acute lymphoblastic leukemia. Cytom Part B Clin Cytom [Internet]. 2013 Nov 1;84(6):359–69. Available from: https://doi.org/10.1002/cyto.b.21101
35. van Dongen JJM, van der Velden VHJ, Brüggemann M, Orfao A. Minimal residual disease diagnostics in acute lymphoblastic leukemia: need for sensitive, fast, and standardized technologies. Blood [Internet]. 2015 Jun 25;125(26):3996–4009. Available from: https://doi.org/10.1182/blood-2015-03-580027
36. Yao H, Price TT, Cantelli G, Ngo B, Warner MJ, Olivere L, Ridge SM, Jablonski EM, Therrien J, Tannheimer S, McCall CM, Chenn A, Sipkins DA. Leukaemia hijacks a neural mechanism to invade the central nervous system. Nature. 2018 Aug;560(7716):55–60.
37. Münch V, Trentin L, Herzig J, Demir S, Seyfried F, Kraus JM, Kestler HA, Köhler R, Barth TFE, te Kronnie G, Debatin KM, Meyer LH. Central nervous system involvement in acute lymphoblastic leukemia is mediated by vascular endothelial growth factor. Blood [Internet]. 2017 Aug 3;130(5):643–54. Available from: https://doi.org/10.1182/blood-2017-03-769315
38. Lenk L, Alsadeq A, Schewe DM. Involvement of the central nervous system in acute lymphoblastic leukemia: opinions on molecular mechanisms and clinical implications based on recent data. Cancer Metastasis Rev [Internet].

2020;39(1):173–87. Available from: https://doi.org/10.1007/s10555-020-09848-z

39. Hong Z, Wei Z, Xie T, Fu L, Sun J, Zhou F, Jamal M, Zhang Q, Shao L. Targeting chemokines for acute lymphoblastic leukemia therapy. J Hematol Oncol [Internet]. 2021;14(1):1–14. Available from: https://doi.org/10.1186/s13045-021-01060-y
40. Price RA. Histopathology of CNS leukemia and complications of therapy. Am J Pediatr Hematol Oncol. 1979;1(1):21–30.
41. Thastrup M, Duguid A, Mirian C, Schmiegelow K, Halsey C. Central nervous system involvement in childhood acute lymphoblastic leukemia: challenges and solutions. Leukemia [Internet]. 2022;36(12):2751–68. Available from: https://doi.org/10.1038/s41375-022-01714-x
42. Glass JP, Melamed M, Chernik NL, Posner JB. Malignant cells in cerebrospinal fluid (CSF): the meaning of a positive CSF cytology. Neurology. 1979 Oct;29(10):1369–75.
43. Thastrup M, Marquart HV, Levinsen M, Grell K, Abrahamsson J, Albertsen BK, Frandsen TL, Harila-Saari A, Lähteenmäki PM, Niinimäki R, Pronk CJ, Ulvmoen A, Vaitkevičienė G, Taskinen M, Schmiegelow K, Wehner P, Frost BM, Norén-Nyström U, Behrendtz M, et al. Flow cytometric detection of leukemic blasts in cerebrospinal fluid predicts risk of relapse in childhood acute lymphoblastic leukemia: a Nordic Society of Pediatric Hematology and Oncology study. Leukemia. 2020;34(2):336–46.
44. Dux R, Kindler-Röhrborn A, Annas M, Faustmann P, Lennartz K, Zimmermann CW. A standardized protocol for flow cytometric analysis of cells isolated from cerebrospinal fluid. J Neurol Sci. 1994 Jan;121(1):74–8.
45. Steele RW, Marmer DJ, O'Brien MD, Tyson ST, Steele CR. Leukocyte survival in cerebrospinal fluid. J Clin Microbiol. 1986 May;23(5):965–6.
46. Sampathi S, Chernyavskaya Y, Haney MG, Moore LH, Snyder IA, Cox AH, Fuller BL, Taylor TJ, Yan D, Badgett TC, Blackburn JS. Nanopore sequencing of clonal IGH rearrangements in cell-free DNA as a biomarker for acute lymphoblastic leukemia. Front Oncol. 2022;12:958673.
47. Lv M, Zhu S, Peng H, Cheng Z, Zhang G, Wang Z. B-cell acute lymphoblastic leukemia-related microRNAs: uncovering their diverse and special roles. Am J Cancer Res. 2021;11(4):1104–20.

48. Rzepiel A, Kutszegi N, Gézsi A, Sági JC, Egyed B, Péter G, Butz H, Nyírő G, Müller J, Kovács GT, Szalai C, Semsei ÁF, Erdélyi DJ. Circulating microRNAs as minimal residual disease biomarkers in childhood acute lymphoblastic leukemia. J Transl Med. 2019 Nov;17(1):372.
49. Egyed B, Kutszegi N, Sági JC, Gézsi A, Rzepiel A, Visnovitz T, Lőrincz P, Müller J, Zombori M, Szalai C, Erdélyi DJ, Kovács GT, Semsei ÁF. MicroRNA-181a as novel liquid biopsy marker of central nervous system involvement in pediatric acute lymphoblastic leukemia. J Transl Med. 2020 Jun;18(1):250.
50. Swerdlow, SH; Campo, E; Harris, NL; Jaffe, ES; Pileri, SA; Stein, H; Thiele, J; Vardiman J. WHO Classification of Tumours of Haematopoietic and Lymphoid Tissues [Internet]. 4th ed. Geneva, Switzerland: WHO Press; 2008. Available from: http://apps.who.int/bookorders/anglais/detart1.jsp?codlan=1&codcol=70&codcch=4002
51. Stary J, Zimmermann M, Campbell M, Castillo L, Dibar E, Donska S, Gonzalez A, Izraeli S, Janic D, Jazbec J, Konja J, Kaiserova E, Kowalczyk J, Kovacs G, Li CK, Magyarosy E, Popa A, Stark B, Jabali Y, et al. Intensive chemotherapy for childhood acute lymphoblastic leukemia: results of the randomized intercontinental trial ALL IC-BFM 2002. J Clin Oncol Off J Am Soc Clin Oncol. 2014 Jan;32(3):174–84.
52. Campbell M, Kiss C, Zimmermann M, Riccheri C, Kowalczyk J, Felice MS, Kuzmanovic M, Kovacs G, Kosmidis H, Gonzalez A, Bilic E, Castillo L, Kolenova A, Jazbec J, Popa A, Konstantinov D, Kappelmayer J, Szczepanski T, Dworzak M, et al. Childhood Acute Lymphoblastic Leukemia: Results of the Randomized Acute Lymphoblastic Leukemia Intercontinental-Berlin-Frankfurt-Münster 2009 Trial. J Clin Oncol Off J Am Soc Clin Oncol. 2023 Jul;41(19):3499–511.
53. Dworzak MN, Buldini B, Gaipa G, Ratei R, Hrusak O, Luria D, Rosenthal E, Bourquin JP, Sartor M, Schumich A, Karawajew L, Mejstrikova E, Maglia O, Mann G, Ludwig WD, Biondi A, Schrappe M, Basso G, International-BFM-FLOW-network on behalf of the. AIEOP-BFM Consensus Guidelines 2016 for Flow Cytometric Immunophenotyping of Pediatric Acute Lymphoblastic Leukemia. Cytom Part B Clin Cytom [Internet]. 2018 Jan 1;94(1):82–93.

Available from: https://doi.org/10.1002/cyto.b.21518

54. Hunyadi A, Kriston C, Szalóki G, Péterffy B, Egyed B, Szepesi Á, Timár B, Erdélyi DJ, Csanádi K, Kutszegi N, Márk Á, Barna G. The significance of CD49f expression in pediatric B-cell acute lymphoblastic leukemia. Am J Clin Pathol. 2024 Sep;

55. Benard-Slagter A, Zondervan I, de Groot K, Ghazavi F, Sarhadi V, Van Vlierberghe P, De Moerloose B, Schwab C, Vettenranta K, Harrison CJ, Knuutila S, Schouten J, Lammens T, Savola S. Digital Multiplex Ligation-Dependent Probe Amplification for Detection of Key Copy Number Alterations in T- and B-Cell Lymphoblastic Leukemia. J Mol Diagn. 2017 Sep;19(5):659–72.

56. Xu C, Gu X, Padmanabhan R, Wu Z, Peng Q, DiCarlo J, Wang Y. smCounter2: an accurate low-frequency variant caller for targeted sequencing data with unique molecular identifiers. Bioinformatics [Internet]. 2019 Apr 15;35(8):1299–309. Available from: https://doi.org/10.1093/bioinformatics/bty790

57. Kopanos C, Tsiolkas V, Kouris A, Chapple CE, Albarca Aguilera M, Meyer R, Massouras A. VarSome: the human genomic variant search engine. Bioinformatics [Internet]. 2019 Jun 1;35(11):1978–80. Available from: https://doi.org/10.1093/bioinformatics/bty897

58. Haas BJ, Dobin A, Li B, Stransky N, Pochet N, Regev A. Accuracy assessment of fusion transcript detection via read-mapping and de novo fusion transcript assembly-based methods. Genome Biol [Internet]. 2019;20(1):213. Available from: https://doi.org/10.1186/s13059-019-1842-9

59. Nicorici D, Şatalan M, Edgren H, Kangaspeska S, Murumägi A, Kallioniemi O, Virtanen S, Kilkku O. FusionCatcher– a tool for finding somatic fusion genes in paired-end RNA-sequencing data [Internet]. bioRxiv; 2014. Available from: http://europepmc.org/abstract/PPR/PPR35712

60. Melsted P, Hateley S, Joseph IC, Pimentel H, Bray N, Pachter L. Fusion detection and quantification by pseudoalignment. bioRxiv [Internet]. 2017 Jan 1;166322. Available from: http://biorxiv.org/content/early/2017/07/20/166322.abstract

61. Zhou X, Edmonson MN, Wilkinson MR, Patel A, Wu G, Liu Y, Li Y, Zhang Z, Rusch MC, Parker M, Becksfort J, Downing JR, Zhang J. Exploring genomic alteration in pediatric cancer using ProteinPaint. Nat Genet [Internet].

2016;48(1):4–6. Available from: https://doi.org/10.1038/ng.3466

62. Péterffy B, Krizsán S, Egyed B, Bedics G, Benard-Slagter A, Palit S, Erdélyi DJ, Müller J, Nagy T, Hegyi LL, Bekő A, Kenéz LA, Jakab Z, Péter G, Zombori M, Csanádi K, Ottóffy G, Csernus K, Vojcek Á, et al. Molecular Profiling Reveals Novel Gene Fusions and Genetic Markers for Refined Patient Stratification in Pediatric Acute Lymphoblastic Leukemia. Mod Pathol [Internet]. 2025 Jun 1;38(6). Available from: https://doi.org/10.1016/j.modpat.2025.100741

63. Péterffy B, Nádasi TJ, Krizsán S, Horváth A, Márk Á, Barna G, Timár B, Almási L, Müller J, Csanádi K, Rakonczai A, Nagy Z, Kállay K, Kertész G, Kriván G, Csóka M, Sebestyén A, Semsei ÁF, Kovács GT, et al. Digital PCR-based quantification of miR-181a in the cerebrospinal fluid aids patient stratification in pediatric acute lymphoblastic leukemia. Sci Rep [Internet]. 2024;14(1):28556. Available from: https://doi.org/10.1038/s41598-024-79733-0

64. Pui CH, Yang JJ, Bhakta N, Rodriguez-Galindo C. Global efforts toward the cure of childhood acute lymphoblastic leukaemia. Lancet Child Adolesc Heal. 2018 Jun;2(6):440–54.

65. Pui CH, Yang JJ, Hunger SP, Pieters R, Schrappe M, Biondi A, Vora A, Baruchel A, Silverman LB, Schmiegelow K, Escherich G, Horibe K, Benoit YCM, Izraeli S, Yeoh AEJ, Liang DC, Downing JR, Evans WE, Relling M V, et al. Childhood Acute Lymphoblastic Leukemia: Progress Through Collaboration. J Clin Oncol Off J Am Soc Clin Oncol. 2015 Sep;33(27):2938–48.

66. Waanders E, Gu Z, Dobson SM, Antić Ž, Crawford JC, Ma X, Edmonson MN, Payne-Turner D, van de Vorst M, Jongmans MCJ, McGuire I, Zhou X, Wang J, Shi L, Pounds S, Pei D, Cheng C, Song G, Fan Y, et al. Mutational Landscape and Patterns of Clonal Evolution in Relapsed Pediatric Acute Lymphoblastic Leukemia. Blood Cancer Discov [Internet]. 2020 Jul 1 [cited 2022 Jun 28];1(1):96–111. Available from: https://aacrjournals.org/bloodcancerdiscov/article/1/1/96/35174/Mutational-Landscape-and-Patterns-of-Clonal

67. Hoelzer D. Personalized medicine in adult acute lymphoblastic leukemia. Vol. 100, Haematologica. Italy; 2015. p. 855–8.

68. Van Der Veer A, Waanders E, Pieters R, Willemse ME, Van Reijmersdal S V.,

Russell LJ, Harrison CJ, Evans WE, Van Der Velden VHJ, Hoogerbrugge PM, Van Leeuwen F, Escherich G, Horstmann MA, Khankahdani LM, Rizopoulos D, De Groot-Kruseman HA, Sonneveld E, Kuiper RP, Den Boer ML. Independent prognostic value of BCR-ABL1-like signature and IKZF1 deletion, but not high CRLF2 expression, in children with B-cell precursor ALL. Blood [Internet]. 2013 Oct 10 [cited 2022 Jun 28];122(15):2622–9. Available from: https://pubmed.ncbi.nlm.nih.gov/23974192/

69. van der Veer A, Zaliova M, Mottadelli F, De Lorenzo P, te Kronnie G, Harrison CJ, Cavé H, Trka J, Saha V, Schrappe M, Pieters R, Biondi A, Valsecchi MG, Stanulla M, den Boer ML, Cazzaniga G. IKZF1 status as a prognostic feature in BCR-ABL1–positive childhood ALL. Blood [Internet]. 2014 Mar 13;123(11):1691–8. Available from: https://doi.org/10.1182/blood-2013-06-509794

70. Mullighan CG, Miller CB, Radtke I, Phillips LA, Dalton J, Ma J, White D, Hughes TP, Le Beau MM, Pui CH, Relling M V, Shurtleff SA, Downing JR. BCR–ABL1 lymphoblastic leukaemia is characterized by the deletion of Ikaros. Nature [Internet]. 2008;453(7191):110–4. Available from: https://doi.org/10.1038/nature06866

71. Tran TH, Harris MH, Nguyen J V, Blonquist TM, Stevenson KE, Stonerock E, Asselin BL, Athale UH, Clavell LA, Cole PD, Kelly KM, Laverdiere C, Leclerc JM, Michon B, Schorin MA, Welch JJG, Reshmi SC, Neuberg DS, Sallan SE, et al. Prognostic impact of kinase-activating fusions and IKZF1 deletions in pediatric high-risk B-lineage acute lymphoblastic leukemia. Blood Adv [Internet]. 2018 Mar 5;2(5):529–33. Available from: https://doi.org/10.1182/bloodadvances.2017014704

72. Boer JM, van der Veer A, Rizopoulos D, Fiocco M, Sonneveld E, de Groot-Kruseman HA, Kuiper RP, Hoogerbrugge P, Horstmann M, Zaliova M, Palmi C, Trka J, Fronkova E, Emerenciano M, do Socorro Pombo-de-Oliveira M, Mlynarski W, Szczepanski T, Nebral K, Attarbaschi A, et al. Prognostic value of rare IKZF1 deletion in childhood B-cell precursor acute lymphoblastic leukemia: an international collaborative study. Leukemia. 2016 Jan;30(1):32–8.

73. Mullighan CG, Su X, Zhang J, Radtke I, Phillips LAA, Miller CB, Ma J, Liu W,

Cheng C, Schulman BA, Harvey RC, Chen IM, Clifford RJ, Carroll WL, Reaman G, Bowman WP, Devidas M, Gerhard DS, Yang W, et al. Deletion of IKZF1 and prognosis in acute lymphoblastic leukemia. N Engl J Med. 2009 Jan;360(5):470–80.

74. Kuiper RP, Waanders E, van der Velden VHJ, van Reijmersdal S V, Venkatachalam R, Scheijen B, Sonneveld E, van Dongen JJM, Veerman AJP, van Leeuwen FN, van Kessel AG, Hoogerbrugge PM. IKZF1 deletions predict relapse in uniformly treated pediatric precursor B-ALL. Leukemia. 2010 Jul;24(7):1258–64.

75. Clappier E, Grardel N, Bakkus M, Rapion J, De Moerloose B, Kastner P, Caye A, Vivent J, Costa V, Ferster A, Lutz P, Mazingue F, Millot F, Plantaz D, Plat G, Plouvier E, Poirée M, Sirvent N, Uyttebroeck A, et al. IKZF1 deletion is an independent prognostic marker in childhood B-cell precursor acute lymphoblastic leukemia, and distinguishes patients benefiting from pulses during maintenance therapy: results of the EORTC Children's Leukemia Group study 58951. Leukemia. 2015 Nov;29(11):2154–61.

76. Hayette S, Grange B, Vallee M, Bardel C, Huet S, Mosnier I, Chabane K, Simonet T, Balsat M, Heiblig M, Tigaud I, Nicolini FE, Mareschal S, Salles G, Sujobert P. Performances of Targeted RNA Sequencing for the Analysis of Fusion Transcripts, Gene Mutation, and Expression in Hematological Malignancies. HemaSphere [Internet]. 2021 Feb 27 [cited 2022 Jun 28];5(2). Available from: https://pubmed.ncbi.nlm.nih.gov/33880432/

77. Schieck M, Lentes J, Thomay K, Hofmann W, Behrens YL, Hagedorn M, Ebersold J, Davenport CF, Fazio G, Möricke A, Buchmann S, Alten J, Cario G, Schrappe M, Bergmann AK, Stanulla M, Steinemann D, Schlegelberger B, Cazzaniga G, et al. Implementation of RNA sequencing and array CGH in the diagnostic workflow of the AIEOP-BFM ALL 2017 trial on acute lymphoblastic leukemia. Ann Hematol [Internet]. 2020;99(4):809–18. Available from: https://doi.org/10.1007/s00277-020-03953-3

78. Kim B, Kim E, Lee ST, Cheong JW, Lyu CJ, Min YH, Choi JR. Detection of recurrent, rare, and novel gene fusions in patients with acute leukemia using next-generation sequencing approaches. Hematol Oncol. 2020 Feb;38(1):82–8.

79. Yasuda T, Tsuzuki S, Kawazu M, Hayakawa F, Kojima S, Ueno T, Imoto N, Kohsaka S, Kunita A, Doi K, Sakura T, Yujiri T, Kondo E, Fujimaki K, Ueda Y, Aoyama Y, Ohtake S, Takita J, Sai E, et al. Recurrent DUX4 fusions in B cell acute lymphoblastic leukemia of adolescents and young adults. Nat Genet [Internet]. 2016;48(5):569–74. Available from: https://doi.org/10.1038/ng.3535

80. Gu Z, Churchman M, Roberts K, Li Y, Liu Y, Harvey RC, McCastlain K, Reshmi SC, Payne-Turner D, Iacobucci I, Shao Y, Chen IM, Valentine M, Pei D, Mungall KL, Mungall AJ, Ma Y, Moore R, Marra M, et al. Genomic analyses identify recurrent MEF2D fusions in acute lymphoblastic leukaemia. Nat Commun [Internet]. 2016;7(1):13331. Available from: https://doi.org/10.1038/ncomms13331

81. Hirabayashi S, Ohki K, Nakabayashi K, Ichikawa H, Momozawa Y, Okamura K, Yaguchi A, Terada K, Saito Y, Yoshimi A, Ogata-Kawata H, Sakamoto H, Kato M, Fujimura J, Hino M, Kinoshita A, Kakuda H, Kurosawa H, Kato K, et al. ZNF384-related fusion genes define a subgroup of childhood B-cell precursor acute lymphoblastic leukemia with a characteristic immunotype. Haematologica. 2017 Jan;102(1):118–29.

82. Hormann FM, Hoogkamer AQ, Beverloo HB, Boeree A, Dingjan I, Wattel MM, Stam RW, Escherich G, Pieters R, den Boer ML, Boer JM. NUTM1 is a recurrent fusion gene partner in B-cell precursor acute lymphoblastic leukemia associated with increased expression of genes on chromosome band 10p12.31-12.2. Vol. 104, Haematologica. Italy; 2019. p. e455–9.

83. Stutterheim J, van der Sluis IM, de Lorenzo P, Alten J, Ancliffe P, Attarbaschi A, Brethon B, Biondi A, Campbell M, Cazzaniga G, Escherich G, Ferster A, Kotecha RS, Lausen B, Li CK, Lo Nigro L, Locatelli F, Marschalek R, Meyer C, et al. Clinical Implications of Minimal Residual Disease Detection in Infants With KMT2A-Rearranged Acute Lymphoblastic Leukemia Treated on the Interfant-06 Protocol. J Clin Oncol Off J Am Soc Clin Oncol. 2021 Feb;39(6):652–62.

84. Meyer C, Larghero P, Almeida Lopes B, Burmeister T, Gröger D, Sutton R, Venn NC, Cazzaniga G, Corral Abascal L, Tsaur G, Fechina L, Emerenciano M, Pombo-de-Oliveira MS, Lund-Aho T, Lundán T, Montonen M, Juvonen V, Zuna J, Trka J, et al. The KMT2A recombinome of acute leukemias in 2023. Leukemia

[Internet]. 2023;37(5):988–1005. Available from: https://doi.org/10.1038/s41375-023-01877-1

85. Issa GC, Aldoss I, DiPersio J, Cuglievan B, Stone R, Arellano M, Thirman MJ, Patel MR, Dickens DS, Shenoy S, Shukla N, Kantarjian H, Armstrong SA, Perner F, Perry JA, Rosen G, Bagley RG, Meyers ML, Ordentlich P, et al. The menin inhibitor revumenib in KMT2A-rearranged or NPM1-mutant leukaemia. Nature [Internet]. 2023;615(7954):920–4. Available from: https://doi.org/10.1038/s41586-023-05812-3

86. Wiemels JL, Zhang Y, Chang J, Zheng S, Metayer C, Zhang L, Smith MT, Ma X, Selvin S, Buffler PA, Wiencke JK. RAS mutation is associated with hyperdiploidy and parental characteristics in pediatric acute lymphoblastic leukemia. Leukemia [Internet]. 2005;19(3):415–9. Available from: https://doi.org/10.1038/sj.leu.2403641

87. Ariës IM, van den Dungen RE, Koudijs MJ, Cuppen E, Voest E, Molenaar JJ, Caron HN, Pieters R, den Boer ML. Towards personalized therapy in pediatric acute lymphoblastic leukemia: RAS mutations and prednisolone resistance. Vol. 100, Haematologica. Italy; 2015. p. e132-6.

88. Irving J, Matheson E, Minto L, Blair H, Case M, Halsey C, Swidenbank I, Ponthan F, Kirschner-Schwabe R, Groeneveld-Krentz S, Hof J, Allan J, Harrison C, Vormoor J, von Stackelberg A, Eckert C. Ras pathway mutations are prevalent in relapsed childhood acute lymphoblastic leukemia and confer sensitivity to MEK inhibition. Blood. 2014 Nov;124(23):3420–30.

89. Jerchel IS, Hoogkamer AQ, Ariës IM, Steeghs EMP, Boer JM, Besselink NJM, Boeree A, van de Ven C, de Groot-Kruseman HA, de Haas V, Horstmann MA, Escherich G, Zwaan CM, Cuppen E, Koudijs MJ, Pieters R, den Boer ML. RAS pathway mutations as a predictive biomarker for treatment adaptation in pediatric B-cell precursor acute lymphoblastic leukemia. Leukemia. 2018 Apr;32(4):931–40.

90. Antić Ž, Yu J, Van Reijmersdal S V, Van Dijk A, Dekker L, Segerink WH, Sonneveld E, Fiocco M, Pieters R, Hoogerbrugge PM, Van Leeuwen FN, Van Kessel AG, Waanders E, Kuiper RP. Multiclonal complexity of pediatric acute lymphoblastic leukemia and the prognostic relevance of subclonal mutations.

Haematologica. 2021 Dec;106(12):3046–55.

91. Sinclair PB, Cranston RE, Raninga P, Cheng J, Hanna R, Hawking Z, Hair S, Ryan SL, Enshaei A, Nakjang S, Rand V, Blair HJ, Moorman A V, Heidenreich O, Harrison CJ. Disruption to the FOXO-PRDM1 axis resulting from deletions of chromosome 6 in acute lymphoblastic leukaemia. Leukemia [Internet]. 2023;37(3):636–49. Available from: https://doi.org/10.1038/s41375-023-01816-0

92. Borst L, Wesolowska A, Joshi T, Borup R, Nielsen FC, Andersen MK, Jonsson OG, Wehner PS, Wesenberg F, Frost BM, Gupta R, Schmiegelow K. Genome-wide analysis of cytogenetic aberrations in ETV6/RUNX1-positive childhood acute lymphoblastic leukaemia. Br J Haematol. 2012 May;157(4):476–82.

93. Sun C, Chang L, Zhu X. Pathogenesis of ETV6/RUNX1-positive childhood acute lymphoblastic leukemia and mechanisms underlying its relapse. Oncotarget. 2017 May;8(21):35445–59.

94. Li JF, Dai YT, Lilljebjörn H, Shen SH, Cui BW, Bai L, Liu YF, Qian MX, Kubota Y, Kiyoi H, Matsumura I, Miyazaki Y, Olsson L, Tan AM, Ariffin H, Chen J, Takita J, Yasuda T, Mano H, et al. Transcriptional landscape of B cell precursor acute lymphoblastic leukemia based on an international study of 1,223 cases. Proc Natl Acad Sci U S A. 2018 Dec;115(50):E11711–20.

95. Passet M, Boissel N, Sigaux F, Saillard C, Bargetzi M, Ba I, Thomas X, Graux C, Chalandon Y, Leguay T, Lengliné E, Konopacki J, Quentin S, Delabesse E, Lafage-Pochitaloff M, Pastoret C, Grardel N, Asnafi V, Lhéritier V, et al. PAX5 P80R mutation identifies a novel subtype of B-cell precursor acute lymphoblastic leukemia with favorable outcome. Vol. 133, Blood. United States; 2019. p. 280–4.

96. Zaliova M, Potuckova E, Lukes J, Winkowska L, Starkova J, Janotova I, Sramkova L, Stary J, Zuna J, Stanulla M, Zimmermann M, Bornhauser B, Bourquin JP, Eckert C, Cario G, Trka J. Frequency and prognostic impact of ZEB2 H1038 and Q1072 mutations in childhood B-other acute lymphoblastic leukemia. Vol. 106, Haematologica. Italy; 2021. p. 886–90.

97. Boer JM, Ilan U, Boeree A, Langenberg KPS, Koster J, Koudijs MJ, Hehir-Kwa JY, Nierkens S, Rossi C, Molenaar JJ, Goemans BF, den Boer ML, Zwaan CM. Oncogenic and immunological targets for matched therapy of pediatric blood cancer patients: Dutch iTHER study experience. HemaSphere [Internet]. 2024 Jul

1;8(7):e122. Available from: https://doi.org/10.1002/hem3.122

98. Stengel A, Schnittger S, Weissmann S, Kuznia S, Kern W, Kohlmann A, Haferlach T, Haferlach C. TP53 mutations occur in 15.7% of ALL and are associated with MYC-rearrangement, low hypodiploidy, and a poor prognosis. Blood [Internet]. 2014 Jul 10;124(2):251–8. Available from: https://doi.org/10.1182/blood-2014-02-558833

99. Hof J, Krentz S, van Schewick C, Körner G, Shalapour S, Rhein P, Karawajew L, Ludwig WD, Seeger K, Henze G, von Stackelberg A, Hagemeier C, Eckert C, Kirschner-Schwabe R. Mutations and deletions of the TP53 gene predict nonresponse to treatment and poor outcome in first relapse of childhood acute lymphoblastic leukemia. J Clin Oncol Off J Am Soc Clin Oncol. 2011 Aug;29(23):3185–93.

100. Stengel A, Kern W, Haferlach T, Meggendorfer M, Fasan A, Haferlach C. The impact of TP53 mutations and TP53 deletions on survival varies between AML, ALL, MDS and CLL: an analysis of 3307 cases. Leukemia [Internet]. 2017;31(3):705–11. Available from: https://doi.org/10.1038/leu.2016.263

101. Holmfeldt L, Wei L, Diaz-Flores E, Walsh M, Zhang J, Ding L, Payne-Turner D, Churchman M, Andersson A, Chen SC, Mccastlain K, Becksfort J, Ma J, Wu G, Patel SN, Heatley SL, Phillips LA, Song G, Easton J, et al. The genomic landscape of hypodiploid acute lymphoblastic leukemia. Nat Genet. 2013 Mar;45(3):242–52.

102. Mühlbacher V, Zenger M, Schnittger S, Weissmann S, Kunze F, Kohlmann A, Bellos F, Kern W, Haferlach T, Haferlach C. Acute lymphoblastic leukemia with low hypodiploid/near triploid karyotype is a specific clinical entity and exhibits a very high TP53 mutation frequency of 93%. Genes Chromosomes Cancer. 2014 Jun;53(6):524–36.

103. Ratei R, Basso G, Dworzak M, Gaipa G, Veltroni M, Rhein P, Biondi A, Schrappe M, Ludwig WD, Karawajew L. Monitoring treatment response of childhood precursor B-cell acute lymphoblastic leukemia in the AIEOP-BFM-ALL 2000 protocol with multiparameter flow cytometry: predictive impact of early blast reduction on the remission status after induction. Leukemia. 2009 Mar;23(3):528–34.

104. Borowitz MJ, Devidas M, Hunger SP, Bowman WP, Carroll AJ, Carroll WL,

Linda S, Martin PL, Pullen DJ, Viswanatha D, Willman CL, Winick N, Camitta BM. Clinical significance of minimal residual disease in childhood acute lymphoblastic leukemia and its relationship to other prognostic factors: a Children's Oncology Group study. Blood. 2008 Jun;111(12):5477–85.

105. Pawinska-Wasikowska K, Bukowska-Strakova K, Surman M, Rygielska M, Sadowska B, Ksiazek T, Klekawka T, Wieczorek A, Skoczen S, Balwierz W. Go with the Flow-Early Assessment of Measurable Residual Disease in Children with Acute Lymphoblastic Leukemia Treated According to ALL IC-BFM2009. Cancers (Basel). 2022 Oct;14(21).

106. László T, Kotmayer L, Fésüs V, Hegyi L, Gróf S, Nagy Á, Kajtár B, Balogh A, Weisinger J, Masszi T, Nagy Z, Farkas P, Demeter J, Istenes I, Szász R, Gergely L, Sulák A, Borbényi Z, Lévai D, et al. Low-burden TP53 mutations represent frequent genetic events in CLL with an increased risk for treatment initiation. J Pathol Clin Res. 2024 Jan;10(1):e351.

107. Malcikova J, Pavlova S, Kunt Vonkova B, Radova L, Plevova K, Kotaskova J, Pal K, Dvorackova B, Zenatova M, Hynst J, Ondrouskova E, Panovska A, Brychtova Y, Zavacka K, Tichy B, Tom N, Mayer J, Doubek M, Pospisilova S. Low-burden TP53 mutations in CLL: clinical impact and clonal evolution within the context of different treatment options. Blood. 2021 Dec;138(25):2670–85.

108. Nadeu F, Delgado J, Royo C, Baumann T, Stankovic T, Pinyol M, Jares P, Navarro A, Martín-García D, Beà S, Salaverria I, Oldreive C, Aymerich M, Suárez-Cisneros H, Rozman M, Villamor N, Colomer D, López-Guillermo A, González M, et al. Clinical impact of clonal and subclonal TP53, SF3B1, BIRC3, NOTCH1, and ATM mutations in chronic lymphocytic leukemia. Blood. 2016 Apr;127(17):2122–30.

109. Bomben R, Rossi FM, Vit F, Bittolo T, D'Agaro T, Zucchetto A, Tissino E, Pozzo F, Vendramini E, Degan M, Zaina E, Cattarossi I, Varaschin P, Nanni P, Berton M, Braida A, Polesel J, Cohen JA, Santinelli E, et al. TP53 Mutations with Low Variant Allele Frequency Predict Short Survival in Chronic Lymphocytic Leukemia. Clin cancer Res an Off J Am Assoc Cancer Res. 2021 Oct;27(20):5566–75.

110. Rossi D, Khiabanian H, Spina V, Ciardullo C, Bruscaggin A, Famà R, Rasi S,

Monti S, Deambrogi C, De Paoli L, Wang J, Gattei V, Guarini A, Foà R, Rabadan R, Gaidano G. Clinical impact of small TP53 mutated subclones in chronic lymphocytic leukemia. Blood. 2014 Apr;123(14):2139–47.

111. Mullighan CG, Zhang J, Kasper LH, Lerach S, Payne-Turner D, Phillips LA, Heatley SL, Holmfeldt L, Collins-Underwood JR, Ma J, Buetow KH, Pui CH, Baker SD, Brindle PK, Downing JR. CREBBP mutations in relapsed acute lymphoblastic leukaemia. Nature [Internet]. 2011;471(7337):235–9. Available from: https://doi.org/10.1038/nature09727

112. Inthal A, Zeitlhofer P, Zeginigg M, Morak M, Grausenburger R, Fronkova E, Fahrner B, Mann G, Haas OA, Panzer-Grümayer R. CREBBP HAT domain mutations prevail in relapse cases of high hyperdiploid childhood acute lymphoblastic leukemia. Leukemia [Internet]. 2012;26(8):1797–803. Available from: https://doi.org/10.1038/leu.2012.60

113. Malinowska-Ozdowy K, Frech C, Schönegger A, Eckert C, Cazzaniga G, Stanulla M, zur Stadt U, Mecklenbräuker A, Schuster M, Kneidinger D, von Stackelberg A, Locatelli F, Schrappe M, Horstmann MA, Attarbaschi A, Bock C, Mann G, Haas OA, Panzer-Grümayer R. KRAS and CREBBP mutations: a relapse-linked malicious liaison in childhood high hyperdiploid acute lymphoblastic leukemia. Leukemia [Internet]. 2015;29(8):1656–67. Available from: https://doi.org/10.1038/leu.2015.107

114. Wada M, Bartram CR, Nakamura H, Hachiya M, Chen DL, Borenstein J, Miller CW, Ludwig L, Hansen-Hagge TE, Ludwig WD. Analysis of p53 mutations in a large series of lymphoid hematologic malignancies of childhood. Blood. 1993 Nov;82(10):3163–9.

115. Tang JL, Tien HF, Lin MT, Chen PJ, Chen YC. Frequent p53 mutation in relapsed acute lymphoblastic leukemia with cytogenetic instability: a longitudinal analysis. Anticancer Res. 1998;18(2B):1273–8.

116. Chiaretti S, Brugnoletti F, Tavolaro S, Bonina S, Paoloni F, Marinelli M, Patten N, Bonifacio M, Kropp MG, Sica S, Guarini A, Foà R. TP53 mutations are frequent in adult acute lymphoblastic leukemia cases negative for recurrent fusion genes and correlate with poor response to induction therapy. Vol. 98, Haematologica. Italy; 2013. p. e59-61.

117. Li B, Brady SW, Ma X, Shen S, Zhang Y, Li Y, Szlachta K, Dong L, Liu Y, Yang F, Wang N, Flasch DA, Myers MA, Mulder HL, Ding L, Liu Y, Tian L, Hagiwara K, Xu K, et al. Therapy-induced mutations drive the genomic landscape of relapsed acute lymphoblastic leukemia. Blood [Internet]. 2020 Jan 2;135(1):41–55. Available from: https://doi.org/10.1182/blood.2019002220
118. Meyer JA, Wang J, Hogan LE, Yang JJ, Dandekar S, Patel JP, Tang Z, Zumbo P, Li S, Zavadil J, Levine RL, Cardozo T, Hunger SP, Raetz EA, Evans WE, Morrison DJ, Mason CE, Carroll WL. Relapse-specific mutations in NT5C2 in childhood acute lymphoblastic leukemia. Nat Genet. 2013 Mar;45(3):290–4.
119. Tzoneva G, Perez-Garcia A, Carpenter Z, Khiabanian H, Tosello V, Allegretta M, Paietta E, Racevskis J, Rowe JM, Tallman MS, Paganin M, Basso G, Hof J, Kirschner-Schwabe R, Palomero T, Rabadan R, Ferrando A. Activating mutations in the NT5C2 nucleotidase gene drive chemotherapy resistance in relapsed ALL. Nat Med. 2013 Mar;19(3):368–71.
120. Dieck CL, Tzoneva G, Forouhar F, Carpenter Z, Ambesi-Impiombato A, Sánchez-Martín M, Kirschner-Schwabe R, Lew S, Seetharaman J, Tong L, Ferrando AA. Structure and Mechanisms of NT5C2 Mutations Driving Thiopurine Resistance in Relapsed Lymphoblastic Leukemia. Cancer Cell. 2018 Jul;34(1):136-147.e6.
121. Dieck CL, Ferrando A. Genetics and mechanisms of NT5C2-driven chemotherapy resistance in relapsed ALL. Blood. 2019 May;133(21):2263–8.
122. McNeer JL, Schmiegelow K. Management of CNS Disease in Pediatric Acute Lymphoblastic Leukemia. Curr Hematol Malig Rep [Internet]. 2022;17(1):1–14. Available from: https://doi.org/10.1007/s11899-021-00640-6
123. Arthur C, Rezayee F, Mogensen N, Saft L, Rosenquist R, Nordenskjöld M, Harila-Saari A, Tham E, Barbany G. Patient-Specific Assays Based on Whole-Genome Sequencing Data to Measure Residual Disease in Children With Acute Lymphoblastic Leukemia: A Proof of Concept Study. Front Oncol. 2022;12:899325.
124. Rapado-González O, Martínez-Reglero C, Salgado-Barreira A, López-López R, Suárez-Cunqueiro MM, Muinelo-Romay L. miRNAs in liquid biopsy for oral squamous cell carcinoma diagnosis: Systematic review and meta-analysis. Oral Oncol. 2019 Dec;99:104465.

125. Sebestyén E, Nagy Á, Marosvári D, Rajnai H, Kajtár B, Deák B, Matolcsy A, Brandner S, Storhoff J, Chen N, Bagó AG, Bödör C, Reiniger L. Distinct miRNA Expression Signatures of Primary and Secondary Central Nervous System Lymphomas. J Mol Diagnostics [Internet]. 2022;24(3):224–40. Available from: https://www.sciencedirect.com/science/article/pii/S152515782100427X
126. Han HS, Jo YN, Lee JY, Choi SY, Jeong Y, Yun J, Lee OJ. Identification of suitable reference genes for the relative quantification of microRNAs in pleural effusion. Oncol Lett. 2014 Oct;8(4):1889–95.
127. Assmann JLJC, Leon LG, Stavast CJ, van den Bogaerdt SE, Schilperoord-Vermeulen J, Sandberg Y, Bellido M, Erkeland SJ, Feith DJ, Loughran Jr TP, Langerak AW. miR-181a is a novel player in the STAT3-mediated survival network of TCRαβ+ CD8+ T large granular lymphocyte leukemia. Leukemia [Internet]. 2022;36(4):983–93. Available from: https://doi.org/10.1038/s41375-021-01480-2
128. Ye F. MicroRNA expression and activity in T-cell acute lymphoblastic leukemia. Oncotarget. 2018 Jan;9(4):5445–58.
129. Lin S, Pan L, Guo S, Wu J, Jin L, Wang JC, Wang S. Prognostic role of microRNA-181a/b in hematological malignancies: a meta-analysis. PLoS One. 2013;8(3):e59532.
130. Ye Z, Li G, Kim C, Hu B, Jadhav RR, Weyand CM, Goronzy JJ. Regulation of miR-181a expression in T cell aging. Nat Commun. 2018 Aug;9(1):3060.
131. Kim C, Ye Z, Weyand CM, Goronzy JJ. miR-181a-regulated pathways in T-cell differentiation and aging. Immun Ageing [Internet]. 2021;18(1):28. Available from: https://doi.org/10.1186/s12979-021-00240-1
132. Tan LP, Wang M, Robertus JL, Schakel RN, Gibcus JH, Diepstra A, Harms G, Peh SC, Reijmers RM, Pals ST, Kroesen BJ, Kluin PM, Poppema S, van den Berg A. miRNA profiling of B-cell subsets: specific miRNA profile for germinal center B cells with variation between centroblasts and centrocytes. Lab Investig [Internet]. 2009;89(6):708–16. Available from: https://doi.org/10.1038/labinvest.2009.26
133. Verduci L, Azzalin G, Gioiosa S, Carissimi C, Laudadio I, Fulci V, Macino G. microRNA-181a enhances cell proliferation in acute lymphoblastic leukemia by targeting EGR1. Leuk Res. 2015 Apr;39(4):479–85.

134. Nabhan M, Louka ML, Khairy E, Tash F, Ali-Labib R, El-Habashy S. MicroRNA-181a and its target Smad 7 as potential biomarkers for tracking child acute lymphoblastic leukemia. Gene. 2017 Sep;628:253–8.
135. Liu X, Liao W, Peng H, Luo X, Luo Z, Jiang H, Xu L. miR-181a promotes G1/S transition and cell proliferation in pediatric acute myeloid leukemia by targeting ATM. J Cancer Res Clin Oncol. 2016 Jan;142(1):77–87.
136. Kato I, Nishinaka Y, Nakamura M, Akarca AU, Niwa A, Ozawa H, Yoshida K, Mori M, Wang D, Morita M, Ueno H, Shiozawa Y, Shiraishi Y, Miyano S, Gupta R, Umeda K, Watanabe K, Koh K, Adachi S, et al. Hypoxic adaptation of leukemic cells infiltrating the CNS affords a therapeutic strategy targeting VEGFA. Vol. 129, Blood. United States; 2017. p. 3126–9.
137. Sun W, Wang X, Li J, You C, Lu P, Feng H, Kong Y, Zhang H, Liu Y, Jiao R, Chen X, Ba Y. MicroRNA-181a promotes angiogenesis in colorectal cancer by targeting SRCIN1 to promote the SRC/VEGF signaling pathway. Cell Death Dis. 2018 Apr;9(4):438.
138. Egyed B, Horváth A, Semsei ÁF, Szalai C, Müller J, Erdélyi DJ, Kovács GT. Co-Detection of VEGF-A and Its Regulator, microRNA-181a, May Indicate Central Nervous System Involvement in Pediatric Leukemia. Pathol Oncol Res. 2022;28:1610096.
139. Muench V, Trentin L, Herzig J, Krauss J, Kestler HA, te Kronnie G, Debatin KM, Meyer LH. Migration of Acute Lymphoblastic Leukemia Cells into the Central Nervous System Is Regulated By VEGF. Blood [Internet]. 2015;126(23):2634. Available from: https://www.sciencedirect.com/science/article/pii/S0006497118496139
140. Braicu C, Gulei D, Cojocneanu R, Raduly L, Jurj A, Knutsen E, Calin GA, Berindan-Neagoe I. miR-181a/b therapy in lung cancer: reality or myth? Mol Oncol. 2019 Jan;13(1):9–25.
141. Takizawa H, Eto K, Yoshikawa A, Nakauchi H, Takatsu K, Takaki S. Growth and maturation of megakaryocytes is regulated by Lnk/Sh2b3 adaptor protein through crosstalk between cytokine- and integrin-mediated signals. Exp Hematol [Internet]. 2008;36(7):897–906. Available from: https://www.sciencedirect.com/science/article/pii/S0301472X08000702

142. Devallière J, Chatelais M, Fitau J, Gérard N, Hulin P, Velazquez L, Turner CE, Charreau B. LNK (SH2B3) is a key regulator of integrin signaling in endothelial cells and targets α-parvin to control cell adhesion and migration. FASEB J Off Publ Fed Am Soc Exp Biol. 2012 Jun;26(6):2592–606.
143. Tokar T, Pastrello C, Rossos AEM, Abovsky M, Hauschild AC, Tsay M, Lu R, Jurisica I. mirDIP 4.1-integrative database of human microRNA target predictions. Nucleic Acids Res. 2018 Jan;46(D1):D360–70.
144. Crespo-Solis E, López-Karpovitch X, Higuera J, Vega-Ramos B. Diagnosis of acute leukemia in cerebrospinal fluid (CSF-acute leukemia). Curr Oncol Rep. 2012 Oct;14(5):369–78.
145. Schwinghammer C, Koopmann J, Chitadze G, Karawajew L, Brüggemann M, Eckert C. A New View on Minimal Residual Disease Quantification in Acute Lymphoblastic Leukemia using Droplet Digital PCR. J Mol Diagn. 2022 Aug;24(8):856–66.

9. BIBLIOGRAPHY TO THE CANDIDATE'S PUBLICATIONS

Publications related to the PhD Thesis:

1. Péterffy, Borbála ; Nádasi, Tamás János ; Krizsán, Szilvia ; Horváth, Anna ; Márk, Ágnes ; Barna, Gábor ; Timár, Botond ; Almási, Laura ; Müller, Judit ; Csanádi, Krisztina ; Rakonczai, Anna ; Nagy, Zsolt ; Kállay, Krisztián ; Kertész, Gabriella ; Kriván, Gergely ; Csóka, Monika ; Sebestyén, Anna ; Semsei, Ágnes ; Kovács, Gábor Tamás ; Erdélyi, Dániel János ; Bödör, Csaba ; Egyed, Bálint* ; Alpár, Donát*.
Digital PCR-based quantification of miR-181a in the cerebrospinal fluid aids patient stratification in pediatric acute lymphoblastic leukemia
SCIENTIFIC REPORTS 14 : 1 Paper: 28556 , 13 p. (2024); * joint senior authors

2. Péterffy, Borbála ; Krizsán, Szilvia ; Egyed, Bálint ; Bedics, Gábor ; Benard-Slagter, Anne ; Palit, Sander ; Erdélyi, Dániel János ; Müller, Judit ; Nagy, Tibor ; Hegyi, Lajos László ; Bekő, Anna ; Kenéz, Lili Anna ; Jakab, Zsuzsanna ; Péter, György ; Zombori, Marianna ; Csanádi, Krisztina ; Ottóffy, Gábor ; Csernus, Katalin ; Vojcek, Ágnes ; Tiszlavicz, Lilla Györgyi ; Gábor, Krisztina Míta ; Kelemen, Ágnes ; Hauser, Péter; Kállay, Krisztián ; Kertész, Gabriella ; Gaál, Zsuzsanna ; Szegedi, István ; Barna, Gábor ; Márk, Ágnes ; Haltrich, Irén ; Hevessy, Zsuzsanna ; Ujfalusi, Anikó ; Kajtár, Béla ; Timár, Botond ; Kiss, Csongor ; Kriván, Gergely ; Matolcsy, András ; Savola, Suvi ; Kovács, Gábor ; Bödör, Csaba ; Alpár, Donát.
Molecular profiling reveals novel gene fusions and genetic markers for refined patient stratification in pediatric acute lymphoblastic leukemia
MODERN PATHOLOGY 38 : 6 Paper: 100741 , 14 p. (2025); * joint senior authors

Other publications:

1. Török, Marianna; Merkely, Petra ; Monori-Kiss, Anna ; Horváth, Eszter Mária ; Sziva, Réka Eszter ; Péterffy, Borbála ; Jósvai, Attila ; Sayour, Alex Ali ; Oláh, Attila ; Radovits, Tamás ; Merkely, Béla ; Ács, Nándor ; Nádasy György László ; Várbíró, Szabolcs.
Network analysis of the left anterior descending coronary arteries in swim-trained rats by an in situ video microscopic technique

BIOLOGY OF SEX DIFFERENCES 12 : 1 Paper: 37 , 17 p. (2021)

2. Tarszabó, Róbert ; Bányai, Bálint ; Ruisanchez, Éva ; Péterffy, Borbála ; Korsós-Novák, Ágnes ; Lajtai, Krisztina ; Sziva, Réka Eszter ; Gerszi, Dóra ; Hosszú, Ádám ; Benkő, Rita ; Benyó, Zoltán ; Horváth, Eszter Mária ; Masszi, Gabriella ; Várbíró, Szabolcs.
Influence of Vitamin D on the Vasoactive Effect of Estradiol in a Rat Model of Polycystic Ovary Syndrome
INTERNATIONAL JOURNAL OF MOLECULAR SCIENCES 22 : 17 Paper: 9404 , 12 p. (2021)

3. Sipos, Miklós ; Péterffy, Borbála ; Sziva, Réka Eszter ; Magyar, Péter ; Hadjadj, Leila ; Bányai, Bálint ; Süli, Anita ; Soltész-Katona, Eszter ; Gerszi, Dóra ; Kiss, Judit ; Szekeres, Mária ; Nádasy, György László; Horváth, Eszter Mária ; Várbíró, Szabolcs.
Vitamin D Deficiency Cause Gender Specific Alterations of Renal Arterial Function in a Rodent Model
NUTRIENTS 13 : 2 Paper: 704 , 13 p. (2021)

4. Lajtai, Krisztina ; Tarszabó, Róbert ; Bányai, Bálint ; Péterffy, Borbála ; Gerszi, Dóra ; Ruisanchez, Éva ; Sziva, Réka Eszter ; Korsós-Novák, Ágnes ; Benkő, Rita ; Hadjadj, Leila ; Benyó, Zoltán ; Horváth, Eszter Mária ; Masszi, Gabriella ; Várbíró, Szabolcs.
Effect of Vitamin D Status on Vascular Function of the Aorta in a Rat Model of PCOS
OXIDATIVE MEDICINE AND CELLULAR LONGEVITY 2021 Paper: 8865979 , 6 p. (2021)

5. Hannah, Armes ; Ana, Rio-Machin ; Krizsán, Szilvia ; Bödör, Csaba ; Fadimana, Kaya ; Findlay, Bewicke-Copley ; Jenna, Alnajar ; Amanda, Walne ; Péterffy, Borbála ; Hemanth, Tummala ; Rouault-Pierre, Kevin ; Dokal, Inderjeet ; Vulliamy , Tom ; Fitzgibbon, Jude.
Acquired somatic variants in inherited myeloid malignancies
LEUKEMIA 36 : 5 pp. 1377-1381. , 5 p. (2022)

6. Krizsán, Szilvia ; Péterffy, Borbála ; Egyed, Bálint ; Nagy, Tibor ; Sebestyén, Endre ; Hegyi, Lajos László ; Jakab, Zsuzsanna ; Erdélyi, Dániel J. ; Müller, Judit ; Péter, György ; Csanádi, Krisztina ; Kállay, Krisztián ; Kriván, Gergely ; Barna, Gábor ; Bedics, Gábor ; Haltrich, Irén ; Ottóffy, Gábor ; Csernus, Katalin ; Vojcek, Ágnes ; Tiszlavicz, Lilla Györgyu ; Gábor, Krisztina Mita, Kelemen, Ágnes ; Hauser, Péter ; Gaál, Zsuzsanna ; Szegedi, István ; Ujfalusi, Anikó ; Kajtár, Béla ; Kiss, Csongor ; Matolcsy, András ; Timár, Botond ; Kovács, Gábor ; Alpár, Donát ; Bödör, Csaba.
Next-Generation Sequencing–Based Genomic Profiling of Children with Acute Myeloid Leukemia
JOURNAL OF MOLECULAR DIAGNOSTICS 25 : 8 pp. 555-568. , 14 p. (2023)

7. Hunyadi, Anna ; Kriston, Csilla ; Szalóki, Gabor ; Péterffy, Borbála ; Egyed, Bálint ; Szepesi, Ágota ; Timár, Botond ; Erdélyi, Dániel János ; Csanádi, Krisztina ; Kutszegi, Nóra ; Márk, Ágnes ; Barna, Gábor.
The significance of CD49f expression in pediatric B-cell acute lymphoblastic leukemia
AMERICAN JOURNAL OF CLINICAL PATHOLOGY 163 : 2 pp. 169-177. , 9 p. (2025)

8. Egyed, Bálint ✉ ; Árvai, Kristóf ; Zajta, Erik ; Hegyi, Lajos ; Andrássy, Blanka ; Kovács, Árpád Ferenc ; Bekő, Anna ; Péterffy, Borbála ; Erdélyi, Dániel János ; Müller, Judit ; Békési, Andrea ; Kállay, Krisztián ; Goda, Vera ; Kriván, Gergely ; Tuboly, Eszter ; Csanádi, Krisztina ; Ottóffy, Gábor ; Szegedi, István ; Kiss, Csongor ; Bödör, Csaba ; Alpár, Donát ; Kovács, Gábor.
A genetikai eredetű gyermekkori krónikus cytopeniák felismerése a molekuláris medicina érájában : Klinikai ajánlás és metodikai útmutató
ORVOSI HETILAP 166 : 1 pp. 3-19. , 17 p. (2025)

10. ACKNOWLEDGEMENT

I am grateful to András Matolcsy, MD, PhD, DSc, Head of the Department of Pathology and Experimental Cancer Research at Semmelweis University, for allowing me to pursue my PhD studies in the host Institute.

I would like to thank my supervisor, Donát Alpár, PhD for his admirable professional attitude and accuracy. He was always available and I could count on him with any questions and problems that arose.

I am thankful to Csaba Bödör, PhD, DSc, Head of the Molecular Oncohematology Research Group for creating a creative and inspiring environment in the working group and for providing the infrastructural background required for my research projects.

I am grateful to Szilvia Krizsán, MD for all the useful practical guidance she provided during my first year of PhD studies.

I would like to thank Bálint Egyed, MD, PhD for all his valuable insights and for providing a clinical perspective, which greatly improved the quality of our research.

I am eternally grateful to the members of the HCEMM-SE Molecular Oncohematology Research Group (Anna Bekő, Lili Anna Kenéz, Gabriella Szepesi, Luca Varga, Lili Kotmayer, Tamás László, Bence Bátai, Gábor Bedics, Balázs Kardos and Ákos Nagy) for their invaluable personal and professional support, even in the most challenging moments.

I am tremendously grateful to my family and friends (especially S.R., A.B., Á.B., F.A., K.S., P.F.) for listening, supporting, and encouraging me at any time during the whole period of my PhD studies.

APPENDIX

Supplementary tables and figures related to the PhD thesis.

Supplementary Table 1. Comparison of the 5th edition of WHO Classification and the latest International Consensus Classification in acute lymphoblastic leukemia(11,12)**.**

WHO Classification, 5th edition	**International Consensus Classification**
B-lymphoblastic leukemia/lymphoma	
B-ALL/LBL with *BCR::ABL1* fusion	B-ALL with t(9;22)(q34.1;q11.2)/*BCR::ABL1* with lymphoid only involvement /with multilineage involvement
B-ALL/LBL with *KMT2A* rearrangement	B-ALL with t(v;11q23.3)/*KMT2A* rearranged
B-ALL/LBL with *ETV6::RUNX1* fusion	B-ALL with t(12;21)(p13.2;q22.1)/*ETV6::RUNX1*
B-ALL/LBL with high hyperdiploidy	B-ALL, hyperdiploid
B-ALL/LBL with hypodiploidy	B-ALL, low hypodiploid
	B-ALL, near haploid
B-ALL/LBL with *IGH::IL3* fusion	B-ALL with t(5;14)(q31.1;q32.3)/*IL3::IGH*
B-ALL/LBL with *TCF3::PBX1* fusion	B-ALL with t(1;19)(q23.3;p13.3)/*TCF3::PBX1*
B-ALL/LBL with *TCF3::HLF* fusion	B-ALL with *HLF* rearrangement
B-ALL/LBL with *BCR::ABL1*-like features	B-ALL, *BCR::ABL1*–like, ABL-1 class rearranged
	B-ALL, *BCR::ABL1*–like, JAK-STAT activated
	B-ALL, *BCR::ABL1*–like, NOS
B-ALL/LBL with iAMP21	B-ALL with iAMP21
B-ALL/LBL with other defined genetic abnormalitites	B-ALL with *MYC* rearrangement
	B-ALL with *DUX4* rearrangement
	B-ALL with *MEF2D* rearrangement
	B-ALL with *ZNF384(362)* rearrangement
	B-ALL with *NUTM1* rearrangement
	B-ALL with *UBTF::ATXN7L3/PAN3,CDX2* (“CDX2/UBTF”)
	B-ALL with mutated *IKZF1* N159Y
	B-ALL with mutated *PAX5* P80R
	B-ALL with recurrent genetic abnormalitites
B-ALL/LBL with *ETV6::RUNX1*-like features	Provisional entity: B-ALL, *ETV6::RUNX1*-like
B-ALL/LBL, NOS	B-ALL, NOS
T-lymphoblastic leukemia/lymphoma	
Early T-precursor ALL/LBL	Early T-cell precursor ALL with rearrangement
	Early T-cell precursor ALL, NOS
T-ALL/LBL, NOS	T-ALL, NOS

Supplementary Table 2. Composition and clinical characteristics of the novel groups after reclassification of patients by considering hsa-miR-181a-5p expression. At categorical variables, the Fisher-Freeman-Halton test was used, while for continuous variables, the Kruskal-Wallis test was applied (63).

	CNSmin/miRmin	**CNSmin/miRsign**	**CNSpos/miRsign**	**p**
Patients, n	17	12	4	-
Excluded from further analysis, n (reason)	2 (TLP)	3 (2 TLP, 1 not fulfilling QC criteria)	1 (outlier, over +3SD)	-
Male %	67%	60%	100%	0.621
Immunophenotype: B-cell, %	87%	80%	67%	0.792
Initial diagnosis: LBL, %	7%	0%	0%	1.000
% of positive cytospins at Dx	0%	33%	100%	0.007
% of positive CSF FCM results at Dx	13%	60%	67%	0.026
Mean normalized hsa-miR-181a-5p copy number; Day 0	744.02±86.81	2503.50±275.89	3300.70±809.69	<0.001
Mean normalized hsa-miR-181a-5p copy number, log; Day 0	2.81±0.064	3.37±0.05	3.49±0.11	<0.001
EOI MRD positivity (BM), %	57%	40%	33%	0.650

End of 2nd induction cycle MRD positivity (BM), %	14%	20%	33%	0.797
Sample numbers at different time points of sample collection:				
At Dx (day 0), n	15	10	3	-
During the induction cycle (day 1 - day 33), n	25	16	7	-
Follow-up after the induction cycle (day 33 – day 100), n	3	2	2	-
Molecular profiling of the BM sample at diagnosis:				
DNAseq was performed, %	100%	100%	100%	-
Genes affected by clonal mutations (list)	*ASMTL, ASXL2, BCL11B, BRAF, CDKN2A, CREBBP, ETV6, EZH2, KRAS, NOTCH1, NRAS, PHF6, VPREB1, WHSC1*	*FLT3, IL7R, NOTCH1, NRAS, PDGFRA, RPL10, SETD2, TP53, VPREB1, ZEB2*	*ASMTL, CDKN2A, DNMT3A, EBF1, PIK3R1, SH2B3*	-

Abbreviations: BM: bone marrow; CSF: cerebrospinal fluid; Dx: diagnosis; EOC: end of consolidation; EOI: end of induction; FCM: flow cytometry; LBL: lymphoblastic lymphoma; MRD: measurable residual disease; QC: quality control; TLP: traumatic lumbar puncture

Supplementary Figure 1.A

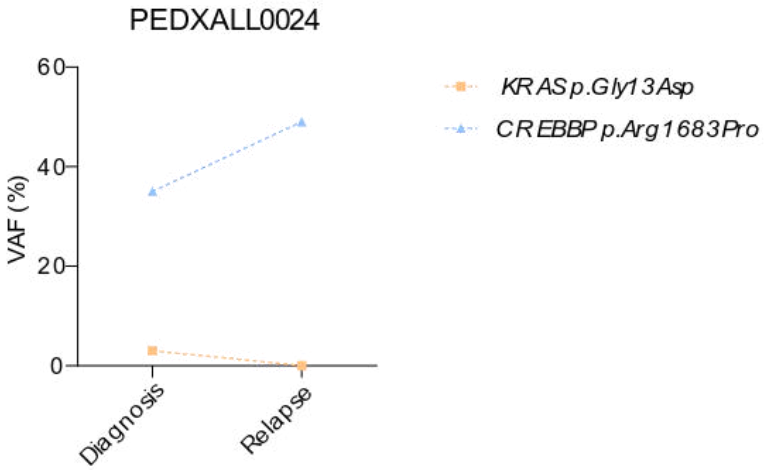

Supplementary Figure 1.B

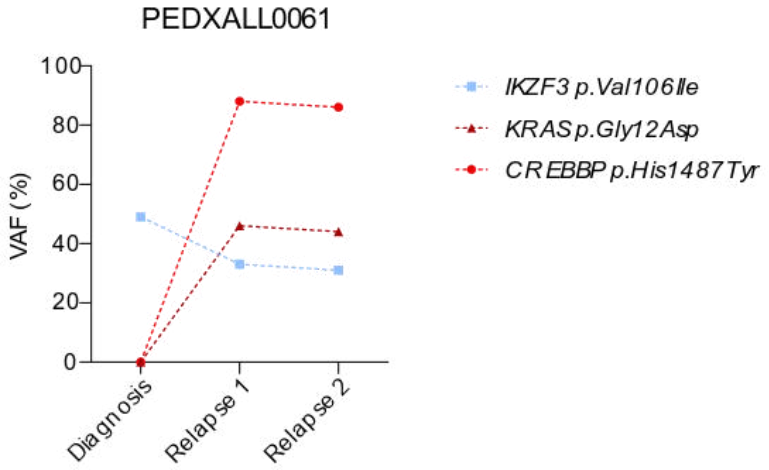

Supplementary Figure 1.C

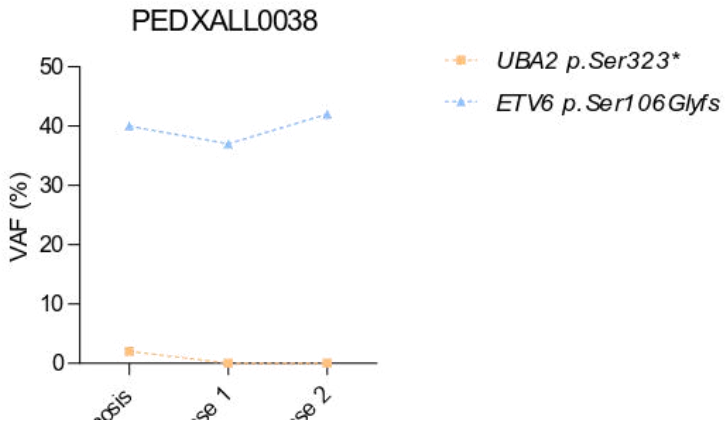

Supplementary Figure 1.D

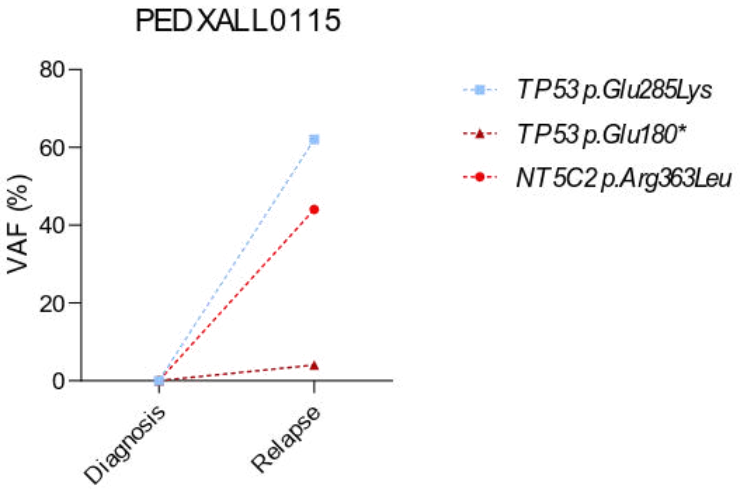

Supplementary Figure 1.E

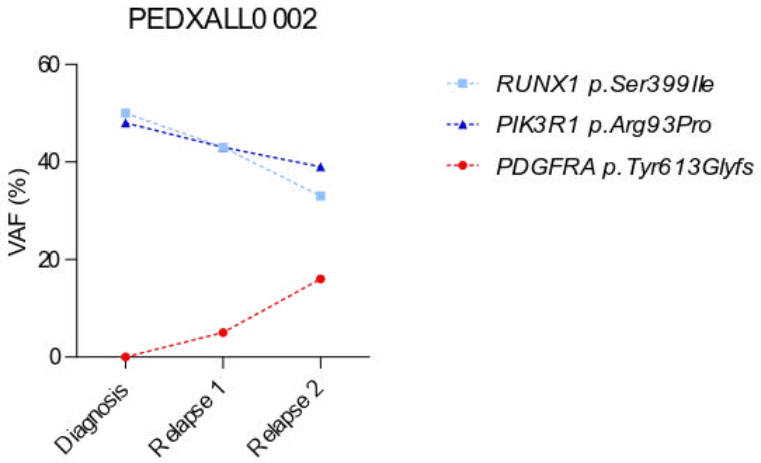

Supplementary Figure 1.F

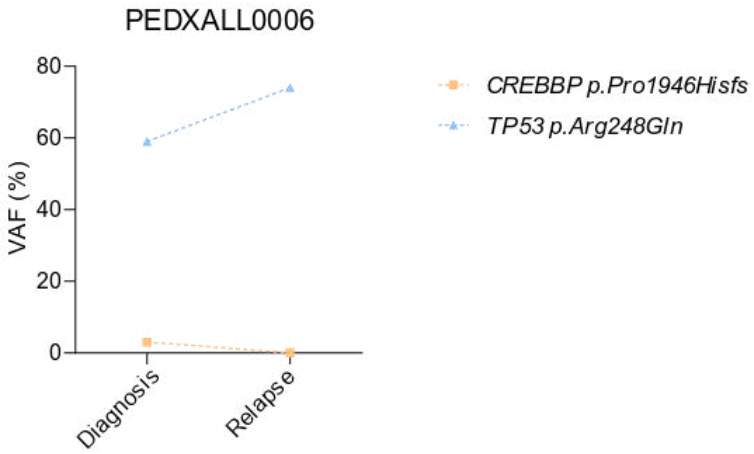

Supplementary Figure 1.G

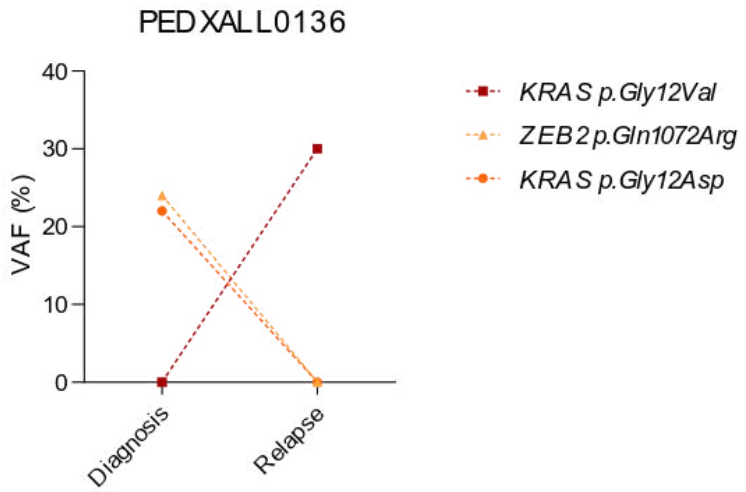

Supplementary Figure 1.H

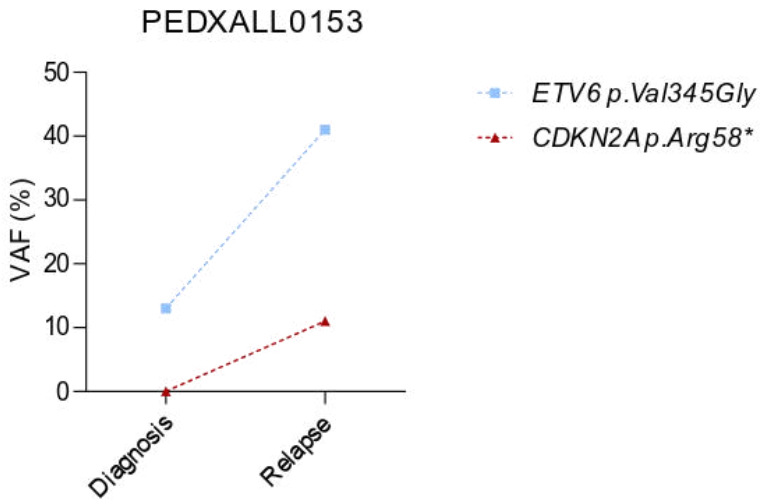

Supplementary Figure 1.I

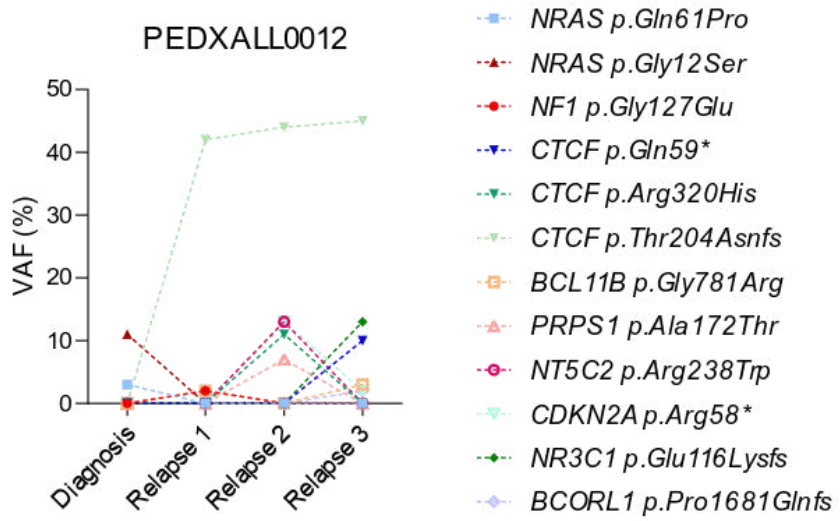

Supplementary Figure 1.J

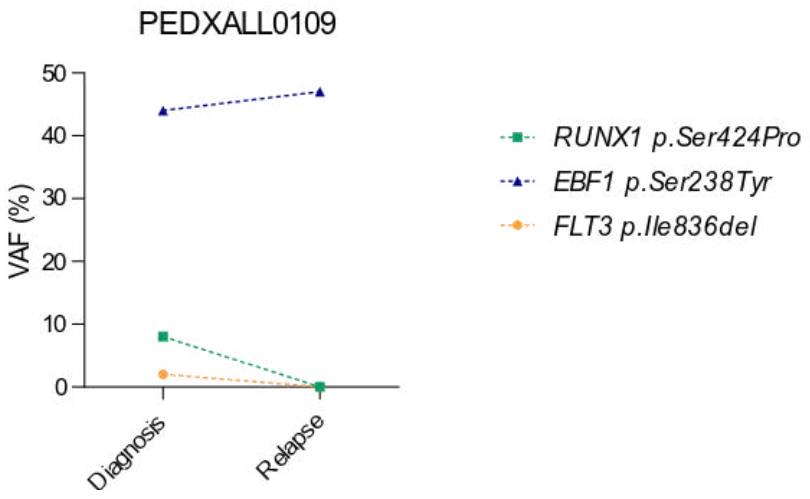

Supplementary Figure 1.K

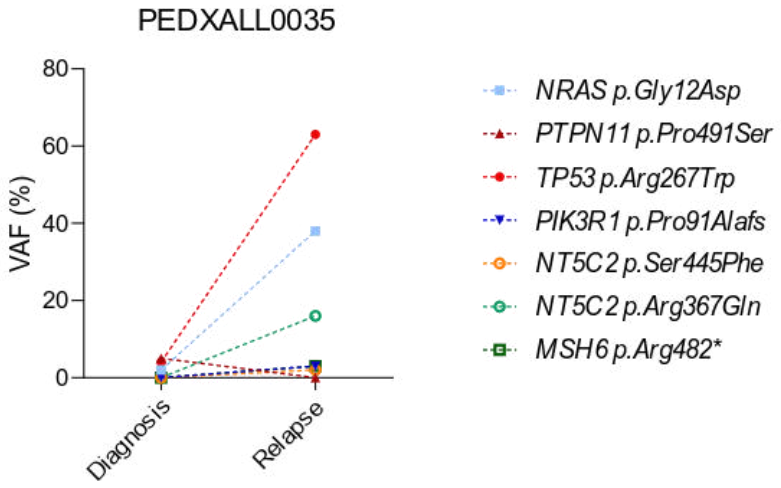

Supplementary Figure 1.L

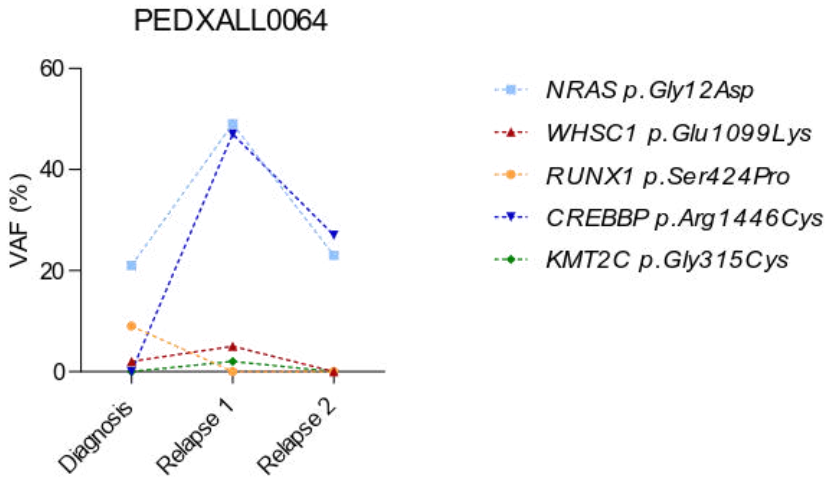

Supplementary Figure 1.M

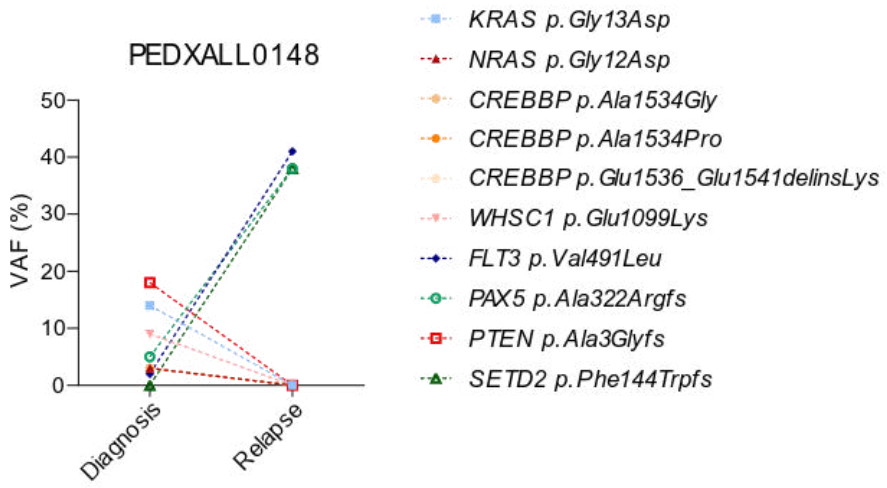

Supplementary Figure 1.N

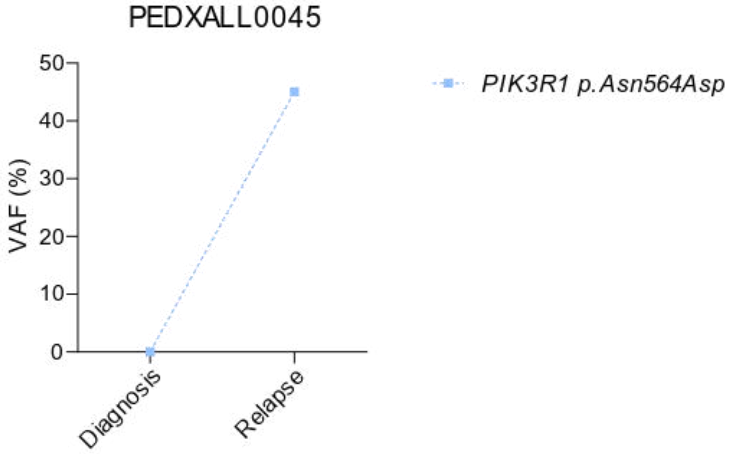

Supplementary Figure 1.O

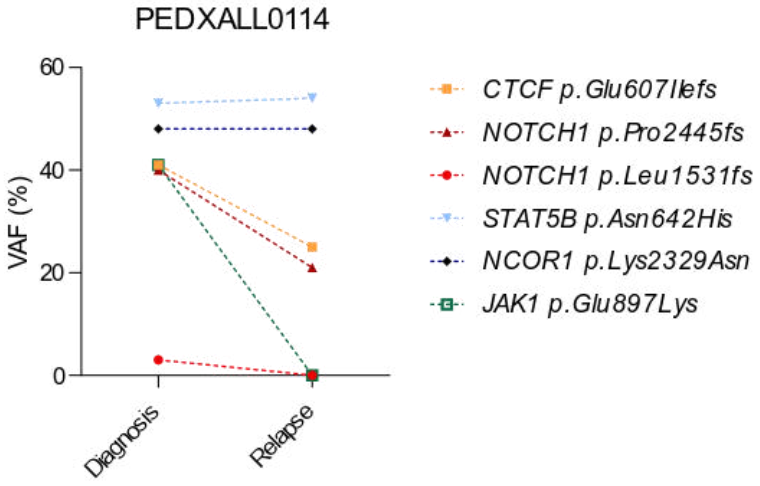

Supplementary Figure 1.P

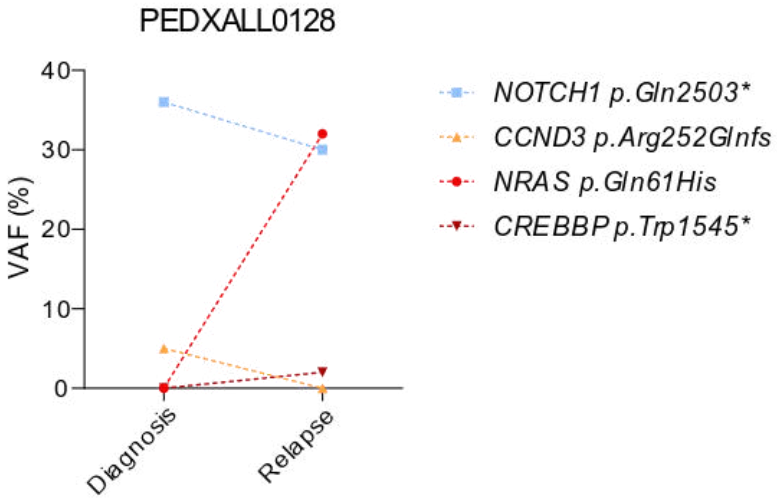

Supplementary Figure 1.Q

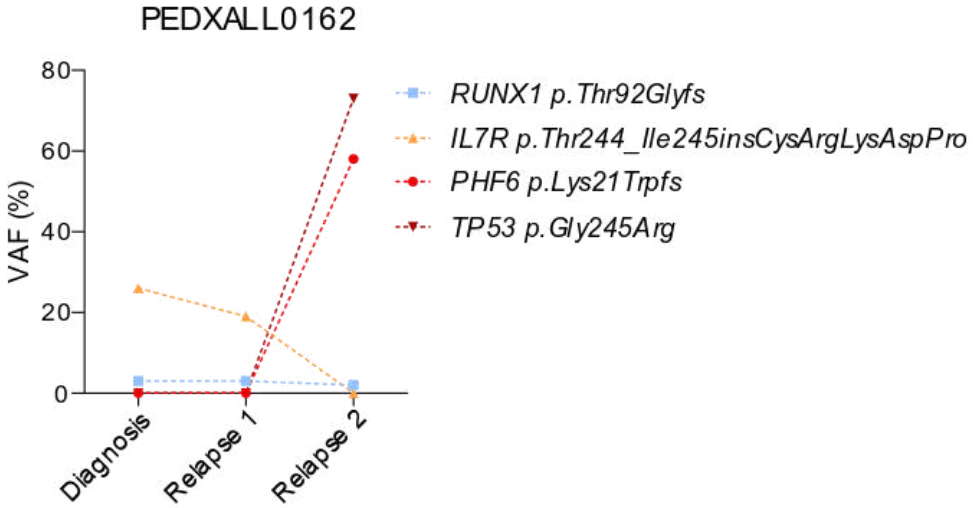

Supplementary Figure 1. Clonal dynamics and composition of mutations at the time of diagnosis and relapse in 17 patients experiencing relapse (62). VAF: variant allele frequency

Supplementary Figure 2.A

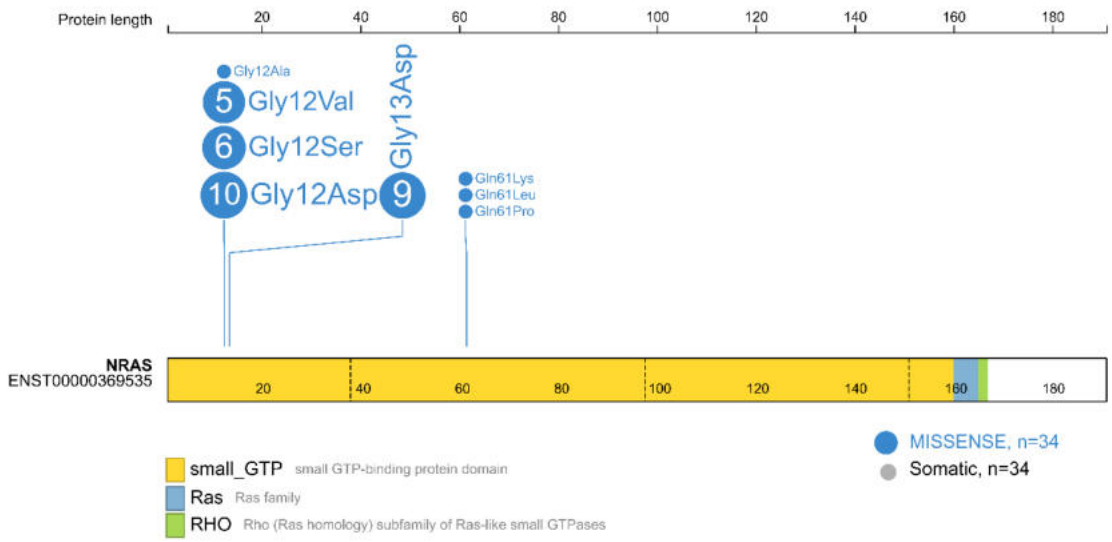

Supplementary Figure 2.B

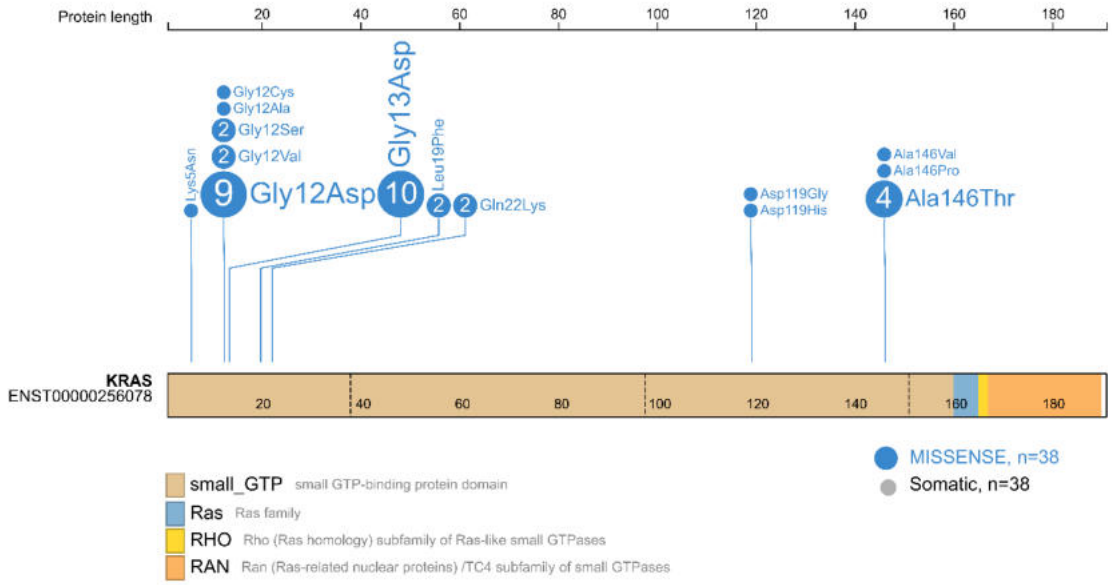

Supplementary Figure 2.C

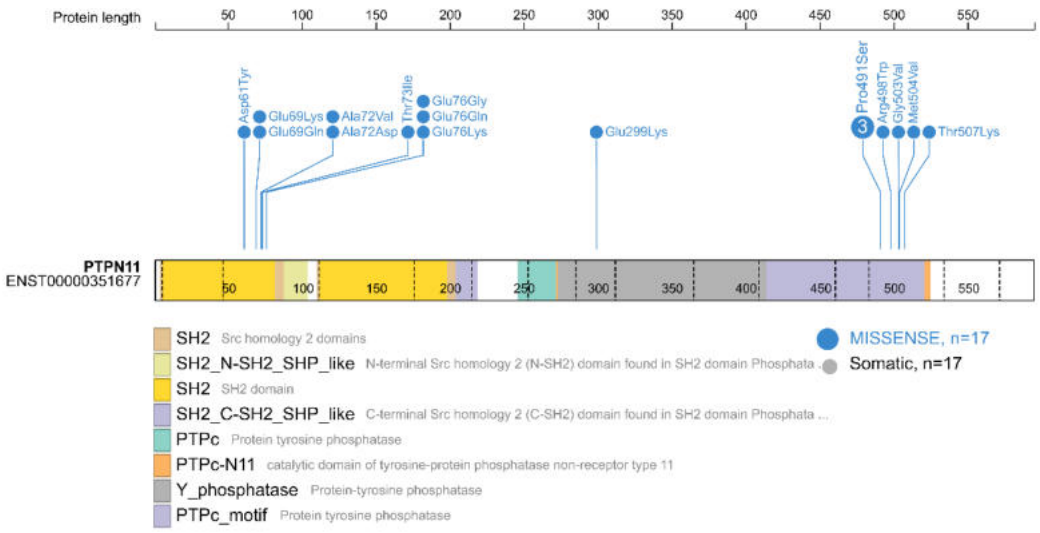

Supplementary Figure 2.D

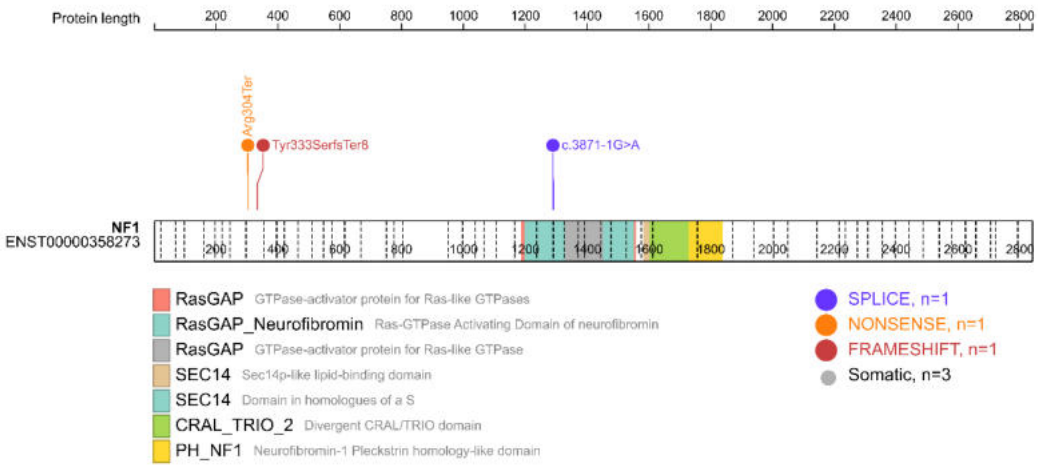

Supplementary Figure 2.E

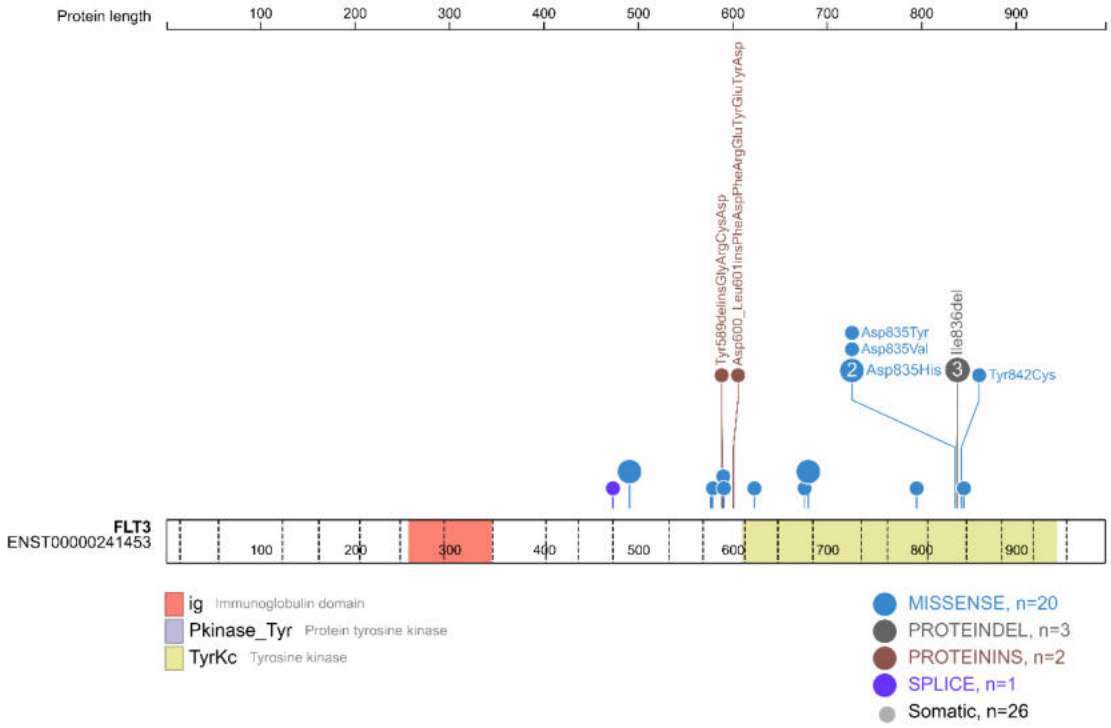

Supplementary Figure 2.F

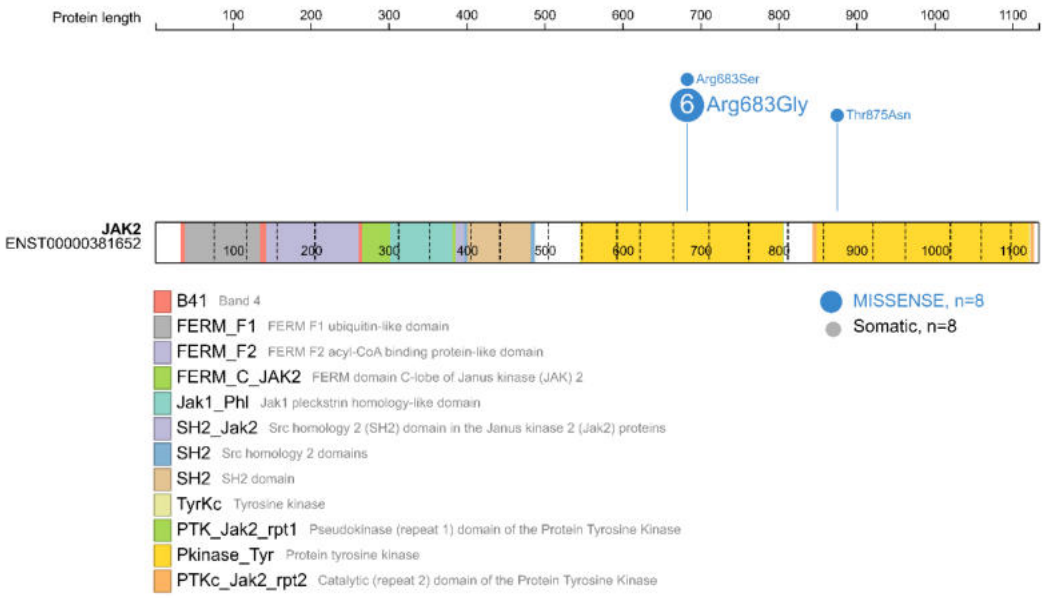

Supplementary Figure 2.G

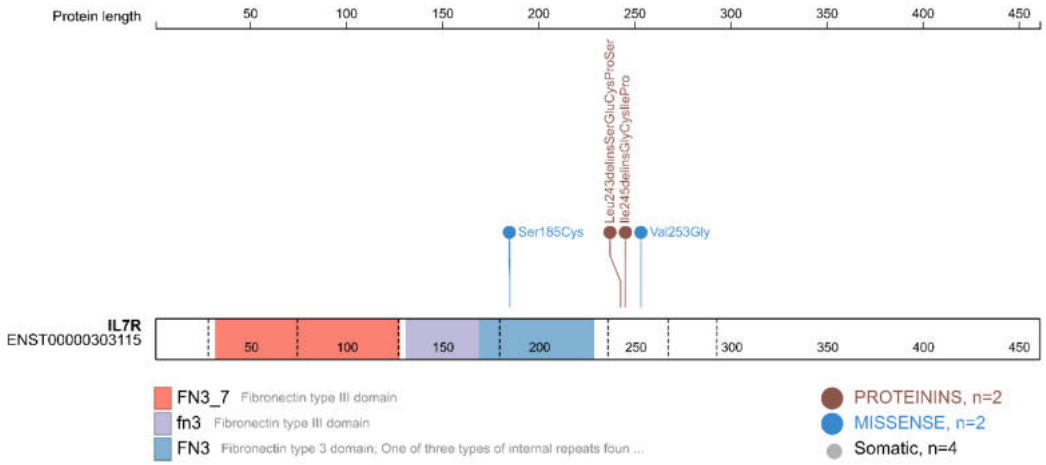

Supplementary Figure 2.H

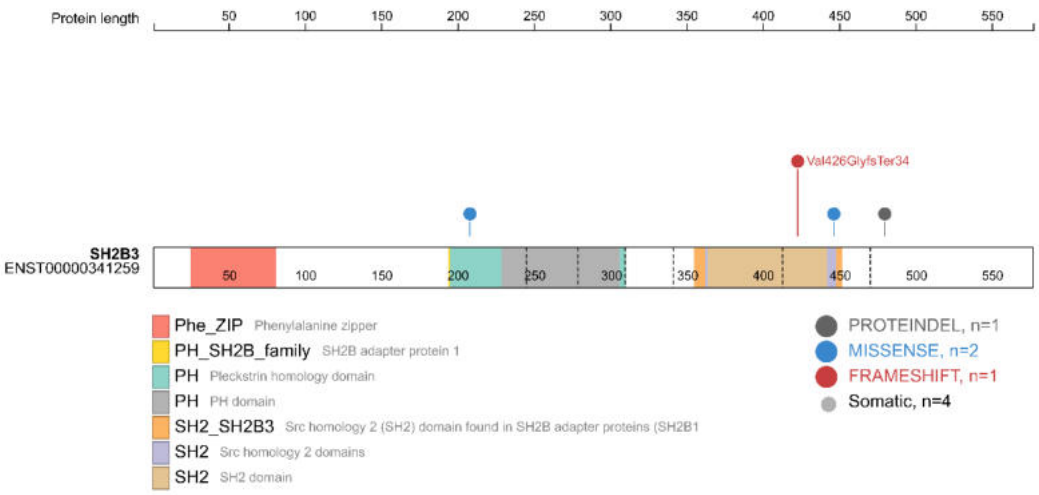

Supplementary Figure 2.I

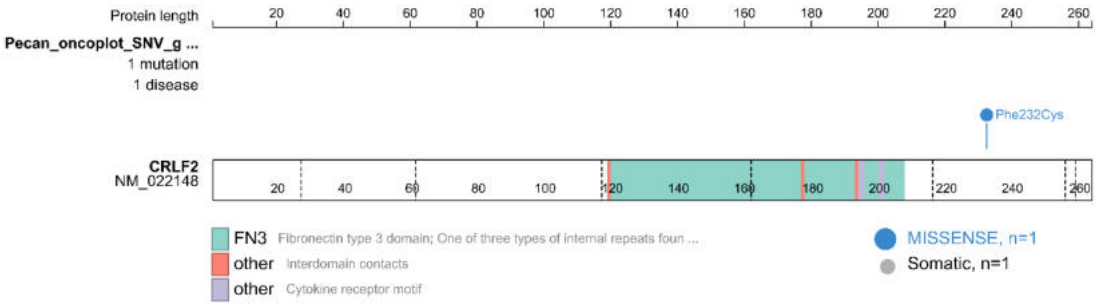

Supplementary Figure 2.J

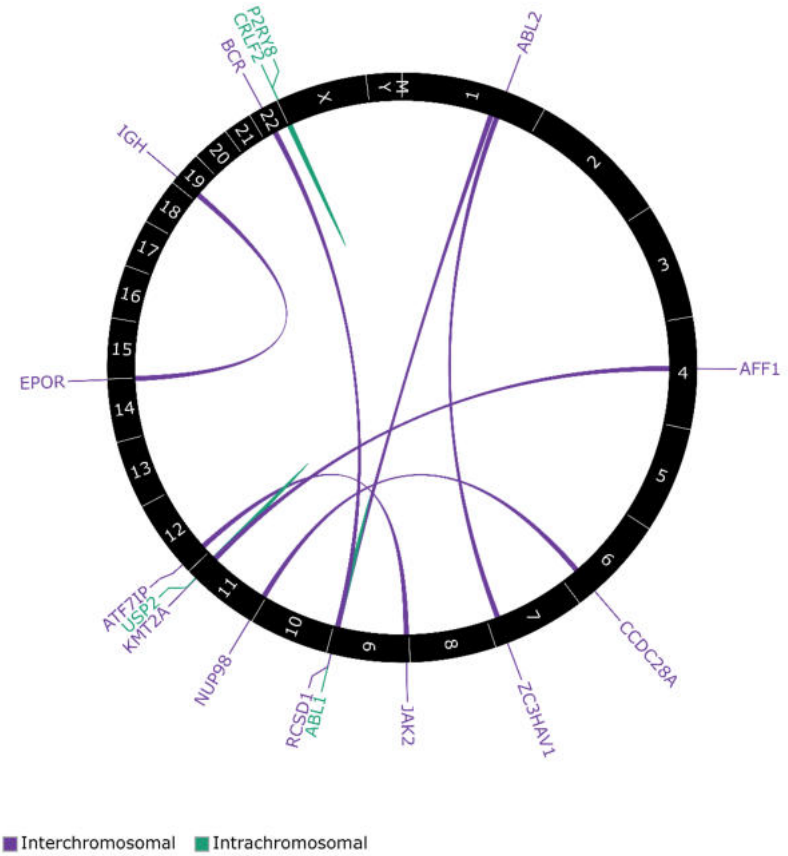

Supplementary Figure 2. A-I Short somatic variants identified in putatively targetable genes, such as *NRAS, KRAS, PTPN11, NF1, FLT3, JAK2, IL7R, SH2B3* and *CRLF2*.

J Gene fusions affecting potentially targetable genes (62).